

INTRACELLULAR IMMUNODYNAMICS OF LENTIVIRAL GENE DELIVERY IN
HUMAN NATURAL KILLER CELLS

by

ECE CANAN SAYITOĞLU

Submitted to the Graduate School of Engineering and Natural Sciences

in partial fulfillment of

the requirements for the degree of

Doctor of Philosophy


Sabanci University

January 2017

INTRACELLULAR IMMUNODYNAMICS OF LENTIVIRAL GENE DELIVERY IN
HUMAN NATURAL KILLER CELLS

APPROVED BY:

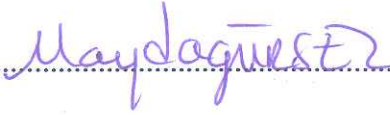
Prof. Dr. Batu Erman
(Thesis Supervisor)



Prof. Dr. İhsan Gürsel



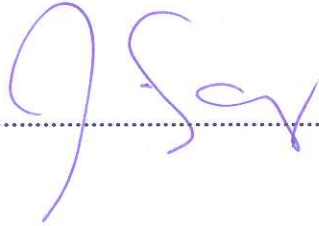
Prof. Dr. Mayda Gürsel



Prof. Dr. O. Uğur Sezerman



Prof. Dr. Zehra Sayers



DATE OF APPROVAL: 06/01/2017



© Ece Canan Sayitođlu 2017

All Rights Reserved

ABSTRACT

INTRACELLULAR IMMUNODYNAMICS OF LENTIVIRAL GENE DELIVERY IN HUMAN NATURAL KILLER CELLS

Ece Canan Sayitođlu

Biological Sciences and Bioengineering, PhD Thesis, 2017

Thesis Supervisor: Batu Erman

Co-supervisor: Tolga Sütlu

Keywords: natural killer cells, immunotherapy, lentiviral vectors

Natural Killer (NK) cells are members of the innate immune system that target tumors and infected cells. Cancer immunotherapy approaches using genetically modified NK cells continue to inspire clinical trials with promising results but the protocols for genetic modification of NK cells are suboptimal. NK cells show strikingly high resistance to lentiviral gene delivery when compared to other cells of the immune system. Previous studies show that the use of BX795, a small molecule inhibitor of TBK1/IKKepsilon complex downstream of Toll-like Receptors and RIG-I-like receptors, significantly enhances lentiviral gene delivery to NK cells. This study shows that while viral vector entry to NK cells can take place without major problems, the activation of antiviral signaling pathways leads to intracellular elimination of the vector. To study the roles of 20 candidate genes in this process, the CRISPR/Cas9 system was used and single genes were knocked out in 293FT and NK-92 cell lines. We demonstrate that, capsid recognition by TRIM5alpha in 293FT cells and dsRNA-induced signaling through RIG-I and TRIM25 in NK-92 cells are major players affecting lentiviral gene delivery. Additionally, viral vector exposure was shown to increase MAPK activity in host cells, specifically p38 and JNK phosphorylation in NK-92 cells, as observed in wildtype HIV infections. Overall, this study confirms that lentiviral gene delivery evokes an innate immune response in NK cells through multiple pattern recognition receptors and cellular restriction factors. Small molecule inhibitors help to overcome this obstacle for promising applications in immunotherapy using genetically modified NK cells.

ÖZET

İNSAN DOĞAL ÖLDÜRÜCÜ HÜCRELERDE LENTİVİRAL GEN AKTARIMININ HÜCREİÇİ İMMÜN DİNAMİĞİ

Ece Canan Sayitođlu

Biyoloji Bilimleri ve Biyomühendislik, Doktora Tezi, 2017

Tez Danışmanı: Batu Erman

Eş Danışman: Tolga Sütü

Anahtar kelimeler: doğal öldürücü hücreler, immünoterapi, lentiviral vektörler

Dođal Öldürücü (NK) hücreler dođal bađışıklık sisteminin kanser hücrelerini ve enfekte olmuş hücreleri hedef alan üyeleridir. Genetiđi deđiştirilmiş NK hücreleri kullanılan kanser immün tedavisi yaklaşımları klinik deneylerde umut verici sonuçlarla ilham kaynađı olmaktadır fakat NK hücrelerinde genetik deđişiklik yöntemleri henüz ideal koşullara ulaşmamıştır. NK hücreleri lentiviral gen aktarımına diđer bađışıklık sistemi hücrelerine kıyasla yüksek direnç gösterirler. Geçmiş çalışmalar Toll-benzeri almaçlar ve RIG-I-benzeri almaçların sinyal yolaklarının aşağısındaki TBK1/IKKepsilon çiftinin küçük molekül inhibitörü BX795'in lentiviral gen aktarımı sırasında kullanımının NK hücrelerinde anlamlı verim artışına yol açtığını göstermiştir. Bu çalışma NK hücrelerine viral vektörlerin girişinde büyük sorunlar yaşanmadığını, fakat virüs karşıtı sinyallerin aktifleşmesi sonucu hücreiçi viral vektörlerin elenmesinin gerçekleştiđini göstermiştir. Bu yanıtta payı olan 20 aday genin rollerini araştırmak için CRISPR/Cas9 sistemi kullanılmış ve bu genler 293FT ve NK-92 hücre hatlarında mutasyona uğratılmıştır. Bizim sonuçlarımız virüsün kılıf bölgesinin 293FT hücrelerinde TRIM5alfa tarafından algılanmasının ve çift-sarmal RNA bazlı sinyallerin NK-92 hücrelerinde RIG-I ve TRIM25 üzerinden algılanmasının lentiviral gen aktarımına karşı dirençte önemli roller oynadıklarını göstermektedir. Buna ek olarak, viral vektöre maruz kalan hücrelerde MAPK aktivitesinde, özellikle vahşitip HIV enfeksiyonlarında görüldüğü gibi NK-92 hücrelerinde p38 ve JNK fosforilasyonunda artış olduđu gözlemlenmiştir. Sonuç olarak, bu çalışma lentiviral gen aktarımının NK hücrelerinde çeşitli kalıp tanıma reseptörleri tarafından dođuştan gelen bađışıklık sistemini uyardığını onaylamıştır. Genetiđi deđiştirilmiş NK hücrelerinin immün tedavide umut vaadeden uygulamaları için küçük molekül inhibitörlerinin kullanımı engelleri aşmaya yardımcı olacaktır.



To my family...

Canım aileme...

ACKNOWLEDGEMENTS

I would like to start by expressing my gratitude to my thesis advisor Prof. Dr. Batu Erman for years of great teaching and brainwashing me to become an immunologist. Without him, I would not have thought about getting a master's degree in this field that I now love and cherish and continue with a PhD degree so dedicated to state-of-the-art trends of the world of molecular biology. I am forever grateful for this opportunity to become a member of his research lab, for endless hours of scientific discussions and professional support that I always received and hope to continue in the future.

I would also like to thank the esteemed members of my thesis jury, Prof. Dr. O. Ugur Sezerman and Prof. Dr. Zehra Sayers for always showing their support and ever welcoming approach whenever I needed their help and guidance; and Prof. Dr. İhsan Gürsel and Prof. Dr. Mayda Gürsel for their valuable feedback and interest in my thesis project and scientific discussions. I also would like to thank Dr. Evren Alici for giving me an opportunity to take part in his lab during my short-term research project and for all helpful scientific input for my project.

I want to express my heartfelt appreciation to my co-advisor Dr. Tolga Sütü for introducing me to the world of NK cells years before I could even think of working in this field, for crossing his path with mine at the most unexpected yet fascinating times and believing in me for building a strong scientific collaboration. Inseparably, I am forever grateful for knowing Dr. Adil Doğanay Duru, who has brought a whole new dimension to my scientific thinking, helped me see the light at the darkest of times, always found a way to put a smile on my face and boosted my confidence at times I needed the most. Without these two amazing friends and scientists, I would not be where I am right now and I believe we are just at the beginning of an exciting journey together.

Great science requires great friendships and I am lucky to have the best colleagues one could ever ask for. I would like to thank all the past and present members of Ermanlab and Sutlulab for giving me such great memories: Dr. Emre Deniz, Dr. Nazlı Keskin, Dr. Bahar Shamloo, Şeyda Temiz, Gülperi Yalçın, Tuğçe Altınuşak, Asma Al Murtadha, Sofia Piepoli, Ahsen Özcan, Ronay Çetin, Hakan Taşkıran, Melike Gezen, Nazife Tolay, Sarah Barakat, Ilgın Kolabaş, Dr. Esen Doğan, Ayhan Parlar, Didem Özkazanç, Aydan Saraç, Cevriye Pamukçu, Mertkaya Aras, Lolai Ikromzoda, Pegah Zahedimaram, Alp Ertunga Eyüpoğlu, Elif Çelik and Hazal Şentürk. Among these great people, I would especially like to show my sincerest appreciation to Emre and Nazlı for teaching me everything they knew with patience and kindness in my first years; and for continuous help and friendship over the following years. I am forever grateful to the day Hazal started working with me and lightened my burden with the sweetest company; the day Ayhan came to be a part of our lab and brought joy into my routine; the day Didem showed up and chose us to continue her path, spent endless hours with me in a few square-meters of cell culture room and always came smiling with great songs when we had countless hours of work to do; the day Ronay came into our lives with all the tech support and put smiles on our faces even at hardest times; the day I picked that desk and enjoyed the desk-mate title with Şeyda, Bahar and Hakan over the years... We had countless great memories and I hope to continue for many more years to come.

One can get lonely and depressed quite more than anyone can imagine during a PhD and I am lucky enough to have the greatest friends who have helped me get through the toughest times. I can confidently say that the friendship of Dr. Beyza Vuruşaner is one of the best presents I gained in my Sabancı grad life. I am forever grateful to Işıl Demir, who I miss and long for the most, for being an inseparable part of my life even from miles away and with hours of time difference, always providing me help and relief. I am equally grateful to Emre Eminoğlu, Faysal Altunbozar, Emirhan Yaltı, İrem Güre, Fahri Demir, Aslıhan Evrensel, Zeynep Paker, Zeynep Serim, Merve Ardil and Seda İlhan who have endured my suffering throughout my studies and brought joy into my life. I would like to thank all of you for all the love and happiness you bring into my world with a short coffee break, a picture, a gift, a text or simply with your presence. I would also like to thank my undergraduate classmates and long-distance role models Dr. İdil Orhon and Dr. İdil Ülengin for setting examples of great women in science.

This PhD could not have been possible without my dearest family, providing me the biggest love and support one can ever wish for. I would like to give my heart-felt gratitude for my mother Nilgün and father Nusret Sayitođlu, my ever-loving sister Aslı and brother-in-law Eren iekdađı, my dearest grandma Gölseren Yıldırım, Emre-Gölgün-İrem-Ecem Günebakan and of course the littlest Ela iekdađı for being the most amazing family in the world, I love you all to the moon and back and I thank you for believing in me and enduring me through my years of struggle in science.



* This thesis was supported by TUBITAK 2232 grant “Novel Approaches in Viral Gene Delivery” Grant Number 114C131. Canan Sayitođlu’s scholarship has been supported by TUBITAK 1001 grants “Identification of New Factors Controlling p53 and the DNA Damage Response in T lymphocytes” Grant Number 11T401; “Investigation of the IL7 Cytokine Receptor (IL7R) Gene Control Mechanism” Grant Number 109T315; and TUBITAK 3501 grant “NK Cell-derived Exosomes as a Nanomedicine Approach in Cancer Immunotherapy” Grant Number 114Z343.

TABLE OF CONTENTS

1. INTRODUCTION.....	1
1.1. Natural Killer Cells of The Immune System.....	1
1.1.1. Description and origin.....	1
1.1.2. Subtypes.....	2
1.1.3. Effector mechanisms.....	3
1.2. NK-92 Cell Line.....	6
1.2.1. Description and origin.....	6
1.2.2. Applications in clinical trials.....	6
1.3. NK Cell Genetic Modification for Uses in Immunotherapy.....	8
1.3.1. Brief history of gene therapy.....	8
1.3.2. Lentivirus.....	11
1.3.3. Lentiviral vectors.....	15
1.3.4. Strategies and examples of NK cell genetic modifications.....	20
1.4. Innate Anti-Viral Immune Response and Signaling.....	22
1.4.1. Pattern recognition receptors (PRRs) in anti-viral signaling.....	22
1.4.1.1. Toll-like receptors (TLRs).....	22
1.4.1.2. C-type lectin receptors (CLRs).....	24
1.4.1.3. NOD-like receptors (NLRs).....	24
1.4.1.4. RIG-I-like receptors (RLRs).....	24
1.4.1.5. Cytoplasmic RNA/DNA sensors.....	26
1.4.1.6. Cellular restriction factors.....	27
1.4.2. Transcription factors involved in anti-viral response.....	29
1.5. CRISPR/Cas9-Mediated Genome Editing.....	32
1.5.1. History and mechanism of genome editing.....	32

1.5.2. Genome-wide approaches with the GeCKO library.....	34
2. AIM OF THE STUDY.....	36
3. MATERIALS AND METHODS.....	38
3.1. Materials.....	38
3.1.1. Chemicals.....	38
3.1.2. Equipment.....	33
3.1.3. Buffers and solutions.....	38
3.1.4. Growth media.....	39
3.1.5. Commercial kits used in this study.....	40
3.1.6. Enzymes.....	40
3.1.7. Antibodies.....	40
3.1.8. Bacterial strains.....	40
3.1.9. Mammalian cell lines.....	41
3.1.10. Plasmids and oligonucleotides.....	41
3.1.11. DNA ladder.....	47
3.1.12. DNA sequencing.....	47
3.1.13. Software, computer-based programs and websites.....	47
3.2. Methods.....	49
3.2.1. Bacterial cell culture.....	49
3.2.2. Mammalian cell culture.....	50
3.2.3. CRISPR design and assembly.....	55
3.2.4. GeCKO v.2 library transduction work flow.....	59
4. RESULTS.....	63
4.1. Optimizing Lentiviral Transduction Parameters in NK Cell Lines.....	63
4.1.1. Optimization of transduction time.....	64
4.1.2. MOI titration.....	65
4.1.3. BX795 dose titration and toxicity determination.....	66
4.1.4. The reversibility of BX795 treatment on NK-92 cells.....	68
4.1.5. Scaling up the transduction protocol.....	69
4.1.6. Serum-free growth of NK-92 cells.....	71
4.1.7. The role of cytokines on lentiviral transduction efficiency.....	72
4.2. The Dynamics of Signals Triggered by Viral Vector Entry in NK-92 Cells.....	74
4.2.1. Intracellular elimination of lentiviral vector.....	74

4.2.2. Analysis of signaling events triggered by viral vector entry.....	76
4.3. Targeting Candidate Genes in 293FT and NK-92 Cell Lines by CRISPR/Cas9-Mediated Genome Editing.....	82
4.3.1. Targeting genes in the 293FT cell line.....	82
4.3.2. Targeting genes in the NK-92 cell line	86
4.4. Preliminary Results for Future Directions.....	89
4.4.1. A p38 inhibitor: a twisted player in anti-viral signaling.....	89
4.4.2. Genome editing using the GeCKO library in NK-92 cells.....	91
4.4.2.1. Transduction, selection and expansion of GeCKO ⁺ NK-92 cells..	91
4.4.2.2. Transduction of GeCKO ⁺ NK-92 populations with LeGO-G2...	92
5. DISCUSSION.....	95
6. CONCLUSION.....	106
REFERENCES.....	107
APPENDIX A: Chemicals Used in This Study.....	125
APPENDIX B: Equipment Used in This Study.....	126
APPENDIX C: Commercial Kits Used in This Study.....	127
APPENDIX D: Antibodies Used in This Study.....	127
APPENDIX E: DNA Ladder.....	127
APPENDIX F: Plasmid Maps.....	128
APPENDIX G: Sequencing Results.....	129
APPENDIX H: CRISPR Target Sites.....	132
APPENDIX I: Immune Cell Signaling Array Results.....	137

LIST OF FIGURES

Figure 1.1. Hematopoiesis and branching of the immune system.....	2
Figure 1.2. NK cell effector mechanisms.....	5
Figure 1.3. Vectors used in gene therapy clinical trials.....	8
Figure 1.4. Examples of commonly used gene delivery systems.....	9
Figure 1.5. HIV-1 structure and genome organization.....	12
Figure 1.6. HIV-1 and lentiviral vector life cycles.....	14
Figure 1.7. Lentiviral vector systems.....	16
Figure 1.8. Lentiviral vector production with 1 st , 2 nd and 3 rd generation vector systems.....	19
Figure 1.9. TLRs and their ligands.....	23
Figure 1.10. RLR signaling.....	26
Figure 1.11. Important signaling pathways activated in anti-viral response.....	31
Figure 1.12. CRISPR/Cas9-mediated genome editing.....	33
Figure 3.1. Sample analysis for virus titer determination.....	52
Figure 3.2. Immune cell signaling array template.....	54
Figure 3.3. GeCKO v.2 library PCR1 and PCR2 strategy.....	61
Figure 3.4. GeCKO v.2 library work flow.....	62
Figure 4.1. Transduction timeline and LeGO-G2 lentiviral construct.....	64
Figure 4.2. NK-92 transduction sample analysis.....	64
Figure 4.3. NK-92 transduction time determination.....	65
Figure 4.4. NK-92 transduction MOI titration.....	66

Figure 4.5. BX795 dose titration during transduction.....	67
Figure 4.6. BX795 toxicity assay with Annexin V/PI staining.....	67
Figure 4.7. The effect of BX795 pre-treatment on NK-92 transduction efficiency.....	68
Figure 4.8. Transduction size comparison and Puromycin selection of NK-92 cells.....	70
Figure 4.9. Serum-starvation and transduction comparison of normal and serum-free grown NK-92 cells.....	72
Figure 4.10. The effect of cytokines added during transduction.....	73
Figure 4.11. The effect of BX795 on intracellular elimination of viral vector in NK-92 cells.....	75
Figure 4.12. Immune cell signaling array with 30-minute IL-21 or IFN α and IFN β treatment.....	77
Figure 4.13. Time-course expression levels of selected proteins from immune cell signaling array.....	79
Figure 4.14. Immune cell signaling array with 30-90 minute-transductions normalized to control (average of two independent experiments).....	80
Figure 4.15. Intracellular flow cytometry with STAT3 P-Ser727, RIG-I and IRF7 P-Ser 477/479 antibodies.....	81
Figure 4.16. RFLP and transduction of 293FT CRISPR/Cas9-modified single cell clones.....	83
Figure 4.17. 293FT lentiCRISPR-transduced cell lines show changes in lentiviral gene delivery.....	85
Figure 4.18. NK-92 lentiCRISPR-transduced cell lines show changes in lentiviral gene delivery.....	87
Figure 4.19. Sequencing of DDX58-lentiCRISPR ⁺ NK-92 genomic DNA pool containing the CRISPR binding site.....	88
Figure 4.20. The role of p38 α inhibitor VX745 when added during transduction of NK-92 cells.....	90
Figure 4.21. GeCKO library timeline.....	92
Figure 4.22. LeGO-G2 transduction of GeCKO ⁺ NK-92 cells.....	93
Figure 4.23. GFP expression of sorted GeCKO ⁺ NK-92 cells.....	94
Figure 5.1. Proposed model for signaling events triggered upon lentiviral vector delivery in NK cells.....	105
Figure E1. 10 kb Gene Ruler DNA Ladder Mix.....	127
Figure F1. The vector map of LeGO-G2.....	128

Figure F2. The vector map of lentiCRISPRv2.....	128
Figure G1. Sequencing results of lentiCRISPR constructs.....	129
Figure H1. DDX58 (lentiCRISPR design) genomic DNA region.....	132
Figure H2. DDX58 (pspCas9(BB) design) genomic DNA region.....	133
Figure H3. IFIH1 (pspCas9(BB) design) genomic DNA region.....	134
Figure H4. TBK1 (pspCas9(BB) design) genomic DNA region.....	135
Figure H5. TRIM5 α (pspCas9(BB) design) genomic DNA region.....	136
Figure I1. Immune cell signaling array with 15-, 30- and 90-minute transductions....	137
Figure I2. Immune cell signaling array with 15-, 30- and 90-minute-transductions normalized to control.....	138
Figure I3. Immune cell signaling array with 30- and 90-minute transductions.....	139
Figure I4. Immune cell signaling array with 30- and 90-minute transductions normalized to control.....	140

LIST OF TABLES

Table 1.1. Features of viral vectors commonly used in gene therapy.....	10
Table 1.2. List of genetic manipulations in primary NK cells and NK cell lines for therapeutic approaches.....	21
Table 1.3. Features of GeCKO library.....	35
Table 3.1. Complete list of plasmids used in this study.....	41
Table 3.2. Complete list of primers and oligonucleotides used in this study.....	44
Table 3.3. Complete list of software and programs.....	48
Table 4.1. 293FT CRISPR/Cas9-modified single cell clones.....	83

LIST OF SYMBOLS AND ABBREVIATIONS

α	Alpha
β	Beta
γ	Gamma
κ	Kappa
μ	Micro
AAV	Adeno-associated virus
ADCC	Antibody-dependent cellular cytotoxicity
Amp	Ampicillin
AP-1	Activator Protein-1
APOBEC3	Apolipoprotein B Editing Complex 3
Arg	Arginine
bp	Basepair
CA	Capsid
CAR	Chimeric Antigen Receptor
CARD	Caspase Activation and Recruitment Domain
Cas	CRISPR-associated
CD	Cluster of Differentiation
CDN	Cyclic dinucleotide
CIAP	Calf Intestine Alkaline Phosphatase
cGAMP	cyclic AMP-GMP
cGAS	cyclic AMP-GMP synthase
CMV	Cytomegalovirus
CLR	C-type Lectin Receptor
cPPT	Central Polypurine Tract
CRISPR	Clustered Regularly Interspaced Short Pallindromic Repeats
CTL	Cytotoxic T Lymphocyte
CypA	Cyclophilin A
Cys	Cysteine
DAI	DNA-dependent Activator of IFN-regulatory factors
DC	Dendritic Cell
DMEM	Dulbecco's Modified Eagle Medium
DMSO	Dimethylsulfoxade
ds	Double-stranded
DSB	Double-stranded break
DTT	dithiothreitol
E.coli	Escherichia coli

EDTA	Ethylenediaminetetraacetic acid
Env	Envelope
FACS	Fluorescence Activated Cell Sorting
FBS	Fetal Bovine Serum
Gag	Group-specific antigen
GAS	Interferon-gamma-activated site
GeCKO	Genome-scale CRISPR Knock-Out
GFP	Green Fluorescent Protein
GOI	Gene-of-interest
gRNA	guide RNA
HDAC	Histone Deacetylase
HDR	Homology-directed repair
HEPES	4-(2-hydroxyethyl)-1-piperazineethanesulfonic acid
HIV	Human Immunodeficiency Virus
HLA	Human Leukocyte Antigen
HSV	Herpes Simplex Virus
IFI16	IFN-gamma-inducible protein 16
IFIH1	Interferon-induced with Helicase C domain-1
IFIT1	Interferon-induced Protein with Tetratricopeptide Repeats 1
IFN	Interferon
I κ B	Inhibitor of κ B
IKK	Inhibitor of κ B Kinase
IL	Interleukin
IN	Integrase
IRF	Interferon Regulatory Factor
ISG	Interferon-Stimulated Gene
ISRE	Interferon-Sensitive Response Element
ITAMs	Immunoreceptor Tyrosine-based Activation Motifs
ITIMs	Immunoreceptor Tyrosine-based Inhibition Motifs
JNK	c-Jun N-terminal Kinase
Kan	Kanamycin
KIR	Killer-cell Immunoglobulin-like Receptor
LB	Luria Broth
LDLR	Low-density lipoprotein receptor
LGP2	Laboratory of Genetics and Physiology 2
LTR	Long Terminal Repeat
LPS	Lipopolysaccharide
MA	Matrix
MAPK	Mitogen-Activated Protein Kinase
MAVS	Mitochondrial Antiviral Signaling
MDA5	Melanoma Differentiation-Associated Protein 5
MHC	Major Histocompatibility Complex
MICA	MHC class I chain-related molecule A
miRNA	micro RNA
MOI	Multiplicity of Infection
NEAA	Non-essential Amino Acid
NC	Nucleocapsid
Nef	Negative effector
NF- κ B	Nuclear Factor kappa B
NGS	Next Generation Sequencing

NHEJ	Non-homologous End Joining
NK	Natural Killer
NLR	NOD-like Receptor
NLRP3	NOD-, LRR- and pyrin domain-containing 3
NOD	Nucleotide-binding Oligomerization Domain
OAS	2'-5' oligoadenylate synthase
ODN	Oligonucleotide
PAM	Protospacer Adjacent Motif
PBMC	Peripheral Blood Mononuclear Cell
PBS	Phosphate Buffered Saline
PCR	Polymerase Chain Reaction
PEI	Polyethylenimine
PI	Propidium Iodide
PI3K	Phosphoinositide 3-kinase
PIPES	piperazine-N,N'-bis (2-ethanesulfonic acid)
PKR	Protein Kinase R
PLL	Poly-L-lysine
Pol	Polymerase
PR	Protease
Puro	Puromycin
qRT-PCR	quantitative Reverse-Transcription PCR
RCR	Replication-competent Retrovirus
Rev	Regulator of virion gene expression
RFLP	Restriction Fragment Length Polymorphism
RIG-I	Retinoic acid-inducible Gene-I
RLR	RIG-I-like Receptor
RPMI	Roswell Park Memorial Institute
RRE	Rev Response Element
RT	Reverse-Transcriptase
RT	Room Temperature
SCGM	Stem Cell Growth Medium
SCID-X1	X-linked Severe Combined Immunodeficiency
SD	Standard Deviation
SEM	Standard Error of Mean
Ser	Serine
SFFV	Spleen Focus Forming Virus
SHP1	Src homology region 2 domain-containing phosphatase-1
SIN	Self-inactivating
siRNA	small interfering RNA
SLTs	Secondary Lymphoid Tissues
SNP	Single Nucleotide Polymorphism
ss	Single-stranded
STAT	Signal Transducer and Activator of Transcription
STING	Stimulator of Interferon Genes
SU	Surface Glycoprotein
TAK1	Transforming Growth Factor Beta-Activated Kinase-1
TALEN	Transcription Activator-like Effector Nuclease
Tat	Trans-activator
TBE	Tris Borate EDTA
TBK1	TANK Binding Kinase-1

TCR	T-cell Receptor
TLR	Toll-like Receptor
TM	Trans-membrane Glycoprotein
TNF	Tumor Necrosis Factor
TRAIL	TNF α -Related Apoptosis-Inducing Ligand
TRIM	Tripartite Motif
Tyr	Tyrosine
Vif	Viral infectivity factor
Vpr	Viral protein r
Vpu	Viral protein u
VRE	Virus Response Elements
wPRE	Woodchuck hepatitis virus post-transcriptional regulatory element
WT	Wild Type
ZFN	Zinc-finger Nuclease



1. INTRODUCTION

1.1 Natural Killer Cells of The Immune System

1.1.1 Description and origin

The immune system (mainly separated into two branches as innate and adaptive immunity) consists of several different components responsible for fighting various intrinsic or extrinsic threats. The term ‘adaptive’ refers to T and B lymphocytes as well as other cellular components and soluble factors that act upon recognition of specific molecules found on pathogens. The term ‘innate’ commonly refers to cells or humoral components of the immune system that mainly rely on the recognition of non-self and danger-associated molecular patterns rather than antigen-specific recognition of pathogens.

Natural killer (NK) cells, identified first in the 1970s (Herberman et al., 1975; Kiessling et al., 1975), are members of the lymphoid lineage, just like T and B lymphocytes, but belong to the innate family of immune cells (Figure 1.1). This rather unexpected classification is derived from the potential of NK cells to exert cellular cytotoxicity without prior stimulation or immunization, upon recognition of ‘missing-self’, a milestone in NK cell history proposed by Kärre in 1980s (Kärre, 2002; Kärre, 2008; Ljunggren & Kärre, 1990). NK cells fill a hole left out from adaptive immunity; recognizing and killing cells like various cancer types and virus-infected cells that

downregulate the major histocompatibility complex (MHC) (Human Leukocyte Antigen (HLA) in humans) molecules at the cell surface and are in turn capable of escaping recognition by T cells.

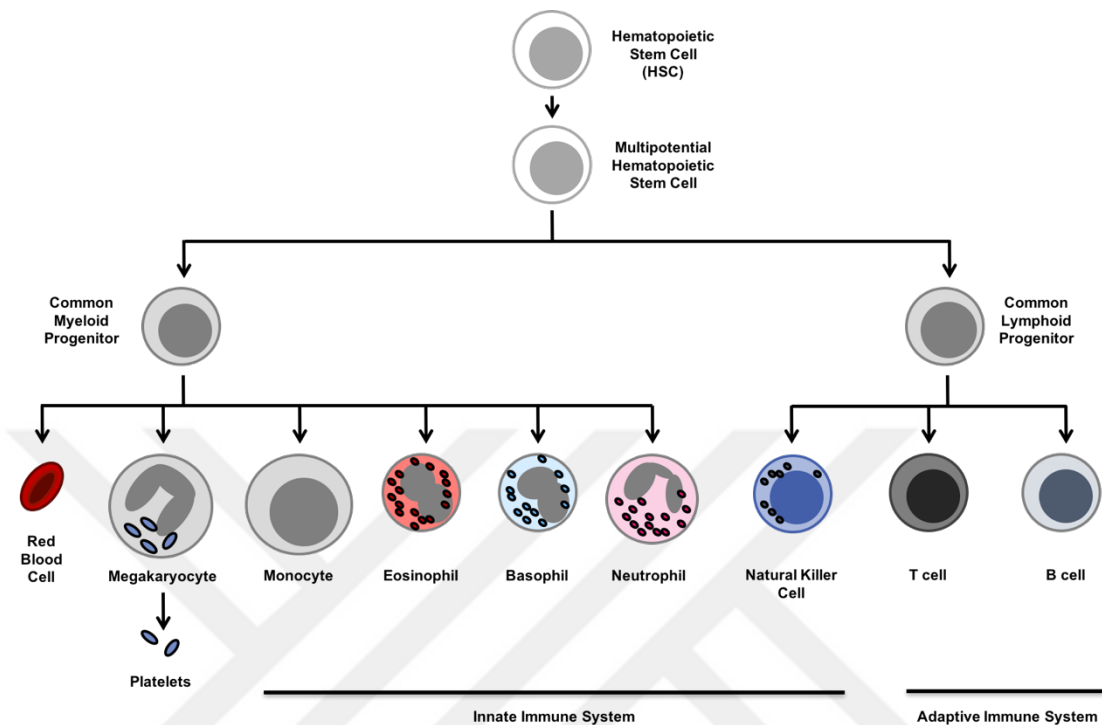


Figure 1.1. Hematopoiesis and branching of the immune system. Hematopoietic Stem Cells (HSCs) that are found in the bone marrow give rise to the two major cell types, myeloid and lymphoid progenitors. Common myeloid progenitors further give rise to red blood cells and platelets as well as members of the innate immune system except for NK cells. NK cells share the lymphoid lineage with adaptive immune system members, T and B cells.

1.1.2 Subtypes

NK cells in humans are characterized as $CD3^-CD56^+$ and are primarily developed in the bone marrow and found in blood, skin, lungs, liver, spleen and lymph nodes (Gregoire et al., 2007). Different NK cell subsets are found in inflamed and malignant tissues and secondary lymphoid tissues (SLTs). In human peripheral blood, more than 90% of NK cells are categorized into the $CD56^{dim}CD16^+$ subset and have higher cytolytic activity with high expression of killer-cell immunoglobulin-like receptors (KIRs) and/or CD94/NKG2A; and less than 10% are categorized into the $CD56^{bright}CD16^-$ subset that have CD94/NKG2A but lack the KIR expression, and secrete $TNF\alpha$ and $IFN\gamma$ upon

activation, acting more as regulatory cells (De Maria et al., 2011; Ferlazzo et al., 2004). Upon contact with fibroblasts, the CD56^{bright}CD16⁻ subset of NK cells can differentiate into CD56^{dim}CD16⁺ cells with high cytolytic activity (Chan et al., 2007).

First developed in the bone marrow, NK cell precursors mature and express different chemokine receptors that are able to direct NK cells to different tissues in the body (Lysakova-Devine & O'Farrelly, 2014). One of these receptors, CCR7, is found predominantly on the CD56^{bright}CD16⁻ subset of NK cells helps the recruitment of these cells to the secondary lymphoid tissues (Campbell et al., 2001). Resting NK cells can be recruited to the site of inflammation during viral or bacterial infections or to the site of tumor formation again by the help of pro-inflammatory chemokines (such as CCL3/MIP1- α or CCL5/RANTES) (Bernardini et al., 2016). Once at the site of encounter with target cells, NK cells get activated via several activating receptors and cytokines triggering effector functions that will be briefly explained in the next section (Pesce et al., 2016).

1.1.3 Effector mechanisms

The importance of NK cells in the host immune response is underlined in cases of NK cell deficiencies where the patient suffers from fatal infections mostly through childhood (Orange & Ballas, 2006). NK cells can detect lowered levels of MHC class I expression on transformed cells like tumors, as well as stress signs like DNA damage and instability as these also cause upregulation of stress-induced ligands of NK cell activating receptors on tumor cells (Raulet & Guerra, 2009).

NK cells have several inhibitory and activating receptors that mediate the interaction with a target cell. The inhibitory receptors have cytoplasmic immunoreceptor tyrosine-based inhibition motifs (ITIMs) and they either belong to the immunoglobulin superfamily or the C-type lectin domain family (Krzewski & Strominger, 2008). In humans, the binding of inhibitory receptors to classical MHC I ligands (HLA-A, -B, -C) is known to induce signals via the Src homology region 2 domain-containing phosphatase-1 (SHP1, also known as PTPN)-mediated phosphorylation of ITIMs (Binstadt et al., 1996) (Figure 1.2).

Activating receptors such as CD16, NKp30, NKp44 and NKp46 couple with immunoreceptor tyrosine-based activation motif (ITAM)-bearing molecules DAP12 and FcR γ -CD3 ζ in their cytoplasmic region while others like NKG2D, 2B4 and CD2 signal through non-ITAM-bearing DAP10 (Smyth et al., 2002). The ligands of activating receptors contain stress-induced molecules like MHC class I chain-related molecule A (MICA) expressed on transformed cells, and the non-classical MHC Ib (HLA-E) ligand which has a distinct transcription pattern from the classical MHC molecules (O'Callaghan, 2000). Upon binding of an activating ligand, ZAP70/SYK or PI3K pathways are turned on to lead the activation of the NK cell (Smyth et al., 2002).

A combination of signals from activating and inhibitory receptors shape NK cell effector functions as well as the fate of the target cells. If activating signals are more dominant, signaling events give rise to the polarization and exocytosis of granules containing perforin and granzyme; perforin making pores on the target's membrane and granzyme upon entering through these pores activating the caspase-cascade that leads to target cell apoptosis (Bryceson et al., 2006; Voskoboinik et al., 2006).

CD16 is another activating receptor that is found on NK cell surface binding to the constant (Fc) region of immunoglobulin, which results in the release of cytolytic granules and death of the target cell. Fc receptors (CD16) enable immune cells detect target specific antibody-coated transformed targets. This mechanism of action is known as antibody-dependent cellular cytotoxicity (ADCC) that can be manipulated for fighting autoimmunity and cancer immunotherapy. Many monoclonal antibody treatments have been studied for a variety of cancers (reviewed in Sliwkowski & Mellman, 2013) that could potentially increase ADCC. Examples include anti-CD20, anti-Her2, anti-CD52, anti-EGFR and anti-CD38 (James et al., 2013) that show promising results for NK cell-mediated elimination of tumors both *in vitro* and *in vivo*.

In addition to inducing apoptosis in target cells via degranulation triggered after activating receptor engagement, NK cells also kill by contact-mediated mechanisms. Fas ligand (FasL) and TNF α -related apoptosis-inducing ligand (TRAIL) on the NK cell surface are known as death receptors and their ligands Fas and TRAILR found on tumor or transformed cells induce apoptosis in the target cell (Medvedev et al., 1997). The immunosuppressive microenvironment of a tumor can lead to downregulation of activating receptors through cytokine secretion (Jinushi et al., 2005; Konjević et al.,

2007). Therefore, it is essential that NK cells can also induce apoptosis in tumor cells with the engagement of death receptors found on the NK cell surface, providing an alternative mechanism for targeting of tumor cells especially in cases where other receptors are shed or NK cell activating receptors are downregulated (Lundqvist et al., 2006).

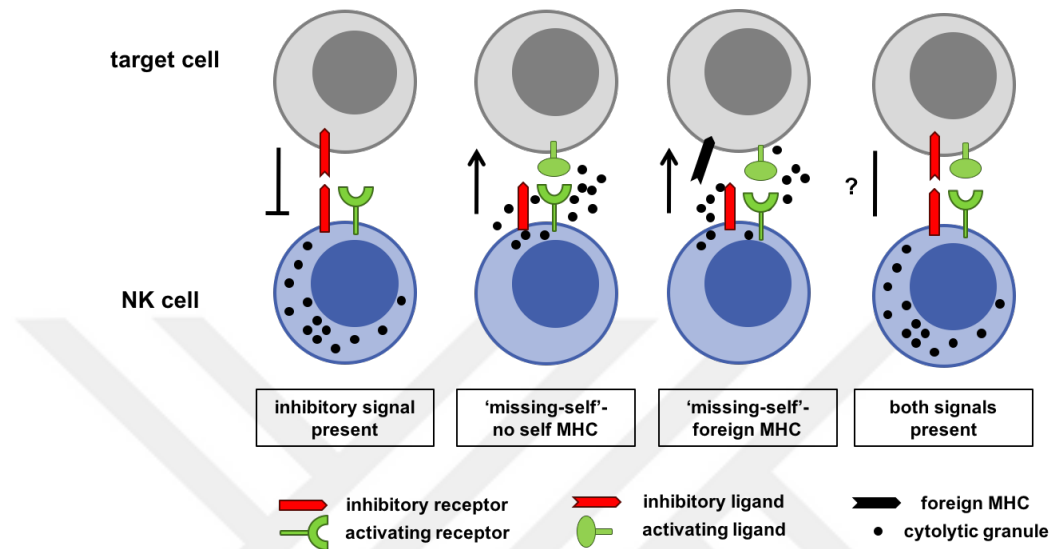


Figure 1.2. NK cell effector mechanisms. When NK cell meets a target, if the only signal received is from an inhibitory ligand (most abundantly self-MHC molecules) engagement to inhibitory receptors, the target is protected from lysis (left-most). If the inhibitory signal is absent, and there is an activating signal, the target cell is killed (middle two). This is usually the case when there is low level of MHC molecules on the surface, and this phenomenon of NK cells recognizing MHC low/absent cells is known as ‘the missing-self recognition’. In the allogeneic setting, a cell with foreign MHC can also be a target for NK cell lysis. When both signals are present, the fate of the target cell is determined by the dominant signal (right-most).

Most of the events taking place during an immune response eventually link innate and adaptive immune systems via contact-mediated interactions between immune cells or soluble factors such as cytokines. When NK cells are recruited to the site of inflammation or tumor, their activation results in production of cytokines like IFN γ and TNF α (Gerosa et al., 2005). The production of IFN γ may result in the recruitment of DCs to the site of inflammation or tumor, and contribute to the differentiation of CD4⁺ T cells towards a T_H1 profile. NK-DC crosstalk based on costimulatory molecule interactions can have different outcomes for the NK cells and DCs; causing activation and maturation in a bi-directional way (Gerosa et al., 2005). This crosstalk is strictly dependent on the formation

of an immunological synapse between the two cell types (Borg et al., 2004) and also requires DC-derived cytokines, primarily IL-12, IL-15 and IL-18 (Brilot et al., 2007; Ferlazzo, Pack, et al., 2004). Maturation of DCs can be referred to as ‘licensing’ by the NK cells of the inflamed site that results in activated DCs capable of antigen-presentation to T cells. Consequently, these events result in the priming of an antigen-specific cytotoxic T lymphocyte (CTL) response. Therefore, NK cells can act as a crucial link between the innate and adaptive immune responses (Moretta et al., 2008).

1.2 NK-92 Cell Line

1.2.1 Description and origin

NK-92 is an immortal natural killer cell line isolated in the year 1992 from a non-Hodgkin’s lymphoma patient (Gong et al., 1994). The cell line is dependent on IL-2 for survival and is highly cytotoxic against target cells such as K562. They are characterized by high surface expression of CD56 but lack the expression of CD16. NK-92 cells also lack the inhibitory KIR receptor family members (except for low levels of KIR2DL4) and are therefore advantageous in allogeneic immunotherapy since no MHC-mediated inhibition of cytotoxic activity will occur when faced with a target cell. It is much feasible to grow and expand NK-92 cells for clinical applications since they can grow in a feeder-free setting and only require IL-2 for growth. These findings place NK-92 cells as promising candidates for cancer immunotherapy. In fact, NK-92 cells are currently tested in various clinical trials (Suck et al., 2015).

1.2.2 Applications in clinical trials

It is a challenging task to grow and expand NK cells from PBMCs, and even more challenging to genetically modify them. In order to achieve better goals in primary NK

cell immunotherapy, NK-92 cells provide an alternative model system. As of 2016, four phase I clinical trials have been conducted with NK-92 cells in three different countries: Canada, USA and Germany. The patients taking part in these trials have advanced cancers that are treatment-resistant. Taking two or three infusions of NK-92 cells, each 48 hours apart, patients showed significant responses against lung cancer (Tonn et al., 2013), kidney cancer and melanoma (Arai et al., 2008). Compared to the difficulties related to harvesting, modification and expansion of primary NK cells, NK-92 cells have a comparably low cost and higher efficiency in theory.

Potential therapies can be planned by taking advantage of the natural receptor composition of NK-92 cells and combining genetic modifications in the future. Firstly, NK-92 cells do not express the CD16 receptor than can bind to the Fc region of antibodies. Expression of a high-affinity CD16 on NK-92 cells along with treatment with a monoclonal IgG1 antibody against a tumor antigen when used in combination show promising outcomes when applied in preclinical setting. Secondly, chimeric-antigen receptor (CAR) designs specific to a tumor antigen can be transduced to NK-92 cells, resulting in patient- and cancer-specific activation of immune cells (Klingemann et al., 2016). For these approaches to come to life, optimal NK cell-specific gene delivery methods should be developed with high safety and genetic modification efficiency.

In the first trials with retroviral and later lentiviral gene delivery to primary NK cells, transduction efficiencies were around 1-2% in general, now ranging from 20 to 90% with several methods defined, using a combination of cytokines and sometimes making serial transductions with high levels of infectious particles (Imamura et al., 2014; Micucci et al., 2006; Nagashima et al., 1998; Sutlu et al., 2012). In all studies mentioned, the cytolytic profile of NK cells were not altered by genetic modifications. To achieve a high efficiency of primary NK cell transduction, it is essential to develop efficient transduction methods that use minimal amounts of lentiviral vectors. The primary aim of this thesis is to develop techniques to transduce NK cell lines that can be applicable to primary NK cells in the clinic.

1.3 NK Cell Genetic Modification for Uses in Immunotherapy

1.3.1 Brief history of gene therapy

Gene therapy is the method of transferring genetic material into cells in order to modulate or correct faulty gene expression leading to various diseases such as cancer, metabolic disorders or immunodeficiencies. As DNA sequencing technologies have developed, the diseases that are related to defects/mutations in certain genes became potentially correctable with the introduction of healthy genes using gene delivery vectors. If a gene deficiency is causing symptoms as in the case of the blood disorder beta-thalassemia, the correction of the beta-globin gene by gene therapy of hematopoietic stem cells can lead to a repaired hematopoietic system. The outcome of such a gene therapy is the rescue of the beta-thalassemia phenotype by the newly transformed blood cells. It is a tricky task to deliver a gene-of-interest to the cells of a patient with high specificity, low or preferably no side effects and maximum efficiency. The distribution of vectors used in gene therapy clinical trials as of 2016 can be summarized in the figure below:

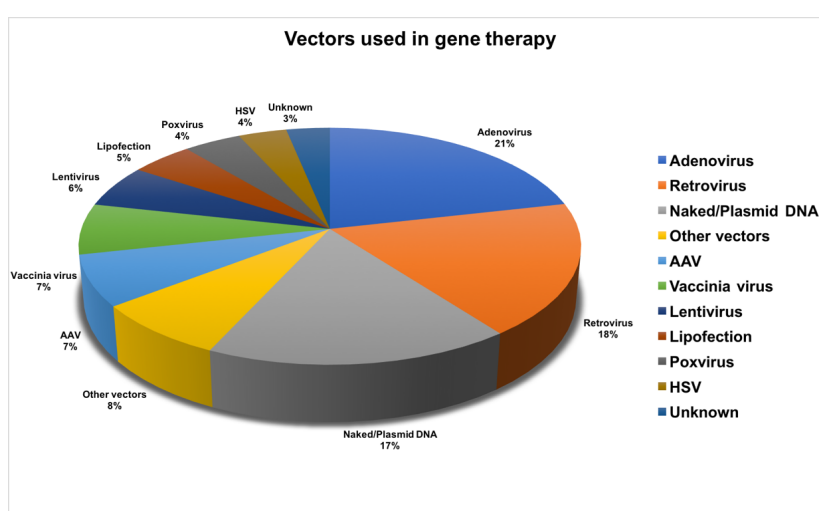


Figure 1.3. Vectors used in gene therapy clinical trials. Information is retrieved from the Journal of Gene Medicine, ©2016 John Wiley and Sons Ltd (updated August 2016).

Since the 1980s, several methods have been developed to increase gene delivery in mammalian cell lines as well as primary cells; however, there are certain obstacles in this process. The genetic material that is introduced to host cells must overcome physical barriers before reaching the nucleus and it is usually one of the major issue resulting in the failure of the gene therapy. There are many factors influencing the stability of cargo and gene expression based on the type of vehicles used for transgene expression (Ibraheem et al., 2014). For introduction of new genes into a mammalian cell, the vehicles used can be classified as non-viral and viral vectors; some major ones schematized in the chart below:

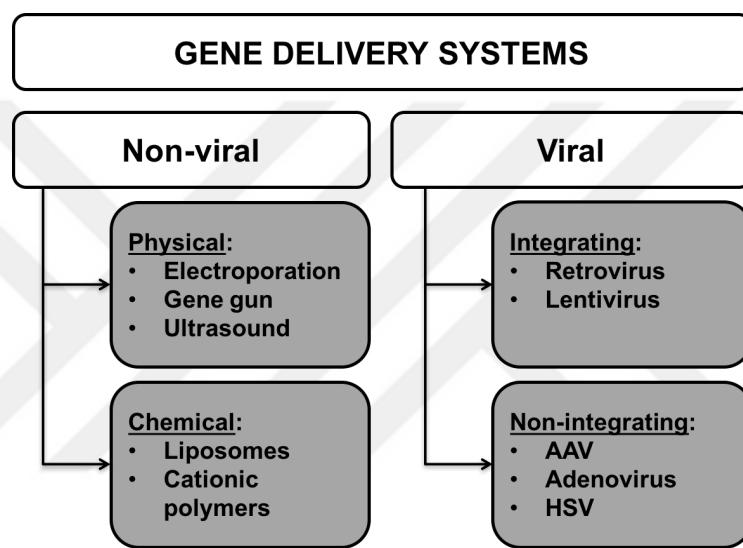


Figure 1.4. Examples of commonly used gene delivery systems.

Non-viral vectors require a mammalian expression cassette delivered as DNA or RNA, that must penetrate through the plasma membrane of the host cell and travel all the way into the nucleus. Once inside the nucleus, the transgene expression depends highly on an intelligent vector design with a strong promoter (usually isolated from virus homologs) and optimized codon sequences with optional accessories like selective markers such as antibiotic resistance genes, fluorescent molecules or tags for protein purification purposes (Gill et al., 2009). The use of non-viral vectors is advantageous in many cases: they are non-pathogenic and they yield high expression of gene-of-interest in a short time with no or low permanent defect in the host cells. However, there are certain barriers that the non-viral vectors need to pass in order to have transgene expression.

First, there are certain limitations of vector delivery due to charge similarity of cell membrane and plasmid DNA. Secondly, naked DNA can only be internalized into the

host cell to a certain extent due to size limitations. Thirdly, getting into the cell is not enough to get transgene expression because nucleases found in the cytoplasm or endosomes of many cell types cause degradation of foreign DNA (Ibraheem et al., 2014). Chemical transfection methods are developed to overcome these barriers, as in the case of cationic polymers such as polyethylenimine (PEI) that form complexes with anionic DNA and make it more stable while increasing uptake by the host cell. However, the increase in transfection efficiency with these reagents might result in cytotoxicity and therefore do not yield the same results in primary cells for gene therapy purposes (Yin et al., 2014). Besides chemical vectors, there are physical methods that result in efficient gene delivery by electroporation, gene gun and ultrasound. For uses in mammalian cells, electroporation methods with brief electric pulses lead to the permeabilization of host cell membranes that causes DNA insertion into the cytoplasm. However, transfection efficiency varies extensively, depending on cell type, size and density; factors which limit the applicability of electroporation in primary cell transfection (Ibraheem et al., 2014).

Compared to non-viral vectors, viral gene delivery is more practical for uses in gene therapy because viruses have naturally evolved to package and deliver essential genetic material in the most efficient way. Still, there are major problems with the natural pathogenicity of viral vectors that need to be thoroughly investigated before use. Many methods have been developed over the years to achieve higher efficiency and safety with these vectors. The features of viral vectors commonly used in past or current gene therapy trials are summarized in Table 1.1.

Virus type	Genetic material	Genome size (kb)	Integration	Key features
Gammaretrovirus	ssRNA	8	Yes	Only infects dividing cells, persistent gene expression
Lentivirus	ssRNA	9	Yes	Infects both non-dividing and dividing cells, persistent gene expression
Adenovirus	dsDNA	30-45	No	Transient high-level gene expression, high immunogenicity
Adeno-associated virus (AAV)	ssDNA	5	No	Long term high-level gene expression, low immunogenicity
Herpes simplex virus (HSV)	dsDNA	150	No	Transient gene expression, difficult to produce

Table 1.1. Features of viral vectors commonly used in gene therapy.

Many factors influence the choice of viral vector for each gene therapy application. Viral vectors that are commonly used in clinical trials can be divided into two groups as non-

integrating and integrating vectors. For long term gene expression in non-dividing cells like neurons, non-integrating vectors are the best choice. Among these type of vectors, AAV and adenovirus are best candidates because they result in transient gene expression; however, adenovirus vectors sometimes suffer from high inflammatory responses (Baker, 2007; Daya & Berns, 2008). On the contrary, integrating viral vectors need to be utilized for gene therapies where continuous gene expression is required as in the case of cells of the hematopoietic lineage. Gammaretroviruses and lentiviruses belong to the family of integrating viral vectors where an RNA genome is packed into the virus particle and reverse-transcribed genetic material is inserted into the host cell genome after infection. Gammaretroviruses lack certain elements that help nuclear import of genomic material so they can only integrate during cell division. Even though they belong to the same family, lentiviruses do not require host cell division and can more readily integrate into the genome (Bukrinsky et al., 1993), thus reaching higher efficiencies of integration in many cell types when used as gene therapy vectors (Sakuma et al., 2012).

Lentiviral vectors that are derived from human immunodeficiency virus (HIV-1) are one of the most promising tools for gene therapy among many other integrating and non-integrating viral vectors (Escors & Breckpot, 2011). Before going through the details of the lentiviral vector design and assembly for uses in gene therapy, lentiviruses will be explained in the following section.

1.3.2 Lentivirus

Lentiviruses are a subgroup of *retroviridae*, which are single-stranded (ss) diploid, sense RNA viruses that use reverse transcriptase to form DNA and insert this synthesized DNA into the host genome for stable viral gene expression. HIV-1 is among the most manipulated pathogenic lentiviruses that are engineered for uses in gene therapy purposes in human hematopoietic cells. A typical lentivirus is almost spherical with a lipid bilayer of the host cell membrane making up the outmost layer, covered with envelope (ENV) protein. Inside, one can find the following proteins: matrix proteins (MA) surround the capsid (CA) that contains the viral RNA genome in complex with nucleocapsid (NC) proteins and essential proteins such as reverse-transcriptase that is required for reverse transcription of RNA genome, integrase (IN) that is required for integration into host

genome and other accessory proteins that block or alter anti-viral responses of the host cell (Figure 1.5A). The genome structure is efficiently ordered in the 5' to 3' direction where three major genes *gag*, *pol* and *env* encode all essential genes. Proteins responsible for structural properties are encoded by the *gag* gene whereas enzymes required for integration, reverse-transcription and HIV-1 life cycle are encoded by the *pol* gene. Envelope proteins are encoded by the *env* gene determine the tropism of the virus (Figure 1.5B).

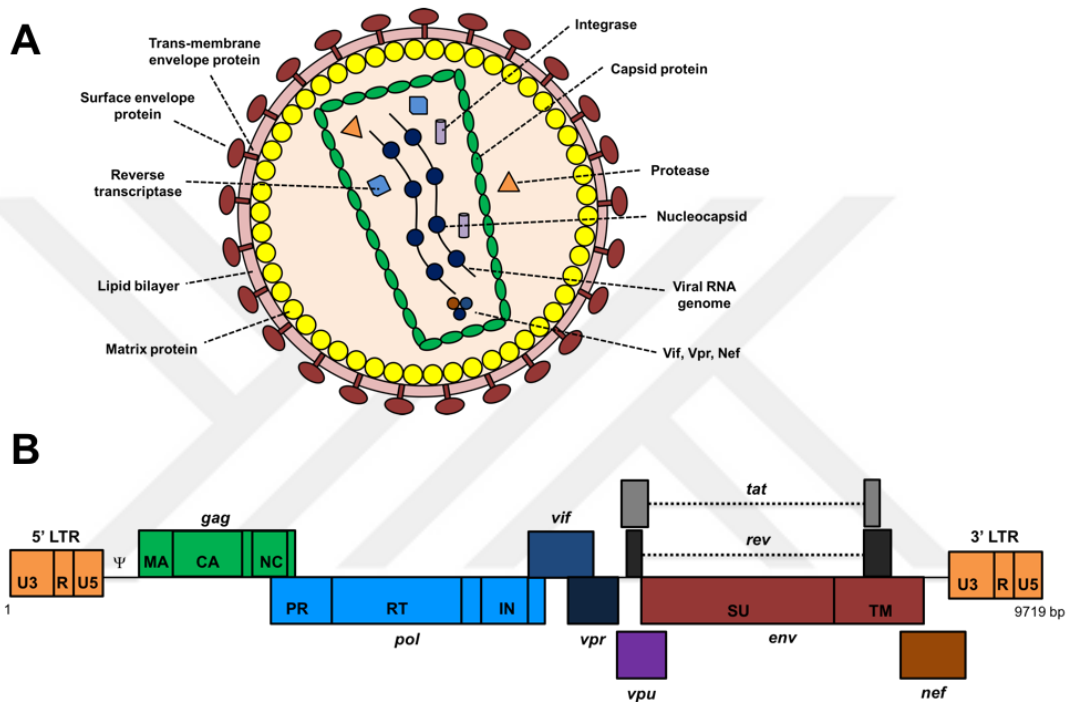


Figure 1.5. HIV-1 structure and genome organization. **(A)** HIV-1 structure can be schematized as shown. **(B)** The viral genome of HIV-1 as seen after integration is enclosed by 5' and 3' Long-terminal repeats (LTRs) where LTR is further subdivided into 3 regions: U3 (promoter), R and U5 acting important roles in transcription and replication. Packaging signal (Ψ) is required for packaging of HIV genome into viral particles. *Gag-pol* and *env* genes encode essential structural proteins, enzymes and envelope proteins respectively. *Vif*, *vpr*, *vpu* and *nef* genes encode accessory proteins. The complete genome size is 9.7 kb as shown on the figure. (MA: matrix, CA: capsid, NC: nucleocapsid, PR: protease, RT: reverse-transcriptase, IN: integrase, SU: surface glycoprotein, TM: trans-membrane glycoprotein, *gag*: group-specific antigen, *pol*: polymerase, *vif*: viral infectivity factor, *vpr*: viral protein r, *vpu*: viral protein u, *env*: envelope, *tat*: trans-activator, *rev*: regulator of virion gene expression, *nef*: negative-effector)

The typical life cycle of HIV-1 starts with docking of surface glycoprotein to CD4 receptor found on helper T cells (T_H cells) of the immune system (Berson et al., 1996; Feng et al., 2011) and to the co-receptor CXCR4 chemokine receptor 4 (CXCR4) found on T cells or CCR5 chemokine receptor 5 (CCR5) found on T cells, macrophages, dendritic cells and microglial cells to a certain extent. Binding of the virus surface protein to its corresponding receptor causes conformational changes in the protein structure that results in membrane fusion and leads to direct entry of the virus particle or entry by endocytosis, releasing the nucleocapsid into the host cell cytoplasm. The capsid structure is highly stable, strengthened by the binding of host protein CypA until the uncoating of the capsid finally releases genomic RNA into the host cell cytoplasm (C. Liu et al., 2016). ssRNA genome of lentiviruses gets reverse-transcribed and translocated to nucleus for integration. Unlike gammaretroviruses, lentiviruses do not require the host cell to go through cell division to have access to genomic DNA because they are already equipped with accessory proteins to translocate synthesized dsDNA through nuclear pores (Bukrinsky et al., 1993; Gallay et al., 1997; Popov et al., 1998).

Once integrated, the viruses take advantage of host cell transcription and translation machinery and start making RNAs and viral proteins required for complete virion assembly. The 5' LTR acts as the enhancer and promoter because it contains binding sites for transcription factors NFAT and NF- κ B abundantly found in activated T cells. The packaging signal found downstream of the 5' LTR maintains the assembly of untranslated ssRNA and viral proteins into mature virion structure. Once transcription is started, Rev binds to the Rev-response element (RRE) found on viral transcripts to manage the export of spliced or non-spliced RNAs (Malim et al., 1989). New viral genome is formed by dimerization of ssRNA copies interacting with Gag proteins on the plasma membrane (J. Chen et al., 2009, 2016). Combining all essential requirements, new viral particles bud off from the host cell's membrane that contains the surface glycoproteins necessary for the next cycle of infection (Sundquist & Kräusslich, 2012) (Figure 1.6 top part).

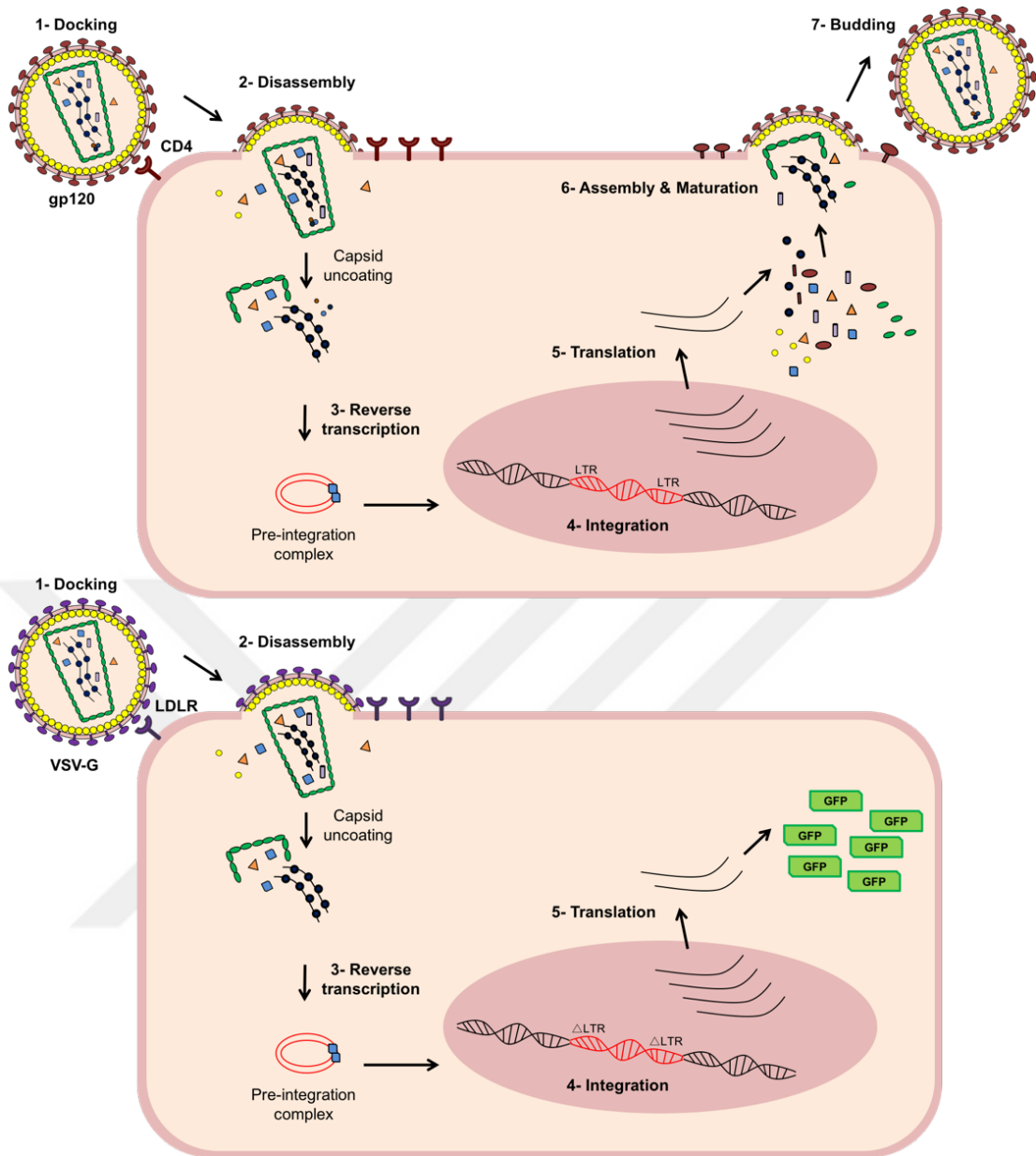


Figure 1.6. HIV-1 and lentiviral vector life cycles. HIV-1 (top) enters the host cell via docking on to the CD4 found on the surface of T_H cells (1). Upon binding to its receptor, conformational changes on the envelope protein leads to fusion of cell membranes and disassembly of viral capsid and proteins (2). Capsid uncoating in cytoplasm releases the RNA genome which then gets reverse-transcribed to form the pre-integration complex (3). Viral genes spanned by the LTRs get integrated into the host cell genome (4) and start producing mRNAs to be used both as the genome of new viral particles and for translation to make the proteins required for the viral life cycle (5). All components come together at the plasma membrane, assembling into the virus structure (6) and bud off from the membrane, later maturing into complete HIV-1 (7). Lentiviral vector (bottom) pseudotyped with VSV-G docks itself to the host cell via the LDLR. The disassembly and reverse transcription occur as above, however; the integrated genetic material contains SIN-LTRs and only expresses the transgene (shown as GFP in this figure). Thus, there are no components found to produce new viral particles.

1.3.3 Lentiviral vectors

The path from naturally occurring HIV to lentiviral vectors required several years of research that led to safer and more efficient design over time. During the course of lentiviral vector production, HEK293 cells are transfected with different plasmids encoding various structural parts of the HIV required to make an infectious particle enclosing the gene of interest. The system we use in the lab is also known as the 3rd generation lentiviral vector system. This process assembles pieces required to make a replication-incompetent virus, that holds a one-way ticket to the cell of interest. Once inside the host cell, lentiviral vectors do get integrated into the genome but are incapable of producing new viral particles, therefore assuring an important level of safety for uses in gene therapy (Figure 1.6 bottom part).

To achieve target-specific gene transfer and reduce the pathogenicity of the virus, several optimizations needed to be completed with 1st, 2nd and 3rd generation of lentiviral vectors (Sakuma et al., 2012). Additionally, envelope proteins are engineered to increase transduction efficiency in a target cell-specific manner and in lentiviral gene therapy the most widely used envelope protein is VSV-G; replacing the CD4-tropism of HIV-1 with low-density lipoprotein receptor (LDLR) expressed on many somatic cells as well as human cell lines (Lévy et al., 2015). VSV-G provides high stability with broad range of targets but when it comes to *in vivo* experiments, human serum is shown to inactivate the VSV-G-pseudotyped viruses so other approaches need to be investigated for clinical use (DePolo et al., 2000).

In the first generation of lentiviral vectors, viral genes except *Env* were cloned into expression plasmids, with a gene-of-interest plasmid enclosed with the LTRs and the packaging signal as found in the wild type virus structure. This was the first attempt for separating viral components to different plasmids. However, all virulent genes were still in the construct, creating a highly pathogenic vector. With the second generation of lentiviral vector system, viral genes were limited to *Gag*, *Pol*, *Rev* and *Tat* and the rest of the system was the same with the 1st generation (Figure 1.7).

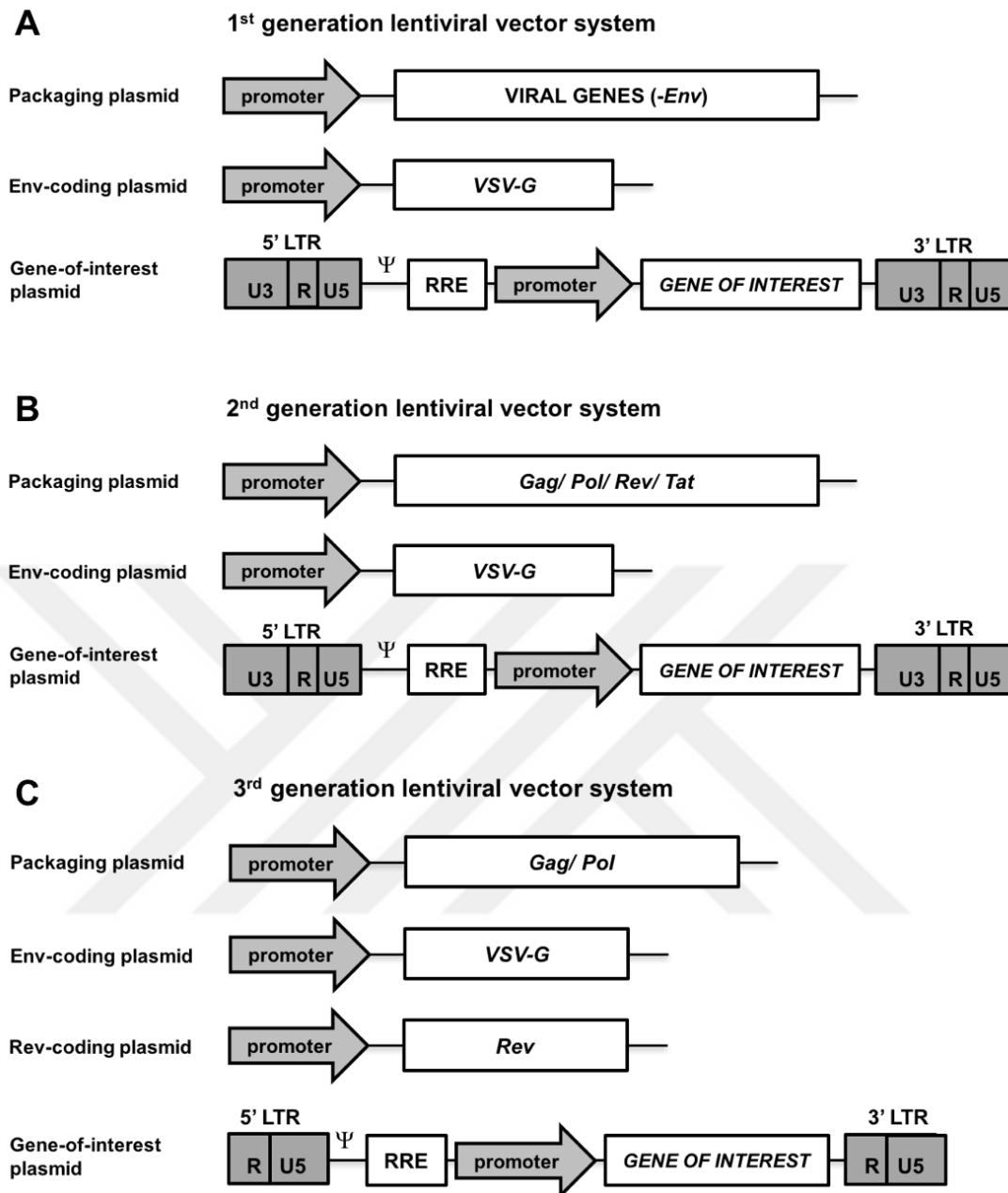


Figure 1.7. Lentiviral vector systems. **(A)** In the 1st generation lentiviral vector system, all viral genes except *Env* were included in the packaging plasmid, still containing all virulent factors. **(B)** In the 2nd generation, packaging plasmid only contained *Gag*, *Pol*, *Rev* and *Tat*. In both 1st and 2nd generation, *VSV-G* plasmid and gene-of-interest plasmids were separate but the LTRs were still intact. **(C)** In the 3rd generation, safety level was maximized by including only *Gag* and *Pol* in the packaging plasmid, and by deleting the U3 region of LTRs in the gene-of-interest plasmid (Sakuma et al., 2012).

Having intact LTRs in the gene-of-interest plasmid creates a high risk of homologous recombination with pre-existing viral components in the cell. In the RNA genome of the wildtype HIV-1, 5'-U3 and 3'-U5 regions are missing; and the RNA is capped by R regions. The copying of the 3'-U3 region to the 5'-LTR occurs right at the reverse transcription stage, prior to the integration of cDNA into the genome. Even though the viral genes are not enclosed by the LTRs in the viral vector, the possibility of complementation by pre-existing viral infections of the host cell could potentially result in a recombination event that results in the creation of replication-competent lentiviruses (RCLs). Studies with retroviral vectors have shown that even 10 bp-long homology regions were enough to end up with replication-competent retroviruses (RCRs) (Otto et al., 1994).

Another major concern regarding the intact LTRs is the issue of LTRs turning on the expression of undesired genes like proto-oncogenes in the host cell that could have drastic effects. In one of the pioneering gene therapy trials for twenty X-linked severe combined immunodeficiency (SCID-X1) patients using gammaretroviral vectors carrying the IL-2 receptor common gamma chain for transduction of CD34⁺ HSCs (Cavazzana-Calvo et al., 2000), results showed positive outcomes that had successful reconstitution of the immune system; however, five of the patients showed serious side-effects related to the vector. Four out of five showed integration of viral vector at the promoter of *LMO2*, a proto-oncogene, leading to insertional mutagenesis and the development of leukemia (Houghton et al., 2015).

To overcome these problems, self-inactivating (SIN)-LTRs were introduced in the later generation of lentiviral vectors that could potentially eliminate insertional mutagenesis issues related to LTRs (Zufferey et al., 1998). Thus, the safest system came out after deletion of the U3 region from the LTRs in the 3rd generation, also limiting the viral genes to *Gag* and *Pol* in one plasmid and *Rev* in another, creating a *Tat*-independent system. With the 3rd generation of lentiviral vectors, standard procedure for virus production requires transfection of HEK293 or HEK293T cells with four different plasmids for packaging, viral regulatory genes and envelope genes along with one plasmid that contains the packaging signal and the gene of interest enclosed by the SIN-LTRs. Separating these plasmids and the packaging signal has been a precaution for viral gene recombination and with this method efficiency of virus production is still very high (Dull et al., 1998; Zufferey et al., 1998).

Increasing safety with the 3rd generation vector systems have helped develop more efficient gene expression from the transgene construct. The addition of central polypurine tract (cPPT) to the construct results in higher transgene expression mainly acting through the nuclear translocation of cDNA (Van Maele et al., 2003). Another element enhancing transgene expression is the woodchuck hepatitis virus (WHV) post-transcriptional regulatory element (WPRE) that helps increase unspliced RNA amount (Zufferey et al., 1999). Likewise, effects of WPRE and specialized poly A termination sequences BGH and SV40 can be used in combination for enhanced transgene expression in lentiviral vector systems (Real et al., 2011).

There are certain limitations regarding the lentiviral vector systems. The primary limitation is the size of genetic material that can be packed into the virion. In the case of HIV-1 the genome size is around 9 kb. A second disadvantage of lentiviral vectors (which is commonly shared by all integrating vectors) is the unknown integration site profile that could potentially lead to the disruption of an essential gene or contrarily turn on the expression of an undesired gene such as a proto-oncogene. Although these issues are tackled to a somewhat successful extent with approaches like SIN-LTRs (Zufferey et al., 1998) or insulator sequences (Ramezani & Hawley, 2010), directing the exact integration site still remains as a challenge.

Current research on employing precise genome editing technologies such as CRISPR/Cas9 within lentiviral vectors shows promise in the development of the next generation of gene therapy vectors. Groundbreaking work by Naldini and colleagues have shed light on site-directed integration by zinc-finger nucleases (ZFNs) at the precise site of mutation in the *IL2RG* in CD34⁺ HSCs that causes the SCID-X1 disease as mentioned above. Their method brought together specific genome editing by ZFNs and integration-deficient lentiviral vectors for homology-directed repair (HDR) that led to the expansion of healthy immune cell populations (Genovese et al., 2014). More recently, another study showed CRISPR/Cas9-mediated genome editing could potentially be used for site-directed integration by using sgRNA-Cas9 protein mixtures along with non-integrating AAV vectors for applications in beta-thalassemia, by the correction of *HBB* gene in CD34⁺ HSCs (Dever et al., 2016). Collectively, these data set examples for a whole new era of targeted genome-editing for the future of gene therapy.

Another limiting factor for viral vectors in general is the intracellular innate immune response by the infected cell that can lead to very low transduction efficiency as in the case of natural killer cells, which will be discussed in detail in the forthcoming sections. Even though the viral vectors are stripped from their natural pathogenicity, they are still composed of immunogenic viral proteins that are sensed as foreign components in the host cell, activating the intracellular immune response via pattern recognition receptors (PRRs), cytoplasmic RNA/DNA sensors and cellular restriction factors. These molecules can each be turned on by the envelope, capsid, RNA or DNA structures inside the cell that overall lead to an inflammatory response (Kajaste-Rudnitski & Naldini, 2015).

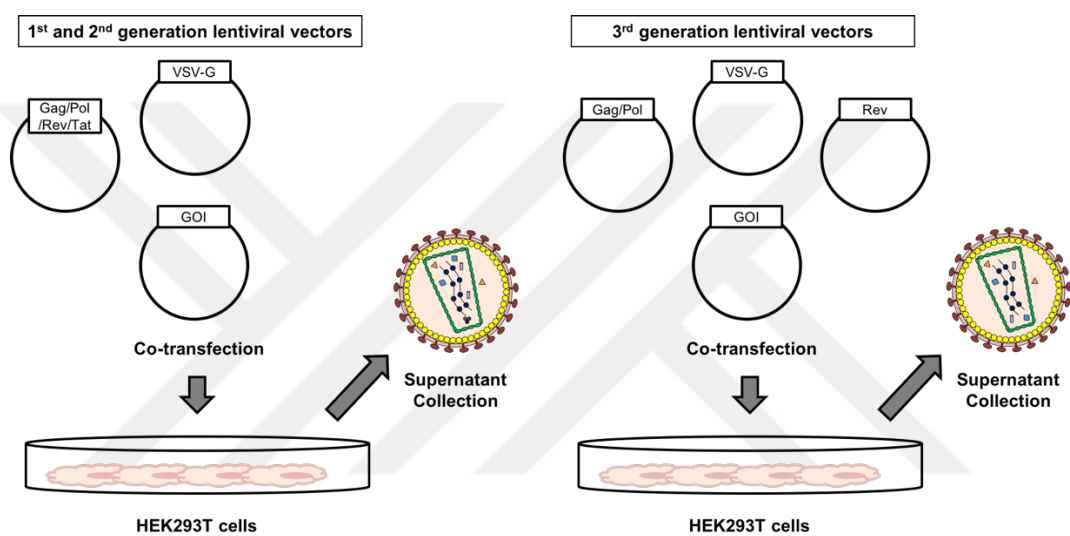


Figure 1.8. Lentiviral vector production with 1st, 2nd and 3rd generation vector systems. 1st and 2nd generation systems (left) result in virus particles with accessory proteins that are highly pathogenic for the host whereas 3rd generation systems (right) have increased safety and decreased immunogenicity. (GOI: gene-of-interest)

Considering the future of gene therapy would require a broad range of lentiviral vectors produced in clinical-grade and large quantity, the transition from research scale to mass production seems to be a challenge at first. For small scale productions, HEK293 or HEK293T cell lines are used as the producing cell line and conventional transfection methods are utilized for transfection of these cells with four plasmids. When scaling up the production, the basic principles are kept constant but with adherent cells, multilayer plates are used for ease of handling (Merten et al., 2011). There have been trials for vector production with suspension cells to reduce cost and the results are promising (Ansorge et al., 2009; Sheu et al., 2015). However, the current approach with adherent cell

transfection is still more beneficial since supernatant collection can be achieved in a cell-independent manner and this is harder to achieve with suspension cells although supernatant collection times can be optimized (Ansorge et al., 2009). Transfection and supernatant collection are just the first steps on the way to mass production, since downstream applications require optimization for purification and quality control of lentiviral vectors to be used in gene therapy in large-scale quantities in the near future (Merten et al., 2016).

1.3.4 Strategies and examples of NK cell genetic modifications

Lentiviral gene therapy in the scope of this study is important for altering gene expression in cells of the immune system, specifically NK cells. In a variety of cancers, NK cells can be manipulated by the suppressive cytokines in the tumor microenvironment and this might result in the escape of cancer cells from immune surveillance or dampening of cytotoxic activity (Baginska et al., 2013; Hasmim et al., 2015). Thus, it is an interesting approach to isolate NK cells from a cancer patient or from an allogeneic donor (or use NK-92 cell line, explained in other sections) and genetically modify them to become unmistakable killers. (i) Upregulation of activating receptors or downregulation of inhibitory receptors, (ii) expression of chimeric antigen receptors (CARs) that target tumor-associated antigens, (iii) expression of chemokine receptors for tumor-homing, (iv) autocrine secretion of proliferative cytokines and (v) protection from suppressive cytokines could potentially provide personalized approaches in cancer immunotherapy. The list of genetic modification approaches in NK cells can be summarized in Table 1.2.

Approach	Transgene	Method	Reference
Cytokine stimulation	IL-2	RV	(Konstantinidis et al., 2005; Nagashima et al., 1998)
	IL-15	RV, LV, EP	(Imamura et al., 2014; W Jiang, Zhang, & Tian, 2008; Wen Jiang, Zhang, Tian, & Zhang, 2014; Sahm, Schönfeld, & Wels, 2012)
Cytotoxicity	α -CD19 CAR	RV, LV, EP	(Boissel et al., 2012, 2013; Boissel et al., 2009; L. Li et al., 2010; Romanski et al., 2016; Shimasaki et al., 2012)
	α -CD20 CAR	RV, LV, EP	(Boissel et al., 2012, 2013; Müller et al., 2008)
	α -CD33 CAR	EP	(Schirrmann & Pecher, 2005)
	α -CD138 CAR	LV	(Chang et al., 2013; H. Jiang et al., 2014)
	α -CS1 CAR	LV	(Chu et al., 2014)
	α -GD2 CAR	RV	(Altvater et al., 2009; Esser et al., 2012)
	α -HER2 CAR	RV, EP	(Kruschinski et al., 2008; J. M. Lee et al., 2010; H. Liu et al., 2015; Schönfeld et al., 2015; C. Zhang et al., 2016)
	α -EGFR CAR	LV, HSV	(X. Chen et al., 2016; Genßler et al., 2016; Han et al., 2015)
	α -CEA CAR	EP	(Schirrmann & Pecher, 2002)
	α -EpCAM CAR	LV	(Sahm et al., 2012)
	α -NKG2D-L CAR α -TRAIL-R1 CAR	RV	(Kobayashi et al., 2014)
α -GPA7 CAR	RV	(Binyamin et al., 2008; G. Zhang et al., 2013)	
Protection from suppressive cytokine	DNT β R1I	EP	(B. Yang et al., 2013)
Silencing inhibitory signal	NKG2A shRNA	LV	(Figueiredo, Seltsam, & Blasczyk, 2009)

Table 1.2. List of genetic manipulations in primary NK cells and NK cell lines for therapeutic approaches (developed from Carlsten & Childs, 2015). RV: Retroviral, LV: Lentiviral, HSV: Herpes Simplex Virus, EP: Electroporation, CAR: Chimeric-antigen receptor.

1.4 Innate Anti-Viral Immune Response and Signaling

Genetic modification of NK cells by using viral vectors has proven to be a taunting task. Several anti-viral signaling events that occur in innate immune cells limit the efficiency of viral vector-mediated gene delivery. Therefore it is essential to fully characterize these signaling pathways to overcome the barriers in a transient process to achieve efficient transgene expression.

Microbial molecules or structural parts named as pathogen-associated molecular patterns (PAMPs) trigger a group of receptors and proteins named as pattern recognition receptors (PRRs) that include a variety of Toll-like receptors (TLRs), C-type Lectin Receptors (CLRs), Nod-like receptors (NLRs), retinoic acid inducible gene-I (RIG-I)-like receptors (RLRs) and other cytosolic RNA/DNA sensors along with cellular restriction factors. Upon virus entry, viral parts activate different pathways that overall lead to anti-viral signaling within the cell mediated by NF- κ B, IRF3/7, AP-1 and STATs, turning on targets named as interferon-stimulated genes (ISGs) and lead to the production of inflammatory cytokines, mainly type I interferons IFN α and IFN β . For the scope of this study, the details will be given on the anti-viral signaling components alarmed exclusively in RNA-virus infections and lentiviral vectors in particular.

1.4.1 Pattern Recognition Receptors (PRRs) in anti-viral signaling

1.4.1.1 Toll-like receptors (TLRs)

There are 10 different TLRs identified in humans, recognizing mainly lipids (TLR1, 2, 4, 6) or nucleic acids (TLR3, 7, 8, 9) coming from foreign organisms (Takeuchi & Akira, 2010) (Figure 1.9). TLR2 and TLR4 are among mostly studied receptors that are localized on the cell surface, recognizing bacterial lipopeptides and lipopolysaccharides (LPS) respectively. They can also recognize some viral glycoproteins found on the surface of

HSV (Leoni et al., 2012), CMV (Boehme et al., 2006), Hepatitis C (Dolganiuc et al., 2004) or VSV (Georgel et al., 2007).

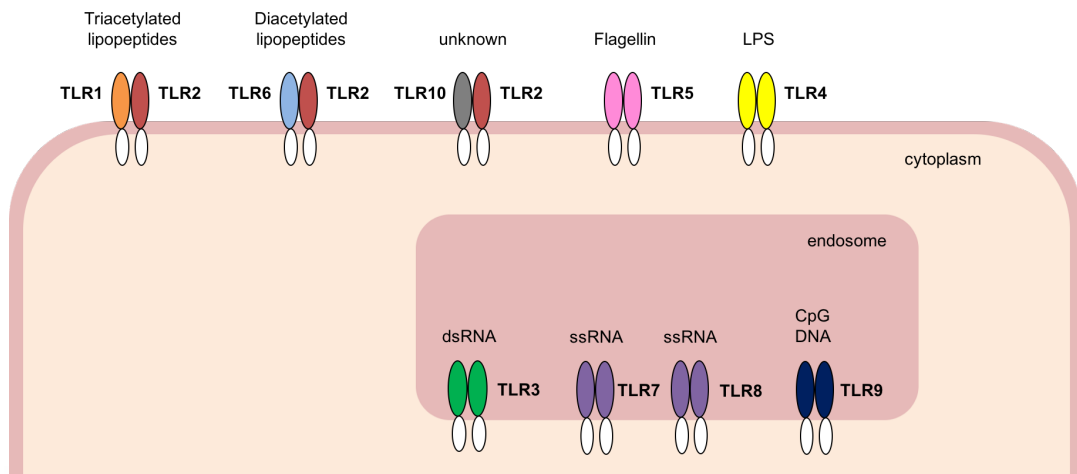


Figure 1.9. TLRs and their ligands. Among TLRs found on the cell surface, TLR1, TLR6 and TLR10 can make heterodimers with TLR2 and recognize lipopeptides. TLR4 recognizes LPS and TLR5 binds to flagellin. Endosomal TLRs recognize nucleic acid structures. (adapted from O’Neill et al., 2013).

The nucleic acid receptors TLR3, TLR7, TLR8 and TLR9 are localized exclusively in endosomes, making it the setting of the first encounter with viruses that enter the host cell via endocytosis. TLR3 is a short, dsRNA sensor that signals through adaptors TRIF and TRAF, inducing NF- κ B, IRF3 or MAPK activation via IKK $\alpha\beta\gamma$ or TBK1/IKK ϵ complex (Fitzgerald et al., 2003). TLR7 and TLR8 recognize ssRNA and signal through MyD88 and induce IRF7 and MAPK activation. TLR9 is a DNA sensor, especially detecting unmethylated CpG motifs associated with viral and bacterial DNA. Both TLR3 and TLR7 have been found to be associated with HIV-1-derived lentiviral vector sensing in dendritic cells (Breckpot et al., 2010). With the VSV-G-pseudotyped lentiviral vectors, the viral particles are shown to enter the cell predominantly via endocytosis in DCs (Breckpot et al., 2010). In primary NK cells, it is shown that using inhibitors that interfere with TLR3 signaling increase transduction efficiency dramatically. BX795, a small molecule inhibitor of TBK1/IKK ϵ , has shown promising advances in transduction of primary NK cells as well as several immune cell lines (Sutlu et al., 2012). Taken together, these results show that it is very likely that endosomal TLRs would be the first line of defense in the course of lentiviral gene delivery systems in some cells of the hematopoietic system (Kajaste-Rudnitski & Naldini, 2015).

1.4.1.2 C-type lectin receptors (CLRs)

CLRs are identified as soluble and transmembrane receptors recognizing viral polysaccharide structures, containing at least one C-type-lectin-like domain (CTLD) traditionally known to recognize fungal parts but have recently been associated with dead or cancerous cells (Dambuza & Brown, 2015). Dendritic cell-specific intracellular adhesion molecule-3-grabbing non-integrin (DC-SIGN) found on the membrane of dendritic cells plays a role in the endocytosis of HIV-1 and its rapid degradation or replication and spread to T cells (Turville et al., 2004). Mannose receptors have similar roles identified in virus entry into macrophages (Lai et al., 2009).

1.4.1.3 NOD-like receptors (NLRs)

NLRs recognize a variety of PAMPs arising from different microbial infections and among their members, NOD2 and NOD-, LRR- and pyrin domain-containing 3 (NLRP3) are best characterized to have roles in viral infections where inflammasomes direct IL-1 β production and inflammasome-independent signals lead to interferon production (Kanneganti, 2010). The pro-inflammatory cytokine IL-1 β production requires NF- κ B-driven signals for making of pro-IL-1 β as well as caspase-1 activation signals. In this context, RIG-I (explained in detail in the following section) is found to act on both NF- κ B signaling and also induction of inflammasome activation independent of NLRP3 to promote IL-1 β production in response to influenza A virus (Poeck et al., 2010).

1.4.1.4 RIG-I-like receptors (RLRs)

Retinoic acid-inducible gene I (RIG-I, also known as DDX58), melanoma differentiation associated 5 (MDA5, also known as IFIH1) and laboratory of genetics and physiology 2 (LGP2) are three known members of the RLRs, each containing a DExD/H-box RNA helicase domain that is required for binding to RNA ligands. Each recognize and bind to specific RNA molecules that have viral origin. RIG-I and MDA5 signal through caspase activation and recruitment domains (CARDs) when met with dsRNA, inducing NF- κ B, IRF3/7 (Yoneyama et al., 2005) or p38 MAPK (Mikkelsen et al., 2009) activation, leading to IL-1 β production (Poeck et al., 2010). LGP2 on the other hand lacks CARDs for

signal transduction and was first identified as a negative regulator of the antiviral signal induced by RIG-I and MDA5 (Yoneyama et al., 2005). Recent studies have shown that LGP2 can also act as a positive regulator of MDA5 signaling by causing more rapid complex formation with viral RNA and stabilizing shorter fragments of MDA5, thus enhancing anti-viral signaling (Bruns & Horvath, 2015; Bruns et al., 2014; Satoh et al., 2010). RIG-I can specifically bind to 5' triphosphate (5'PPP) motif that is only found in viral RNA, that is present in the cytoplasm during infection of the host cell. The ssRNA templates can be matching to create dsRNA or can be found as ssRNA. However, MDA5 is proposed to recognize longer base-paired RNA molecules, thus acting on different ligands (Kato et al., 2006).

Upon binding to their target PAMPs, most PRRs induce signals via their corresponding adapters. In the case of RIG-I and MDA5, the activation due to 5'PPP RNA leads to a cascade of events by mitochondrial antiviral signaling protein (MAVS). In the absence of their ligand, RIG-I and MDA5 are found at a phosphorylated state at specific serine or threonine residues in the CARD or C-terminal domains. Ligand binding initiates a conformational change, stimulated by protein kinase R (PKR) activator (PACT). This change then brings phosphatases PPI α or PPI γ to remove the phosphate residues from the CARDS, bringing it to a signaling-active form. During RIG-I signaling, tripartite motif protein 25 (TRIM25) and Riplet that are E3 ubiquitin ligases, add ubiquitin chains to the CARD and C-terminal domains respectively, which is a crucial step leading to the tetramerization of RIG-I and its interaction with MAVS on the mitochondrial membrane (Gack et al., 2007). On the other hand, MDA5 binding to longer stretches of RNA goes through a different conformational change that leads to its elongated structure, bringing it closer to MAVS (Wu et al., 2013). MAVS further recruits either the TBK1/IKK ϵ complex leading to IRF3/7 activation or the inhibitor of- κ B (I κ B) kinase (IKK) complex leading to NF- κ B activation in addition to AP-1 (Kai Chan & Gack, 2016) (Figure 1.10). Using the small molecule inhibitor BX795 results in an increase in lentiviral gene delivery efficiency in primary NK cells either interfering with the endosomal TLR3 pathway or the RIG-I/MDA5 pathway (Sutlu et al., 2012).

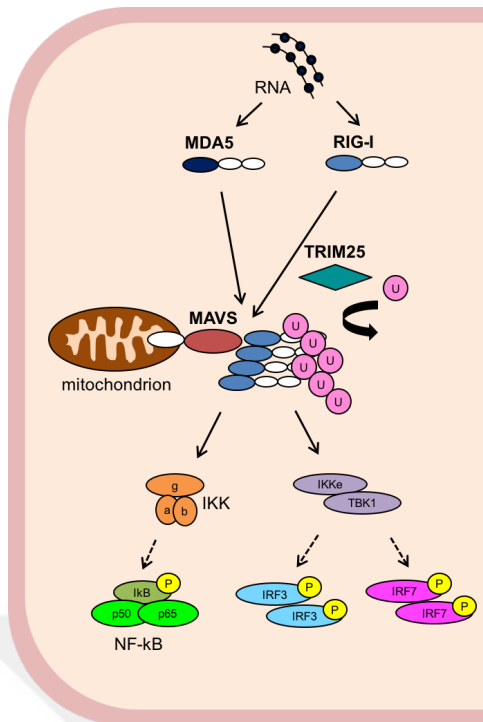


Figure 1.10. RLR signaling. Upon binding to their relative PAMPs, MDA5 and RIG-I are recruited to the adapter MAVS found on the mitochondria, as a result of ubiquitination (pink spheres) by TRIM25 and Riplet (not shown here). MAVS further activates the IKK $\alpha\beta\gamma$ complex that leads to NF- κ B activation or the TBK1/IKK ϵ complex that results in IRF3 and IRF7 activation and translocation to nucleus to turn on the expression of pro-inflammatory cytokines. (Adapted from Kai Chan & Gack, 2016)

1.4.1.5 Cytoplasmic RNA/DNA sensors

Interferon-induced protein with tetratricopeptide repeats 1 (IFIT1) is an RNA sensor recently described to bind to 5'PPP motif found in viral RNA, suggested to act on a different network than RLRs (Pichlmair et al., 2011). Similarly, Protein Kinase R (PKR) is a cytoplasmic kinase again recognizing viral RNA, interfering with the RLR signaling pathways (Nallagatla et al., 2007). Additionally, RNA polymerase III is also shown to have a role in converting dsRNA of viruses into small 5'PPP-containing RNAs that turn on the RLR signaling pathways (Ablasser et al., 2009; Chiu et al., 2009). Together, these cytoplasmic RNA sensors act as additional forces against viral RNA parts especially after induction of ISGs in the later stages of anti-viral response.

IFN-gamma-inducible protein 16 (IFI16) and cyclic AMP-GMP synthase (cGAS) are cytoplasmic DNA sensors, known to have roles in HSV and HIV infections. IFI16, like PKR, is one of the many ISGs triggered by the innate immune response and IFI16 can particularly bind to reverse-transcription products of HIV-1; signaling through the adapter protein stimulator of IFN genes (STING) found on the ER, inducing IKK and TBK1 pathways as explained for the RLRs (Altfeld & Gale Jr, 2015; Jakobsen et al., 2013). cGAS can bind to dsDNA, further forming cyclic GMP-AMP (cGAMP) that is

capable of binding to STING and inducing anti-viral signaling that results in type I interferon production (Sun et al., 2013). Triggering the immune response with oligonucleotides (ODN) and cyclic dinucleotides (CDNs) via DNA sensors cGAS through the adapter STING are among many influential uses of cytoplasmic DNA sensors for immunization strategies (Yildiz et al., 2015).

2'-5' oligoadenylate synthase (OAS) is another sensor turned on by the cytosolic dsDNA, forming 2'-5' oligoadenylates, further activating RNase L that blocks viral replication by degrading RNA and feeding into the RLR pathways (Hornung et al., 2014; Malathi et al., 2007). Similarly, DNA-dependent activator of IFN-regulatory factors (DAI) is a cytoplasmic DNA sensor that can recognize DNA viruses, leading to IRF3 activation and type I IFN production (Takaoka et al., 2007). Last but not least, Absent in melanoma 2 (AIM2) is also a cytoplasmic DNA sensor shown to have roles in the caspase-1-related inflammasome signaling rather than the IRF3 pathway (Fernandes-Alnemri et al., 2009; Hornung et al., 2009).

Having such a variety of RNA and DNA sensors might be the ultimate outcome of years of evolution in highly complex mammalian cells that are under continuous attack by an ever-changing selection of viruses. There are still many other sensors discovered recently with intrinsic cell- and pathogen-specific roles such as DDX41, DXH9, DXH36, DNA-dependent protein kinase (DKR) and MRE11 (Dempsey & Bowie, 2015).

1.4.1.6 Cellular restriction factors

The outstanding variety of cytoplasmic sensors are not limited to the nucleic acid ligands but also serve to interfere with the machinery adapted by viral invaders of the host system. These molecules are named as the cytoplasmic restriction factors that have distinct roles in pathogen intrusion, multiplication and interference with the host cell metabolism. For example, Apolipoprotein B editing complex 3 (APOBEC3) proteins are members of ISGs, transcribed as a result of IFN signaling and further act on HIV-1 and other viruses by introducing G to A mutations during the viral reverse transcription process (Stavrou & Ross, 2015). Another factor named as SAM domain and HD domain-containing protein 1 (SAMHD1) is shown to inhibit HIV-1 replication, predominantly in cells of myeloid lineage, by degradation of cellular dNTPs (Hrecka et al., 2011; Laguette et al., 2011;

Lahouassa et al., 2012). Schlafen11 (SLFN11) is another host cell restriction factor described in the recent years to inhibit HIV-1 protein production by selectively binding to tRNAs in a codon-usage-dependent manner (M. Li et al., 2012).

Among many cellular restriction factors, Tripartite motif 5 α (TRIM5 α) is an important inhibitor of the HIV-1 life cycle that recognizes the capsid protein and causes pre-mature uncoating of the capsid. TRIM5 α contains a RING E3 ubiquitin ligase domain and signals through the transforming growth factor-beta (TGF β)-activated kinase 1 (TAK1) leading to the activation of MAPK pathways and induction of the transcription factors AP-1 and NF- κ B in a broad range of cell types (Lascano et al., 2016; Pertel et al., 2011). On the contrary, Cyclophilin A (CypA) is known for binding to the capsid lattice of HIV-1 and unlike TRIM5 α , plays a role in the viral life cycle that might increase the infectivity of the virus. Recent crystallography results have shown that a new binding site in CypA correlates with a structurally more stable curved capsid lattice, thus helping the protection of the capsid. However, in the case of high abundance of CypA along with TRIM5 α , it is suggested that the structure of the lattice is no longer steady, thus resulting in pre-mature uncoating (C. Liu et al., 2016).

Another interesting member of the tripartite motif containing protein family is TRIM28, also known as Kruppel-associated box protein-1 (KAP-1), that can act as an antiviral agent. Besides its antiviral activity, it plays significant roles in DNA damage responses and gene silencing during embryonic stem cell differentiation. Shown in the recent years, TRIM28 interacts with the integrase of HIV-1, inhibiting integration to host genome. This interaction occurs through the acetylated residues on the integrase and causes deacetylation by recruiting histone deacetylase 1 (HDAC1). TRIM28 knock down causes increased viral activity in some cell lines that are natural targets of HIV-1 (Allouch et al., 2011).

Taken together, these cellular restriction factors have shown the multiple ways the host cell can fight against pathogens like HIV-1 in order to stop the life cycle of the virus before completion.

1.4.2 Transcription factors involved in anti-viral response

Type I interferons are the ultimate factors playing major roles in viral infections as a result of multiple anti-viral signaling pathways. The 5' region of *IFN α* and *IFN β* genes named as the virus response elements (VREs) contain multiple repetitions of GAAANN consensus sequence (Altfeld & Gale Jr, 2015). Upon anti-viral signaling, IRFs, AP-1 (c-Jun and ATF-2 subunits) and NF- κ B (p50 and p65 subunits) are recruited to the VREs and turn on the expression of *IFN β* (Panne et al., 2007). The VRE of *IFN α* gene does not contain the GAAANN consensus, thus cannot recruit NF- κ B and is only controlled by IRF proteins that bind to the AANNGAAA repeats that are found in abundance. Among other members of the IRF family, IRF3 and IRF7 are known as the anti-viral IRFs that can form homo- or hetero-dimers with each other and contribute to the expression of interferon-stimulated genes (Paun & Pitha, 2007).

The abundance of type I interferons in the environment during viral infections induces signals through the cytokine receptor, resulting in phosphorylation of STAT1 and STAT2 by JAK1 and TYK2 found in the cytoplasmic tail region of the receptor. IRF9 is another member of this family, again playing a significant role in anti-viral signaling by binding to the interferon-sensitive response element (ISRE) sites on the 5' region of ISGs. STAT1 and STAT2 also form homo- or hetero-dimers and form a complex with IRF9 for the expression of ISGs (Rustagi & Gale, 2014).

As mentioned before in various PRR pathways, IRF3 is directly phosphorylated by TBK1/IKK ϵ complex and gets activated whereas NF- κ B activation requires the phosphorylation of I κ B by IKK $\alpha\beta\gamma$ complex. Additionally, AP-1 transcription factor is downstream of MAPK pathways that play essential roles in anti-viral signaling, induced by TRIM5 α , TLR7/8 and cytokine signaling pathways. NF- κ B and AP-1 both have broad effects on survival and proliferation of immune cells that are far beyond the scope of this thesis (Figure 1.11).

Interestingly, there are several studies supporting the relationship between MAPK pathways and WT HIV-1 infections. Among the members of MAPK family, p38 is shown to be required for AP-1 induction during HIV-1 infection where p38 phosphorylation is rapidly observed upon lentiviral entry in Jurkat cells or PBMCs (Muthumani et al., 2005).

Introducing p38 inhibitors block the lentiviral life cycle and therefore show potential applications as anti-viral drugs in HIV-1 (Muthumani et al., 2004) or influenza infections (Börgeling et al., 2014). The activation of p38 leads to Serine-727 phosphorylation of STAT1 which is observable upon viral entry and the use of p38 inhibitors cause a reduction in the type I interferon production in the host cell (Börgeling et al., 2014). It is evident that viral protein Nef is responsible for PD-1 upregulation in HIV-1-infected cells that requires p38 phosphorylation (Muthumani et al., 2008). In different RNA virus infections, the presence of cytoplasmic 5'PPP-RNA initiates RIG-I signaling that activates p38 and JNK (Mikkelsen et al., 2009; Poeck et al., 2010). Inhibition of JNK is also shown to reduce lentiviral infection of fibroblasts and keratinocytes (Lee et al., 2011). Additionally, the involvement of p38 and JNK in viral infections are not restricted to RNA viruses and the viral signaling could potentially be abrogated by the use of MAPK inhibitors in DNA virus infections (Pan et al., 2006). Taken together, the involvement of MAPKs in lentiviral gene delivery shows exciting paths to be discovered.

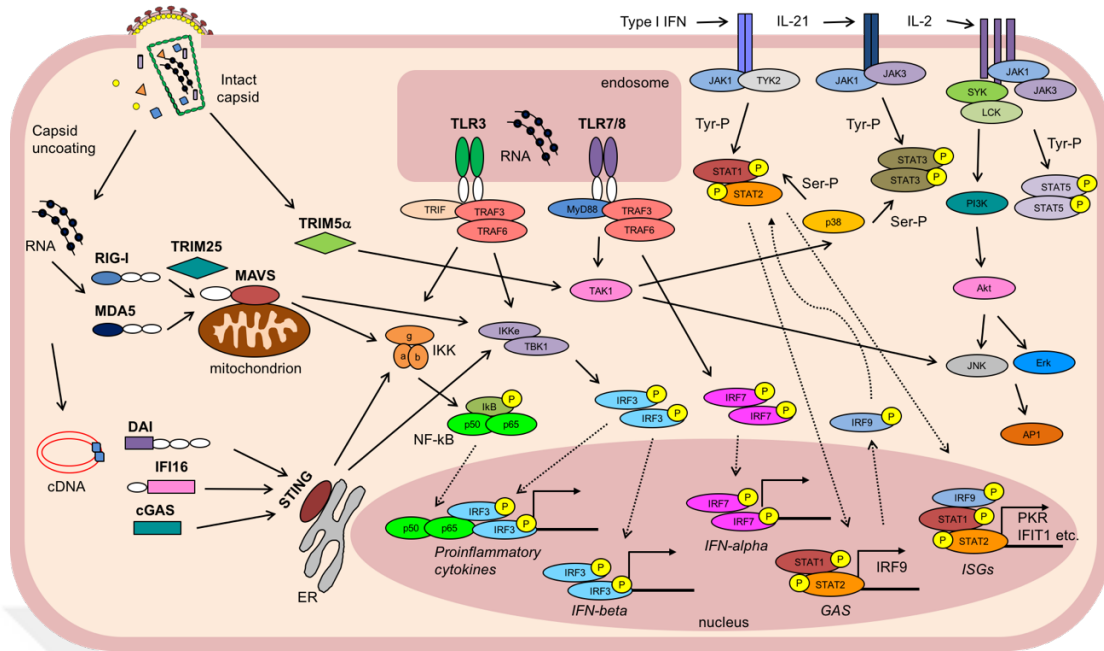


Figure 1.11. Important signaling pathways activated in anti-viral response. WT viruses or lentiviral vectors that enter the host cell cytoplasm cause differential signals to be induced by the genomic RNA, cDNA or the capsid proteins. The capsid lattice is detected by TRIM5 α in the cytoplasm, signaling through TAK1 and MAPKs to induce AP-1. Viral RNA that contains the 5'PPP motif gets detected by RIG-I and MDA5 in the cytoplasm, signaling via MAVS with a role of TRIM25 causing the ubiquitination of RIG-I. This brings together the signaling molecules required for the downstream signal transduction towards IKK and TBK1 pathways, further causing the activation of NF- κ B and IRF3 respectively. The result of reverse-transcribed viral genome is detected by cytoplasmic DNA sensors, DAI, IFI16 and cGAS, that require the adaptor STING found on ER to induce NF- κ B and IRF3 activation. Alternatively, viral RNA detected in the endosomes induce signals from TLR3 that results in NF- κ B and IRF3 activation or TLR7/8, leading to MAPKs or IRF7 phosphorylation. IRF3 and IRF7 homo and heterodimers bind to their corresponding VREs on the 5' region of *IFN α* and *IFN β* genes, resulting in cytokine production. *IFN α* and *IFN β* secreted in an autocrine manner or from neighboring cells end up activating STAT1 and STAT2 signaling due to the phosphorylation of Tyrosine residues by JAK and TYK found on the cytoplasmic tail of cytokine receptor. STAT1/STAT2 can further bind to GAS elements in the genome, turning on the expression of a variety of IRF genes including IRF9. IRF9 forms a complex with STAT1/STAT2 and together they bind to the ISRE elements in the ISGs, expressing genes associated with anti-viral response. IL-2 and IL-21 receptors are shown to include other main signaling events occurring in the NK cell culture environment that could potentially interfere with the anti-viral pathways. Dashed lines indicate translocation, black lines indicate activation (adapted partially from Melchjorsen, 2013).

1.5 CRISPR/Cas9-Mediated Genome Editing

1.5.1 History and mechanism of genome editing

Targeted genome editing has been the major hurdle of all genetic engineers around the world for many years who have been in search of altering and investigating specific roles of genes. Astonishingly, the tools required for the most efficient genome editing came from the nature itself, found in the world of microorganisms. CRISPR/Cas9 technology has been the most exciting discovery of this decade, with accelerated findings about the nature of genome editing used in a variety of cell types and broad applications.

Looking back at the most applied genome editing systems of the past twenty years, Zinc-finger nucleases (ZFNs), Transcription activator-like effector nucleases (TALENs) and most recently CRISPR/Cas9 have all adapted the same basic principle of creating double-stranded breaks (DSBs) at the target sequence. ZFNs and TALENs rely on a protein-DNA interaction for the recognition of target sequence and utilize a nuclease, mostly FokI, for the DSB at desired location. On the other hand, the CRISPR/Cas9 system derived from *Streptococcus pyogenes* revolutionized this approach by introducing RNA-DNA interactions mainly through complementation and cut the genome with an RNA-targeted nuclease, Cas9 (Ran et al., 2013).

The introduction of DSBs in the genome alerts DNA repair systems of the host cell that results in two outcomes: non-homologous end joining (NHEJ) where random insertion or deletions (together known as INDELS) occur at the cut site or homology-directed repair (HDR) that uses a DNA template to fill the missing parts (Figure 1.12). In an attempt to knock-in specific sequences, DNA templates in the form of plasmids or single-stranded oligonucleotides (ssODNs) can be co-transfected with the genome-editing system. Even though their mechanisms of action seem similar, ZFNs and TALENs require a very troublesome cloning procedure that combines the specific DNA-binding proteins in the

necessary order and bases the DSB on the dimerization of nucleases that span the upstream and downstream sequences of the target site. On the contrary, CRISPR/Cas9 system only requires the cloning of a 20 nucleotide-long guide RNA sequence to the RNA backbone of the construct where RNA-guided Cas9 is produced from a single plasmid.

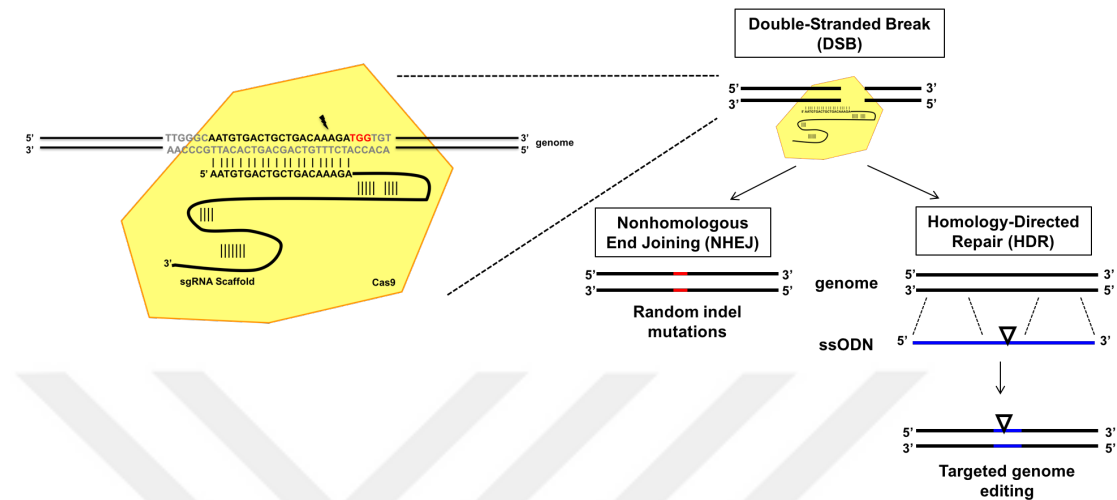


Figure 1.12. CRISPR/Cas9-mediated genome editing. Example shows a genomic DNA sequence where CRISPR target site (black) has a PAM sequence (red) in the 5' to 3' direction where hypothetical double-stranded break (DSB) will occur at the annotated site (lightning sign). The outcome of DSB can either be non-homologous end joining (NHEJ) with random indel mutations or homology-directed repair (HDR) where a single-stranded oligonucleotide (ssODN, blue) or a plasmid can be used to serve as a template for repair. (Dashed lines indicate homology regions) Single cell clones can be isolated to identify specific mutants.

The only requirement for CRISPR design is the existence of a protospacer adjacent motif (PAM) sequence that is generically an NGG at the 3' end of the target sequence and it is suggested that the theoretical cut site is 3 bp upstream of this sequence (Ran et al., 2013). Thus, any sequence in the genome that contains this motif can theoretically be altered by the CRISPR/Cas9 system which is now named as Sp-Cas9 to define its origin. Additionally, the discoveries of new Cas9 homologs from other species, Cpf1 just to name a recent one (Zetsche et al., 2015), and engineering of the original construct have enlightened the path for researchers to use different PAM sequences in the genome for targeted editing (Hirano et al., 2016; Kleinstiver et al., 2015). The biggest concern about the use of CRISPR/Cas9 system for genome editing is the issue of off-target binding possibility. This is due to the complementation of gRNA to other sequences with partial matches in the genomic DNA that is currently trying to be predicted with smart software

design. The predictions lead the users to pick sites with the least off-target effects but still remain to be resolved for future therapeutic uses.

With recent advances in the field, CRISPR/Cas9 system has evolved beyond imagination, serving specific needs to change or alter genes, create knock-out or knock-ins, stimulate large deletion or inversions, turn the expression of genes on and off by interacting with DNA modifications and imaging of genomic loci by the help of fluorescent tags (Sander & Joung, 2014). It is also the new tool in the field of gene therapy as mentioned earlier in the section 1.3.3 with new advances in directing viral vector integration into a specific site in the genome for precise targeted therapy. The first clinical trial with CRISPR gene editing in humans was announced in the second half of 2016 that would potentially target T cells of cancer patients (Cyranoski, 2016).

1.5.2 Genome-wide approaches with the GeCKO library

Genome-scale CRISPR-Cas9 knock-out (GeCKO) library is a tool for complete knock-out screen in human cells, targeting more than 19,000 genes with a variety of gRNAs. It consists of two sets of libraries, named as Library A and Library B where each library has 3 unique guide RNA sequences targeting one gene in the human genome, increasing the total number of guide RNA sequences to 6 per gene. Library A additionally contains guide RNA sequences targeting miRNAs. There are also 1000 non-targeting control guide RNAs (Sanjana et al., 2014; Shalem et al., 2014). The complete description of the contents of the library can be listed in Table 1.3.

Current applications of GeCKO library in mammalian cells aim to screen genes that play roles in a certain limitation factor. For example, chemotherapeutic drug vemurafenib resistance, related to certain types of chemo-resistant cancers, can be mapped to genes playing roles in this process. Melanoma cells have been utilized for this approach in one study (Shalem et al., 2014) where GeCKO-transduced cells were further introduced with the drug and the surviving cells were sequenced in order to figure out which genes complemented in cancer cell survival in the presence of the drug. This tool can be adapted to many different biological questions, in theory to any cell line that is efficiently transduced with lentiviral vectors, further creating complete loss-of-function screens.

<i>Species</i>	human
<i>Total number of genes targeted</i>	19,050
<i>Targeting constructs per gene</i>	6 per gene (3 in Library A, 3 in Library B)
<i>Number of miRNA targeted</i>	1,864
<i>Targeting constructs per miRNA</i>	4 per miRNA
<i>Control (non-targeting) sgRNAs</i>	1,000
<i>Total sgRNA constructs</i>	122,411 (65,383 in Library A, 58,028 in Library B)
<i>Viral plasmid backbone</i>	lentiCRISPRv2

Table 1.3. Features of GeCKO Library (adapted from www.genome-engineering.org/gecko/).



2. AIM OF THIS STUDY

NK cells show resistance to lentiviral gene delivery and the reasons behind this resistance have not yet been fully identified in HIV-1-based, VSV-G-pseudotyped 3rd generation lentiviral vector systems. The use of small molecule inhibitor of the TBK1/IKK ϵ complex, BX795, enhances lentiviral gene delivery in primary NK cells as well as many other cells of hematopoietic lineage. However, the exact pathways playing roles in this effect have not been assessed. The main suspected pathways included viral RNA sensors that induced an overall anti-viral response in the host cell, RIG-I-like receptors that utilize TBK1/IKK ϵ complex and their corresponding transcription factors NF- κ B, IRF3 and IRF7. Additionally, endosomal sensing of viral RNA through TLR3 also may induce signals by the TBK1/IKK ϵ complex. However, another cytoplasmic restriction factor TRIM5 α recognizing the capsid structure of HIV-1 mainly activates TAK1 and related MAPK pathways that could result in the activation of NF- κ B and AP-1 transcription factors with diverse effects in immune cells. The induction of these pathways resulting in an overall anti-viral response and production of type I interferons that could further activate STAT signaling. The relationship between WT HIV-1 infection and MAPK pathways have been identified but the specific interactions with NK cells in lentiviral gene delivery have not yet been found. The studies involving WT HIV-1 and host interactions included the natural hosts of the virus, namely T cells, macrophages and DCs to some extent. The responses to the lentiviral vectors have been investigated, to some

extent, in some cell lines but not specifically in NK cells. How and why lentiviral vectors fail in gene delivery to NK cells is unknown. Thus, this study aimed:

- I. To identify specific roles of anti-viral signaling components and the kinase inhibitor BX795 in NK-92 cells by molecular pathway analysis and gene knock out strategies using CRISPR/Cas9-mediated genome editing,
- II. To map the potential pathways playing a role in anti-viral signaling in NK cells by genome-wide approaches,
- III. To shed light on novel pathways and other inhibitors that might have higher success in lentiviral gene delivery and provide potential use in gene therapy.



3. MATERIALS AND METHODS

3.1 Materials

3.1.1 Chemicals

All the chemicals used in this thesis are listed in Appendix A.

3.1.2 Equipment

All the equipment used in this thesis is listed in Appendix B.

3.1.3 Buffers and solutions

Calcium Chloride (CaCl₂) Solution: 60mM CaCl₂ (diluted from 1M stock), 15% Glycerol, 10mM PIPES (pH 7.00) were mixed and sterilized by autoclaving at 121°C for 15 minutes and stored at 4°C.

Agarose Gel: For 100 ml 1% w/v gel, 1 g of agarose powder was dissolved in 100 ml 0.5X TBE buffer by heating. 0.01% (v/v) ethidium bromide was added to the solution.

Phosphate-buffered saline (PBS): For 1000 ml 1X solution, 100 ml 10X DPBS was added to 900 ml ddH₂O and the solution was filter-sterilized.

Tris-Borate-EDTA (TBE) Buffer: For 1 L 5X stock solution, 54 g Tris-base, 27.5 g boric acid, and 20 ml 0.5M EDTA (pH 8.00) were dissolved in 1 L of ddH₂O. The solution is stored at room temperature (RT) and diluted 1 to 10 with ddH₂O for working solution of 0.5X TBE.

3.1.4 Growth media

Luria Broth (LB): For 1 L 1X LB media, 20 g LB powder was dissolved in 1 L ddH₂O and then autoclaved at 121°C for 15 minutes. For selection, kanamycin at a final concentration of 50 µg/ml or ampicillin at a final concentration of 100 µg/ml was added to liquid medium just before use.

LB-Agar: For 1X agar medium in 1L, 20 g LB powder and 15 g bacterial agar powder were dissolved in 1 L ddH₂O and then autoclaved at 121°C for 15 minutes. Then, autoclaved LB agar is mixed with antibiotic of interest at desired ratio. Kanamycin at a final concentration of 50 µg/ml or ampicillin at a final concentration of 100 µg/ml was added to prepared medium just before pouring onto sterile petri dishes. Sterile agar plates were kept at 4°C.

DMEM: 293FT cells were maintained in culture in DMEM supplemented with 10% heat-inactivated fetal bovine serum, 2mM L-Glutamine, 1mM Sodium Pyruvate, 0.1mM MEM Non-essential amino acid solution, and 25mM HEPES solution.

RPMI: YTS cell line is maintained in culture in RPMI1640 supplemented with 20% heat-inactivated fetal bovine serum, 25mM HEPES, 2mM L-Glutamine, 1X MEM vitamins, 0.1mM MEM Non-essential amino acid solution, 1mM Sodium Pyruvate and 0.1 mM 2-mercaptoethanol.

SCGM: NK-92 cell line is maintained in culture in CellGro SCGM supplemented with 20% heat-inactivated fetal bovine serum. 1000 U/ml Interleukin-2 is added to culture every 48 hours.

Freezing medium: All the cell lines were frozen in heat-inactivated fetal bovine serum containing 6% DMSO (v/v).

3.1.5 Commercial kits used in this study

All the commercial kits used in this thesis is listed in Appendix C.

3.1.6 Enzymes

All the restriction enzymes, polymerases and PCR reaction supplements are obtained from either Fermentas or New England Biolabs.

3.1.7 Antibodies

Antibodies used in this study are listed in Appendix D.

3.1.8 Bacterial strains

Escherichia coli (*E.coli*) DH-5 α strain is used for general plasmid amplifications and Top10 strain is used for lentiviral construct amplifications.

3.1.9 Mammalian cell lines

293FT: Human embryonic kidney 293 (HEK293) cell line derivative that stably express the large T antigen of SV40 virus and has fast-growing specificity (Invitrogen R70007).

NK-92: Human natural killer cell line isolated in the year 1992 from a non-Hodgkin's lymphoma patient (ATCC® CRL 2407™).

YTS: Derivative of YT cell line that was originally from a 15-year old male with acute lymphoblastic leukemia (ALL) were TCR-negative cells with NK cell activity (DSMZ ACC 434).

3.1.10 Plasmids and oligonucleotides

The plasmids and the oligonucleotides used in this thesis are listed in Table 3.1 and Table 3.2, respectively.

PLASMID NAME	PURPOSE OF USE	SOURCE
pMDLg/pRRE	Virus production/packaging plasmid (<i>Gag/Pol</i>)	Addgene (#12251)
pRSV-REV	Virus production/packaging plasmid (<i>Rev</i>)	Addgene (#12253)
pCMV-VSV-g	Virus production/packaging plasmid (<i>Env</i>)	Addgene (#8454)
LeGO-G2	Lentiviral construct for GFP expression	Kind gift from Prof. Boris Fehse of University Medical Center Hamburg-Eppendorf, Hamburg, Germany
LeGO-G2-Puro	Lentiviral construct for GFP expression with Puromycin resistance gene	Kind gift from Prof. Boris Fehse of University Medical Center Hamburg-Eppendorf, Hamburg, Germany
lentiCRISPRv2	Lentiviral construct for CRISPR/Cas9 expression with Puromycin resistance gene	Addgene (#52961)
lentiCRISPRv2-GeCKO Human Library A	Lentiviral construct for CRISPR/Cas9 expression with Puromycin resistance gene – GeCKO Human knock out Library A	Addgene (#1000000048)
lentiCRISPRv2-GeCKO Human Library B	Lentiviral construct for CRISPR/Cas9 expression with Puromycin resistance gene – GeCKO Human knock out Library B	Addgene (#1000000048)

pspCas9(BB)-2A-GFP	Mammalian expression plasmid for CRISPR/Cas9 system with GFP	Addgene (#48138)
pspCas9(BB)-2A-Puro	Mammalian expression plasmid for CRISPR/Cas9 system with Puro	Addgene (#48139)
DDX58_pspCas9(BB)-2A-GFP	Mammalian expression plasmid with DDX58-targeting CRISPR/Cas9 and GFP	Lab construct
DDX58_pspCas9(BB)-2A-Puro	Mammalian expression plasmid with DDX58-targeting CRISPR/Cas9 and Puromycin resistance	Lab construct
IFIH1_pspCas9(BB)-2A-GFP	Mammalian expression plasmid with IFIH1-targeting CRISPR/Cas9 and GFP	Lab construct
IFIH1_pspCas9(BB)-2A-Puro	Mammalian expression plasmid with IFIH1-targeting CRISPR/Cas9 and Puromycin resistance	Lab construct
TBK1_pspCas9(BB)-2A-GFP	Mammalian expression plasmid with TBK1-targeting CRISPR/Cas9 and GFP	Lab construct
TBK1_pspCas9(BB)-2A-Puro	Mammalian expression plasmid with TBK1-targeting CRISPR/Cas9 and Puromycin resistance	Lab construct
TRIM5a_pspCas9(BB)-2A-GFP	Mammalian expression plasmid with TRIM5a-targeting CRISPR/Cas9 and GFP	Lab construct
TRIM5a_pspCas9(BB)-2A-Puro	Mammalian expression plasmid with TRIM5a-targeting CRISPR/Cas9 and Puromycin resistance	Lab construct
DDX58_lentiCRISPRv2	Lentiviral construct for DDX58-targeting CRISPR/Cas9 expression with Puromycin resistance	Lab construct
IFIH1_lentiCRISPRv2	Lentiviral construct for IFIH1-targeting CRISPR/Cas9 expression with Puromycin resistance	Lab construct
IRF3_lentiCRISPRv2	Lentiviral construct for IRF3-targeting CRISPR/Cas9 expression with Puromycin resistance	Lab construct
IRF7_lentiCRISPRv2	Lentiviral construct for IRF7-targeting CRISPR/Cas9 expression with Puromycin resistance	Lab construct
IRF9_lentiCRISPRv2	Lentiviral construct for IRF9-targeting CRISPR/Cas9 expression with Puromycin resistance	Lab construct
JAK3_lentiCRISPRv2	Lentiviral construct for JAK3-targeting CRISPR/Cas9 expression with Puromycin resistance	Lab construct
LCK_lentiCRISPRv2	Lentiviral construct for LCK-targeting CRISPR/Cas9 expression with Puromycin resistance	Lab construct
MAP3K7_lentiCRISPRv2	Lentiviral construct for MAP3K7-targeting CRISPR/Cas9 expression with Puromycin resistance	Lab construct

MAPK8_lentiCRISPRv2	Lentiviral construct for MAPK8-targeting CRISPR/Cas9 expression with Puromycin resistance	Lab construct
MAPK14_lentiCRISPRv2	Lentiviral construct for MAPK14-targeting CRISPR/Cas9 expression with Puromycin resistance	Lab construct
MAVS_lentiCRISPRv2	Lentiviral construct for MAVS-targeting CRISPR/Cas9 expression with Puromycin resistance	Lab construct
PIK3CA_lentiCRISPRv2	Lentiviral construct for PIK3CA-targeting CRISPR/Cas9 expression with Puromycin resistance	Lab construct
SYK_lentiCRISPRv2	Lentiviral construct for SYK-targeting CRISPR/Cas9 expression with Puromycin resistance	Lab construct
TBK1_lentiCRISPRv2	Lentiviral construct for TBK1-targeting CRISPR/Cas9 expression with Puromycin resistance	Lab construct
TLR3_lentiCRISPRv2	Lentiviral construct for TLR3-targeting CRISPR/Cas9 expression with Puromycin resistance	Lab construct
TLR7_lentiCRISPRv2	Lentiviral construct for TLR7-targeting CRISPR/Cas9 expression with Puromycin resistance	Lab construct
TMEM173_lentiCRISPRv2	Lentiviral construct for TMEM173-targeting CRISPR/Cas9 expression with Puromycin resistance	Lab construct
TRIM5a_lentiCRISPRv2	Lentiviral construct for TRIM5a-targeting CRISPR/Cas9 expression with Puromycin resistance	Lab construct
TRIM25_lentiCRISPRv2	Lentiviral construct for TRIM25-targeting CRISPR/Cas9 expression with Puromycin resistance	Lab construct
TRIM28_lentiCRISPRv2	Lentiviral construct for TRIM28-targeting CRISPR/Cas9 expression with Puromycin resistance	Lab construct

Table 3.1. Complete list of plasmids used in this study.

OLIGO NAME	SEQUENCE (5' to 3')	PURPOSE OF USE
DDX58_top	CACCGTCGCTGCTCGGTGGTCATGC	pspCas9 cloning
DDX58_bottom	AAACGCATGACCACCGAGCAGCGAC	pspCas9 cloning
DDX58_forward	ATACTAAGGAAGAGCCCT	Genomic DNA PCR for RFLP and sequencing of DDX58 CRISPR target site
DDX58_reverse	TCGGAAAATCCCTGCTTT	Genomic DNA PCR for RFLP and sequencing of DDX58 CRISPR target site
DDX58 ssODN	CGGATATAATCCTGGAAGGCTTGCAGGCT GCGTCGCTGCTCGGTGGAATCCCGGCCTC TGCTTGCAGCTAGCTACGTTCCCCGCAGGC TGTGCCTC	For HDR in DDX58 transcription start site
IFIH1_top	CACCGTGAGAAAGAAAGATGTCAA	pspCas9 cloning
IFIH1_bottom	AAACTTCGACATCTTTCTTCTCAC	pspCas9 cloning
IFIH1_forward	ATGCACTTATCCAAGACG	Genomic DNA PCR for RFLP and sequencing of IFIH1 CRISPR target site
IFIH1_reverse	GACCCTGCTTCTCTAAGT	Genomic DNA PCR for RFLP and sequencing of IFIH1 CRISPR target site
IFIH1 ssODN	CAGCACCATCTGCTTGGGAGAACCCTCTCC CTTCTCTGAGAAAGAGTCGACTCGAATGG GTATTCCACAGACGAGAATTTCCGCTATCT CATCTCGT	For HDR in IFIH1 transcription start site
TBK1_top	CACCGAGAGCACTTCTAATCATCTG	pspCas9 cloning
TBK1_bottom	AAACCAGATGATTAGAAGTGCTCTC	pspCas9 cloning
TBK1_forward	ACATTGGCTAGAACTGAAC	Genomic DNA PCR for RFLP and sequencing of TBK1 CRISPR target site
TBK1_reverse	TCTTCAGACAAAGGGATCAA	Genomic DNA PCR for RFLP and sequencing of TBK1 CRISPR target site
TBK1 ssODN	TATAACAAGAGGATTGCCTGATCCAGCCA AGATTCAGAGCACTTCGAATTCTCTGTGGC TTTTATCTGATATTTTAGGCCAAGGAGCTA CTGCAAAT	For HDR in TBK1 transcription start site
TRIM5a_top	CACCGGAATAGCTACTATGGCTTC	pspCas9 cloning
TRIM5a_bottom	AAACGAAGCCATAGTAGCTATTCCC	pspCas9 cloning

TRIM5a_forward	CACAAAGCCAGCAAATGA	Genomic DNA PCR for RFLP and sequencing of TRIM5a CRISPR target site
TRIM5a_reverse	CCTTTTCTTATTCTCCCT	Genomic DNA PCR for RFLP and sequencing of TRIM5a CRISPR target site
TRIM5a ssODN	AGAGGAACCTCAGCAGCCAGGACAGGCAG GAGCAGTGGAAATAGCTGAATTCGCTTCTGG AATCCTGGTTAATGTAAAGGAGGAGGTGA CCTGCCCA	For HDR in TRIM5a transcription start site
TBK1_A2_top	CACCGCATAAGCTTCCTTCGTCCAG	LentiCRISPRv2 cloning
TBK1_A2_bottom	AAACCTGGACGAAGGAAGCTTATGC	LentiCRISPRv2 cloning
DDX58_A1_top	CACCGGGTCTTCCGGATATAATCC	LentiCRISPRv2 cloning
DDX58_A1_bottom	AAACGGATTATATCCGGAAGACCCC	LentiCRISPRv2 cloning
IFIH1_A1_top	CACCGCGAATTCCCGAGTCCAACCA	LentiCRISPRv2 cloning
IFIH1_A1_bottom	AAACTGGTTGGACTCGGAATTCGC	LentiCRISPRv2 cloning
TRIM5a_A2_top	CACCGGTATGACAAAACCAACGTCT	LentiCRISPRv2 cloning
TRIM5a_A2_bottom	AAACAGACGTTGGTTTTGTCATACC	LentiCRISPRv2 cloning
TRIM25_A2_top	CACCGAAAGCCAGTCTACATCCCCG	LentiCRISPRv2 cloning
TRIM25_A2_bottom	AAACCGGGGATGTAGACTGGCTTTC	LentiCRISPRv2 cloning
TLR3_A1_top	CACCGTTCGGAGCATCAGTCGTTGA	LentiCRISPRv2 cloning
TLR3_A1_bottom	AAACTCAACGACTGATGCTCCGAAC	LentiCRISPRv2 cloning
TLR7_A1_top	CACCGAAGGAATAGTCACCTCCGTA	LentiCRISPRv2 cloning
TLR7_A1_bottom	AAACTACGGAGGTGACTATTCCTTC	LentiCRISPRv2 cloning
IRF3_B1_top	CACCGATCTACGAGTTTGTGAACTC	LentiCRISPRv2 cloning
IRF3_B1_bottom	AAACGAGTTCACAACTCGTAGATC	LentiCRISPRv2 cloning
IRF7_A2_top	CACCGCGCTCGCTTCGTGATGCTG	LentiCRISPRv2 cloning
IRF7_A2_bottom	AAACCAGCATCACGAAGCGACGCGC	LentiCRISPRv2 cloning
IRF9_A1_top	CACCGGAAGTGTGCTGTCGCTTGA	LentiCRISPRv2 cloning

IRF9_A1_bottom	AAACTCAAAGCGACAGCACAGTTCC	LentiCRISPRv2 cloning
MAPK14_A2_top	CACCGCTTATCTACCAAATTCTCCG	LentiCRISPRv2 cloning
MAPK14_A2_bottom	AAACCGGAGAATTTGGTAGATAAGC	LentiCRISPRv2 cloning
MAP3K7_A2_top	CACCGTAGACCAACAACGAGTCATC	LentiCRISPRv2 cloning
MAP3K7_A2_bottom	AAACGATGACTCGTTGTTGGTCTAC	LentiCRISPRv2 cloning
MAVS_A2_top	CACCGTTCAGTAGTCAGACGCCGC	LentiCRISPRv2 cloning
MAVS_A2_bottom	AAACGCGGGCTGCACTAGTGAAC	LentiCRISPRv2 cloning
TMEM173_A1_top	CACCGGCGGGCCGACCGCATTGGG	LentiCRISPRv2 cloning
TMEM173_A1_bottom	AAACCCCAAATGCGGTCGGCCCCGCC	LentiCRISPRv2 cloning
JAK3_A2_top	CACCGAATCCTTGCGTAGCCGAAG	LentiCRISPRv2 cloning
JAK3_A2_bottom	AAACCTTCGGGGCTACGCAAGGATTC	LentiCRISPRv2 cloning
PIK3CA_A1_top	CACCGTACACAGACACTCTAGTATC	LentiCRISPRv2 cloning
PIK3CA_A1_bottom	AAACGATACTAGAGTGTCTGTGTAC	LentiCRISPRv2 cloning
MAPK8_A2_top	CACCGTAGTAGCGAGTCACTACATA	LentiCRISPRv2 cloning
MAPK8_A2_bottom	AAACTATGTAGTGACTCGCTACTAC	LentiCRISPRv2 cloning
TRIM28_B3_top	CACCGTTGCACATAACCAGATCGCC	LentiCRISPRv2 cloning
TRIM28_B3_bottom	AAACGGCGATCTGGATATGTGCAAC	LentiCRISPRv2 cloning
LCK_A3_top	CACCGGCCAGATCTCCGTCGTGAG	LentiCRISPRv2 cloning
LCK_A3_bottom	AAACCTCACGACGGAGATCTGGGCC	LentiCRISPRv2 cloning
SYK_A1_top	CACCGGAAAAGAAGTTCGACACGCTC	LentiCRISPRv2 cloning
SYK_A1_bottom	AAACGAGCGTGTGCGAACTTCTTCC	LentiCRISPRv2 cloning
hU6_forward	GAGGGCCTATTTCCCATGATTCC	LentiCRISPRv2 sequencing primer
V2 adapter forward	AATGGACTATCATATGCTTACCGTAACTTG AAAGTATTTTCG	PCR1 of GeCKO Library A and B samples

V2 adapter reverse	TCTACTATTCTTTCCCCTGCACTGTTGTGGG CGATGTGCGCTCTG	PCR1 of GeCKO Library A and B samples
GECKO F01	AATGATACGGCGACCACCGAGATCTACAC TCTTTCCCTACACGACGCTCTTCCGATCTTA AGTAGAGTCTTGTGGAAAGGACGAAACAC CG	PCR2 of GeCKO Library A samples used for NGS
GECKO F02	AATGATACGGCGACCACCGAGATCTACAC TCTTTCCCTACACGACGCTCTTCCGATCTAT ACACGATCTCTTGTGGAAAGGACGAAACA CCG	PCR2 of GeCKO Library B samples used for NGS
GECKO R02	CAAGCAGAAGACGGCATAACGAGATGTGAC TGGAGTTCAGACGTGTGCTCTTCCGATCTT TCTACTATTCTTTCCCCTGCACTGT	PCR2 of GeCKO Library A and B samples used for NGS

Table 3.2. Complete list of primers and oligonucleotides used in this study.

3.1.11 DNA Ladder

DNA ladder used in this study is shown in Appendix E.

3.1.12 DNA sequencing

Sequencing service was commercially provided by McLab, CA, USA. (<http://www.mclab.com/>).

3.1.13 Software, computer-based programs and websites

The software and computer based programs used in this project are listed in Table 3.3.

SOFTWARE, PROGRAM, WEBSITE NAME	COMPANY/ADDRESS	PURPOSE OF USE
FlowJo v10	Tree Star Inc.	Viewing and analyzing flow cytometry data
CLC Main Workbench v7.7	CLC bio	Constructing vector maps, restriction analysis, DNA sequencing analysis, DNA alignments, etc
Ensembl Genome Browser	http://www.ensembl.org/index.html	Human genome sequence information
LightCycler 480 SW 1.5	ROCHE	Analyzing qPCR results
Image Studio	LI-COR Biosciences, Lincoln, Nebraska, USA	Analyzing immune cell signaling array output
MIT CRISPR design tool	http://crispr.mit.edu/	Website for CRISPR design and off-target analysis
Addgene	https://www.addgene.org/	Plasmid map and sequence information, CRISPR design tool guidelines
GeCKO v.2 Library	http://www.genome-engineering.org/gecko/	Plasmid map, protocols and sequence information of all CRISPR constructs used in the GeCKO v.2 Library
GraphPad Prism v7	GraphPad Software, Inc., San Diego, CA, USA	Data analysis, statistical analysis

Table 3.3. Complete list of software and programs.

3.2 Methods

3.2.1 Bacterial cell culture

Bacterial culture growth: *E.coli* cells were cultured in LB media with required antibiotics and grown at 37°C with 220 rpm shaking. For single colony picking, cells were spread on petri dishes prepared with required antibiotics by the use of glass beads and incubated overnight at 37°C without shaking. For long term storage of bacteria, single colonies grown overnight in liquid culture were further diluted 1:3 and were grown for another 3 hours at 37°C with 220 rpm shaking. Bacteria were taken at log phase of growth and mixed with glycerol in 1ml at final 10% (w/v) and preserved in cryotubes at -80°C.

Preparation of competent bacteria: Previously obtained competent *E.coli* cells were incubated in 50 ml LB without any antibiotics in a 250ml-flask and grown overnight (approximately 16 hours) at 37°C with 220 rpm shaking. The following day, 4 ml of overnight-grown culture was added into 400 ml of LB without any antibiotics in a 2L-flask and incubated at 37°C with 220 rpm shaking until OD₅₉₀ is around 0.375. The culture is aliquoted into eight 50ml-tubes and incubated on ice for 5-10 minutes. Cells were kept cold and centrifuged at 1600g for 10 minutes always at 4°C from then on. Then supernatant was discarded and each pellet was resuspended in 10 ml of ice-cold CaCl₂ solution and centrifuged at 1100g for 5 minutes again at 4°C. Then supernatant was discarded and each pellet was resuspended in 2 ml of ice-cold CaCl₂ solution. Cells were kept on ice for 30 minutes and finally all were combined in one tube and distributed into 200 µl aliquots that were snap-frozen in liquid nitrogen and stored at -80°C.

Transformation of competent bacteria: Competent *E.coli* cells were kept in 200 µl aliquots at -80°C. For each transformation, plasmid DNA and competent *E.coli* cells were thawed on ice. Plasmid DNA was added to competent *E.coli* cells at desired amounts and cells were further incubated on ice for 30 minutes. The cells were then taken to heat block

pre-adjusted to 42°C and heat shocked for 90 seconds and immediately taken to ice for another minute. 800 µl of LB was added to each tube and competent cells were incubated at water bath pre-adjusted to 37°C for 45 minutes. All cells were centrifuged at 13,200 rpm for 1 minute and the pellet was resuspended in 100 µl volume to be spread on petri dishes. Glass beads were placed on petri dishes prepared with LB agar containing appropriate antibiotic and 100 µl bacterial cell suspension was spread equally on the plate surface. Plates were then incubated at 37°C without shaking overnight.

Plasmid DNA isolation: Invitrogen or Macherey-Nagel Mini-Midiprep Kits were applied according to manufacturer's protocols. The resultant DNA concentration and purity were obtained by a NanoDrop spectrophotometer.

3.2.2 Mammalian cell culture

Maintenance of cell lines: 293FT cells were maintained in complete DMEM medium in sterile tissue culture flasks with filtered caps at an incubator set to 37°C with 5% CO₂. Cells were split when maximum 90% confluency was reached. Cells were washed with PBS and trypsin was added to cell culture flasks and incubated at an incubator set to 37°C with 5% CO₂ for 5-6 minutes. Then the cells were resuspended in complete DMEM and split at 1:3 to 1:8 ratio and split every two days, never letting them reach full confluency. NK-92 cells were maintained in SCGM supplied with 20% heat-inactivated fetal bovine serum and 1000 U/ml human Interleukin-2 (IL-2) in sterile tissue culture flasks with filtered caps at an incubator set to 37°C with 5% CO₂. Cells were kept at a density between 300,000 cells/ml to 1,000,000 cells/ml and fresh IL-2 was added every 48 hours. YTS cells were maintained in complete RPMI medium in sterile tissue culture flasks with filtered caps at an incubator set to 37°C with 5% CO₂. Cells were kept at a density between 300,000 cells/ml to 1,000,000 cells/ml.

Cell freezing: Regardless of cell type, cells were split one day before freezing to a concentration of 500,000 cells/ml for suspension cells and to a confluency of 30-40% for adherent cells. The next day, cells to be frozen were counted and at least 3x10⁶ cells were frozen per vial. For each vial, cells were centrifuged at 300g for 5 minutes where supernatant was discarded and the pellet was resuspended in 0.5ml FBS and incubated on

ice for 15-20 minutes. In the meantime, 0.5 ml FBS with 12% DMSO was prepared fresh and incubated on ice. When the incubation was over, 0.5 ml cell suspension was mixed with 0.5 ml freezing medium to reach 6% DMSO in 1 ml. Cells were stored in cryotubes first in -80°C, then in liquid nitrogen for long term storage.

Cell thawing: Cells preserved in liquid nitrogen in cryotubes were taken on ice and slowly brought to RT. 15 ml tubes were prepared for each cell with 5 ml FBS. When the cell suspension was at RT, 1 ml frozen sample was pipetted very carefully into FBS, taking 2-3 minutes in total to avoid harming cells and dilute remnants of DMSO. The cells were then centrifuged at 300g for 5 minutes and supernatant was discarded. The cell pellet was resuspended with complete media to reach 500,000-700,000 cells/ml concentration and the cells were followed every day after thaw.

Lentiviral vector production: For lentiviral vector production, 14×10^6 293FT cells were cultured overnight in poly-L-lysine-coated 150mm cell culture plates. Next morning, cells were transfected with 30µg gene-of-interest (GOI) plasmid (LeGO-G2, LeGO-G2-Puro or LeGO-T2 unless specified differently) (Weber, Bartsch, Stocking, & Fehse, 2008) expressing eGFP (or tdTomato) in combination with 15ug pMDLg/pRRE (*Gag/Pol*), 10µg pRSV-Rev (*Rev*) and 5µg pHCMV-VSV-G (*Env*) plasmids using Calcium Phosphate transfection kit in the presence of 25 µM chloroquine. Approximately 10-12hr later medium was changed and afterwards virus containing media was collected at 24hr and 36hr time points, filtered with 0.45 µm filters. Aliquots were taken from each virus production and stored at -80°C with no repeated freeze and thaw cycle. Serum-free virus batches were obtained by purifying 40 ml viral supernatant using Vivapure LentiSELECT 40 kit according to manufacturer's protocol.

Virus titer determination: Virus titer was obtained by transducing 5×10^5 293FT cells per well in 24-well plates with serial dilution of viral supernatant for 16 hours in the presence of 8 µg/ml Protamine Sulfate. GFP for LeGO-G2 virus was analyzed by flow cytometry on day 3 after transduction. GFP vs SSC plots were used to calculate GFP⁺ cell numbers (likewise, PE was used for LeGO-T2 virus). Flow cytometry plots for a sample analysis are represented in Figure 3.1. GFP percentages that were below 20% are selected for titer calculation (Kustikova et al., 2003) (the linearity of virus amount and GFP percentage are reliable up until this limit; above that value there can be one cell getting more than one infectious particle so the titer would not be correct).

For 0.1 μl and 0.5 μl viral supernatant, GFP percent was converted to cell numbers to get the values for infectious particles, assuming that starting cell number was exactly 5×10^5 and one cell was infected by one viral particle. Then the average of these two calculations are used as the titer of viral vector in terms of infectious particles per ml.

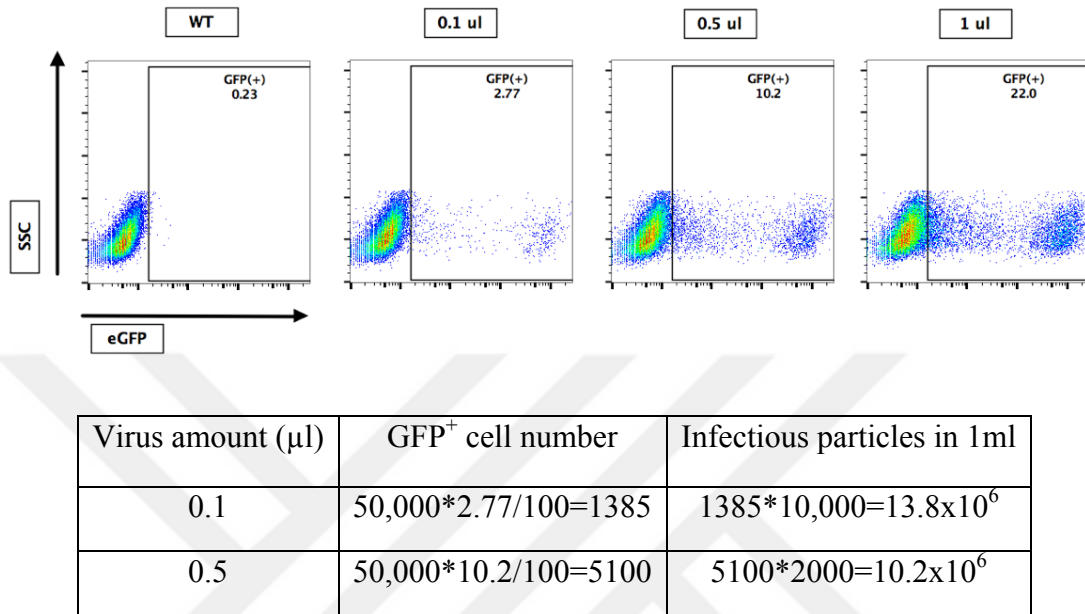


Figure 3.1. Sample analysis for virus titer determination. 293FT cells were transduced with 0.1, 0.5 or 1 μl viral supernatant and GFP percent was analyzed by flow cytometry on day 3 post transduction.

Lentiviral transduction: Lentiviral transduction of NK-92 cells was done with 2×10^5 cells per well in 24-well tissue culture plates, at specified multiplicity of infection (MOI) in the presence or absence of inhibitor BX795 (3 to 6 μM final concentration was used), 1000 U/ml IL-2 and 8 $\mu\text{g/ml}$ Protamine Sulfate for 6 hours unless specified otherwise. After culturing cells in virus containing media for the given time, plates were centrifuged for 15 minutes at 1000g with acceleration 9 and deceleration 4 for transductions done in 24-well plates. For larger scale transductions, cells were taken to sterile tubes and centrifuged at 300g for 5 minutes. Virus containing supernatant was completely removed and cells were cultured in their regular growth media for 72 hours before GFP expression was assessed by flow cytometry. Same procedure was followed for YTS cells, except for culturing media conditions.

Flow cytometry: For surface staining, NK-92 cells were washed once with PBS and stained with anti-CD56-APC as required according to provider's protocol on ice and in

dark for 30 minutes. Cells were washed once more and carried on to analysis. Gating strategy was always the same in all flow cytometry experiments; first on single cells then to CD56^{high} GFP⁺ cell percentage was indicated in the results. Cells were acquired by using FACScanto and analysis was done by FlowJo software. For intracellular staining with P-STAT3, RIG-I or IRF7 required amount of antibody was used following manufacturer's protocol. As a positive control for P-STAT3 detection, cells were cultured with 20 ng/μl IL-21. Transduction was done in the presence of 6 μM BX795 or DMSO control and virus was used at MOI 20. After 30 minutes of culture, cells were diluted 1:2 in 4% PFA solution pre-warmed to 37°C and incubated for another 15 minutes for fixation. Cells were then washed with ice-cold PBS, and resuspended in 500 μl ice-cold Methanol (100%) for permeabilization, that was added drop by drop while vortexing. Samples were stored on ice for 15 minutes and washed twice with ice-cold PBS. Antibody was added in required amounts and incubated on ice and dark for 30 minutes. Cells were washed twice again as indicated and acquired at FACScanto.

Immune cell signaling array: Normal or serum-free growing NK-92 cells were transduced with normal or serum-free virus at MOI 20 as indicated above, at various conditions. 5x10⁵ to 1x10⁶ cell lysates were collected according to manufacturer's protocol. The PathScan® Immune Cell Signaling Antibody Array Kit (Fluorescent Readout) is a multi-sample immunoblotting kit that enables one to compare 16 different conditions and 21 different protein levels of the signaling events in immune cells on the same slide (Figure 3.2). The antibodies readily found on the slide were Erk1/2 (Thr202/Tyr204), Akt (Ser473), p38 MAPK (Thr180/Tyr182), SAPK/JNK (Thr183/Tyr185), Caspase-7 (Asp198 cleavage), IκBα (total), IκBα (Ser32/36), TAK1 (Ser412), Stat1 (Tyr701), Stat1 (Ser727), Stat3 (Tyr705), Stat3 (Ser727), Stat5a (Tyr694), Stat6 (Tyr641), Lck (Tyr416), Syk (Tyr352), Zap-70 (Tyr319), RIG-I (total), and IRF-3 (total). A biotinylated detection antibody was used as a secondary antibody and then streptavidin was used to detect fluorescence by an image scanner. Images were analyzed by Image Studio.

	Target	Site	Modification
1	Positive control		N/A
2	Negative control		N/A
3	Erk1/2	Thr202/Tyr704	phosphorylation
4	Akt	Ser473	phosphorylation
5	p38 MAPK	Thr180/Tyr182	phosphorylation
6	SAPK/JNK	Thr183/Tyr185	phosphorylation
7	Caspase-7	Asp198	cleavage
8	IκBa	Total	N/A
9	IκBa	Ser32/36	phosphorylation
10	TAK1	Ser412	phosphorylation
11	STAT1	Tyr701	phosphorylation
12	STAT1	Ser727	phosphorylation
13	STAT3	Tyr705	phosphorylation
14	STAT3	Ser727	phosphorylation
15	STAT5α	Tyr694	phosphorylation
16	STAT6	Tyr641	phosphorylation
17	Lck	Tyr416	phosphorylation
18	Syk	Tyr352	phosphorylation
19	ZAP70	Tyr319	phosphorylation
20	RIG-I	Total	N/A
21	IRF3	Total	N/A

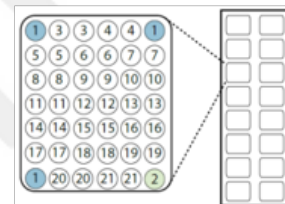
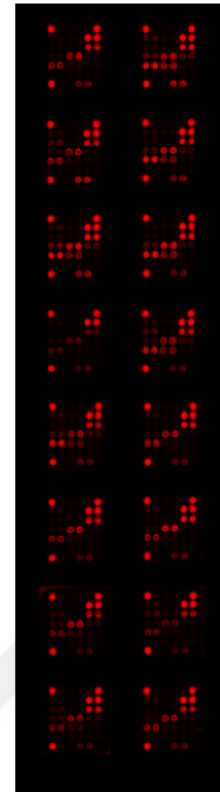


Figure 3.2. Immune cell signaling array template. On a multi-sample immunoblotting kit, one can compare 16 different conditions and 21 different protein levels of the signaling events in immune cells on the same slide. A biotinylated detection antibody is used as a secondary antibody and then fluorescence-labelled streptavidin is used to detect emitted light by an image scanner. Image Studio software is used for quantification of signal values. Image is from one representative experiment where all 16 conditions are different.

Apoptosis assay: NK-92 cells were harvested at 2.5×10^5 cells per well amount in 24-well plates in 0.5 ml volume per well in the presence of indicated amounts of BX795 or DMSO control for 6 hours. Cells were first stained with antiCD56-APC as explained above and then stained with FITC Annexin V Apoptosis Detection Kit according to manufacturer's protocol.

RNA isolation and qRT-PCR: $3-4 \times 10^6$ cells were used for RNA isolation as suggested by manufacturer's protocol. qRT-PCR was performed with TaqMan probes in LightCycler-480 according to TaqMan Universal Master Mix II program suggestion.

3.2.3 CRISPR design and assembly

Throughout this study, there are two types of CRISPRs used: the ones cloned into pspCas9(BB) plasmids for transient expression by transfection method and the ones cloned into lentiCRISPRv2 for stable expression by lentiviral transduction method.

CRISPR design and off-target analysis: CRISPR design was carried out using human genome sequences for required target genes retrieved from ensembl.org and CLC Main Workbench software following guidelines from Zhang Lab provided on addgene.org. Required CRISPR target sequences were uploaded on crispr.mit.edu website provided by Zhang Lab of MIT for off-target score analysis of the designed CRISPRs. CRISPRs with lowest off-target binding were selected for assembly. Selected guide RNA sequences were ordered in top and bottom strand oligonucleotide format with flanking sequences that would ligate with the pspCas9(BB) plasmids with BbsI enzyme and lentiCRISPRv2 plasmid after digestion with BsmBI restriction enzyme. For selected genes, guide RNA sequences from GeCKO v.2 library were obtained and included in lentiCRISPR construct design.

Oligo annealing: For each CRISPR design, top and bottom oligos were ordered from The Midland Certified Reagent Co (TX, USA). After arrival, each oligo was diluted in sterile water to 100 μ M concentration. Then the following reaction was set up for each pair of top and bottom oligos and reaction was completed in a thermocycler as follows:

sgRNA top oligo (100 μ M)	1 μ l
sgRNA bottom oligo (100 μ M)	1 μ l
10X T4 Ligase Buffer	1 μ l
T4 PNK NEB	1 μ l
ddH ₂ O	6 μ l
Total volume	10 μ l

37°C	30 minutes
95°C	5 minutes
Ramp down to 25°C	-5°C per minute

Synthesized oligo pairs were then run on 2% Agarose gel with 0.5X TBE along with single oligo pairs to visualize a shift in oligo-duplex due to increased size when compared to single oligos.

pspCas9 (BB) vectors digest and ligation reactions: pspCas9 (BB)-2A-GFP and pspCas9 (BB)-2A-Puro plasmids were used as the vector in mammalian expression system CRISPR designs used for transfection purposes. Vector digest and ligation with the oligo duplex were completed in the same reaction set up as the following and then treated with Exonuclease V for 30 minutes at 37°C to eliminate non-ligated DNA fragments. Exonuclease V inactivation is completed with final 10mM EDTA at 70°C for 30 minutes.

pspCas9(BB) plasmid	100 ng
Oligo-duplex (1:200)	1 µl
NEB BbsI (10,000 U/ml)	1 µl
NEB T4 ligase	0.5 µl
NEB 10X T4 ligase buffer	2 µl
DTT (10 mM)	1 µl
ATP (10 mM)	1 µl
ddH ₂ O	Up to 20 µl
Total volume	20 µl

37°C	5 minutes
21°C	5 minutes
Repeat cycles 5 times	Total 1 hour

NEB Exonuclease V	1 μ l
NEB 10X Buffer 4	3 μ l
ATP (10 mM)	3 μ l
ddH ₂ O	Up to 30 μ l with the total 20 μ l reaction

These samples were stored at -20oC and 2 μ l out of 35 μ l reaction was used for transformation of each plasmid. For all constructs, negative control ligations were prepared with tubes that did not contain the oligo duplex.

lentiCRISPRv2 vector digest and ligation reactions: lentiCRISPRv2 plasmid was used as the vector in all lentiviral CRISPR designs. First of all, vector was digested according to the following set up with BsmBI restriction enzyme for 2 hours at 55°C at a thermocycler and a filler sequence was removed. Then the full reaction was carried on to CIAP treatment at 37°C for 30 minutes at a thermocycler as follows:

lentiCRISPRv2 plasmid	5 μ g
NEB BsmBI (10,000 U/ml)	3 μ l
NEB 10X 3.1 Buffer	3 μ l
DTT (10 mM)	5 μ l
ddH ₂ O	Up to 30 μ l
Total volume	30 μ l

Full BsmBI digestion reaction	30 μ l
Fermentas CIAP	3 μ l
Fermentas 10X CIAP Buffer	5 μ l
ddH ₂ O	12 μ l
Total volume	50 μ l

The larger sequence (12.5kb) was visualized and extracted from a 1% Agarose gel prepared with 0.5X TBE. Gel extraction was carried out with Macherey-Nagel commercial kit according to manufacturer's protocol. Resultant elution concentration containing the plasmid was measured by a NanoDrop spectrophotometer.

Ligation reaction of gel extracted vector and oligo-duplex was carried out for 15 minutes at RT as follows:

lentiCRISPRv2 gel extract	50 ng
Oligo-duplex (1:200)	1 μ l
NEB T4 DNA ligase	1 μ l
NEB 10X T4 DNA ligase buffer	2 μ l
ddH ₂ O	Up to 20 μ l
Total volume	20 μ l

Transformation and confirmation of positive colonies: For pspCas9(BB) samples, 2 μ l of the above described ligation reaction was used to transform 200 μ l DH5 α competent *E.coli* cells and for lentiCRISPRv2 samples, 10 μ l to 200 μ l Top10 competent *E.coli* cells as described in section 3.2.1. Next day, three colonies were picked from each transformation and miniprep cultures were started. Minipreps for plasmid DNA were carried out the following day with Macherey-Nagel commercial kit according to manufacturer's protocol. Completed minipreps were sent for sequencing of the guide RNA ligation region, with a forward primer binding to human U6 promoter sequence upstream of ligation site (hU6_forward). All CRISPR constructs contained the 20-nucleotide target sequence of relevant genes after the cloning procedure (sequence results can be found in Appendix G).

Transfection with pspCas9(BB) plasmids and ssODNs: 3×10^5 293FT cells were incubated in 6-well plates in the evening. The next morning, 1 μ g of relevant pspCas9(BB)-2A-GFP or -2A-Puro CRISPR construct plasmid (DDX58, IFIH1, TBK1 and TRIM5a) and 2 μ l of 10 μ M relevant ssODN were co-transfected by Calcium Phosphate transfection kit as explained before. pspCas9(BB)-2A-GFP CRISPR transfections were used as control where GFP expression was analyzed 48 hours after transfection. For pspCas9(BB)-2A-

Puro CRISPR transfections, Puromycin selection was started 24 hours after transfection and continued for 3 days.

Single-cell analysis and RFLP: After complete selection, pspCas9(BB)-2A-Puro CRISPR transfection samples were diluted and plated in 96-well plates, by making calculations aiming for 0.5 cell/well in 200 µl volume. On day 7, wells that contain single cell growth were marked. On day 14, cells were expanded to 24-well plates and later to flasks for expansion, genomic DNA isolation, freezing and transduction purposes. Genomic DNA isolation was carried out according to manufacturer's protocol. Each transfection sample (DDX58, IFIH1, TBK1 and TRIM5a) single-cell clone were subjected to PCR spanning the CRISPR binding site and PCR products were further digested with enzymes inserted in the relevant ssODN sequences. IFIH1 colonies were digested with Sall and DDX58, TBK1 and TRIM5a colonies were digested with EcoRI for 2 hours at 37°C. Each PCR and digest product were run on 1.5% agarose gels side-by-side and restriction fragment length polymorphism (RFLP) results were used for mutant colony selection. If digests worked, this was a sign for HDR where ssODN was used as a template for repair. The regions of PCR did not have any other restriction site for the selected enzymes. The design and binding sites of each primer, CRISPR and restriction enzyme can be found in Appendix H.

Sequencing of gDNA PCR products: For selected lentiCRISPRv2 transduced and Puro selected NK-92 cells (DDX58-lentiCRISPR transduction) genomic DNA isolation was followed and PCR products were cloned into InsTA Clone Kit according to manufacturer's protocol. The ligation product was transformed into DH5α competent cells and 24 colonies were picked for miniprep and sent for sequencing.

3.2.4 GeCKO v.2 library transduction work flow

GeCKO v.2 library plasmid prep: Plasmids arrived in two separate stocks, as Library A and B therefore the following protocol was followed for both libraries. The transformation, expansion and plasmid prep were all done according to provider's protocol from www.genome-engineering.org/gecko website.

GeCKO v.2 lentivirus production: Lentivirus production containing Library A or Library B were completed following the protocol explained in section 3.2.2 only with the change of 30 µg of gene-of-interest plasmid with Library A or Library B plasmid prep DNA. Virus titer was obtained by transducing NK-92 cells with serial dilution of viral supernatant. 24 hours after transduction, WT or transduced NK-92 cells were started on 0 or 1µg/ml Puromycin. The growth of cells in terms of cell count was recorded every day afterwards, both from 0 and 1µg/ml Puromycin containing samples. The cell count in Puromycin-containing wells was then divided to the cell count in normal growing wells, finally showing a percent viability directly related to the percentage of transduced cells. According to titration results, optimal amount of virus to be used in experiments was recorded, aiming for at most 20% transduction efficiency in order to make sure there would be only one construct per cell and not more.

Transduction of NK-92 cells with GeCKO v.2 Library A or Library B: 10^7 NK-92 cells were transduced with GeCKO v.2 Library A or Library B virus for 6 hr in the presence of 3 µM BX, aiming for 10-20% transduction efficiency to ensure one construct entry per cell. 24 hr post-transduction, Puromycin selection was started and cells were counted every two days to set the concentration to 0.5×10^6 cells/ml and the surviving cells were named as GeCKO⁺NK-92 cells from then on. Cells were expanded until 50×10^6 cells were reached (two weeks of selection) and 40×10^6 cells from each library were used for genomic DNA isolation and PCR for next generation sequencing of base library.

Transduction of GeCKO⁺NK-92 cells with LeGO-G2 lentiviral vector: 10^7 cells from each GeCKO⁺NK-92 population were transduced with LeGO-G2 virus at MOI 10 for 6 hr in the absence of inhibitor to assess the loss of function effect of candidate genes on lentiviral gene delivery in NK cells. 3 days after LeGO-G2 transduction, GFP expression was analyzed with flow cytometry and GFP⁺ and GFP⁻ populations were sorted and further expanded. 20×10^6 cells from each library GFP⁺ and GFP⁻ populations were used for genomic DNA isolation and PCR for next generation sequencing (NGS).

PCR1 and PCR2 for Next-Generation Sequencing: There were two steps of sequencing sample preparation and they were named as PCR1 and PCR2. The lentiviral construct of lentiCRISPRv2 backbone was the same for all GeCKO targets, therefore it was known which sequences would be integrated into the genome of host cell. PCR1 aimed for amplifying the constructs starting from U6 promoter region of the lentiCRISPR vector,

containing the target sequence and the beginning of the sgRNA scaffold sequence. Once the PCR1 products were obtained, PCR2 was set up with NGS forward and reverse primers that were almost 100 bp in length and add flow cell adapters and barcode sequences. Both PCR protocols were obtained from Shalem et al., 2014 and further optimized.

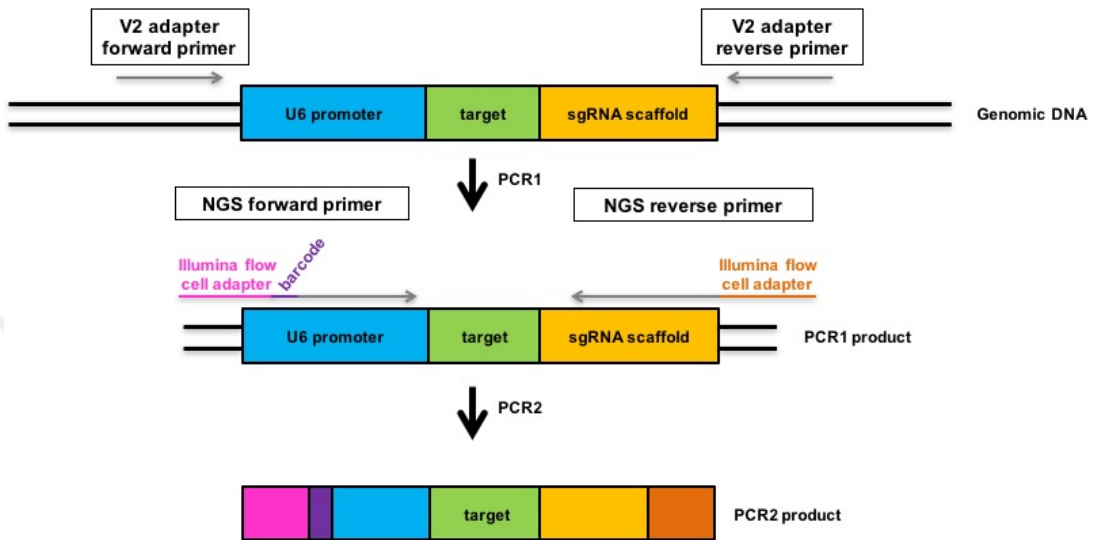


Figure 3.3. GeCKO v.2 library PCR1 and PCR2 strategy. PCR1 with forward and reverse primers amplifies the region integrated into host cell genome, containing the unique sgRNA sequence (green). Then PCR2 uses PCR1 products as templates and adds flow cell adapters for NGS.

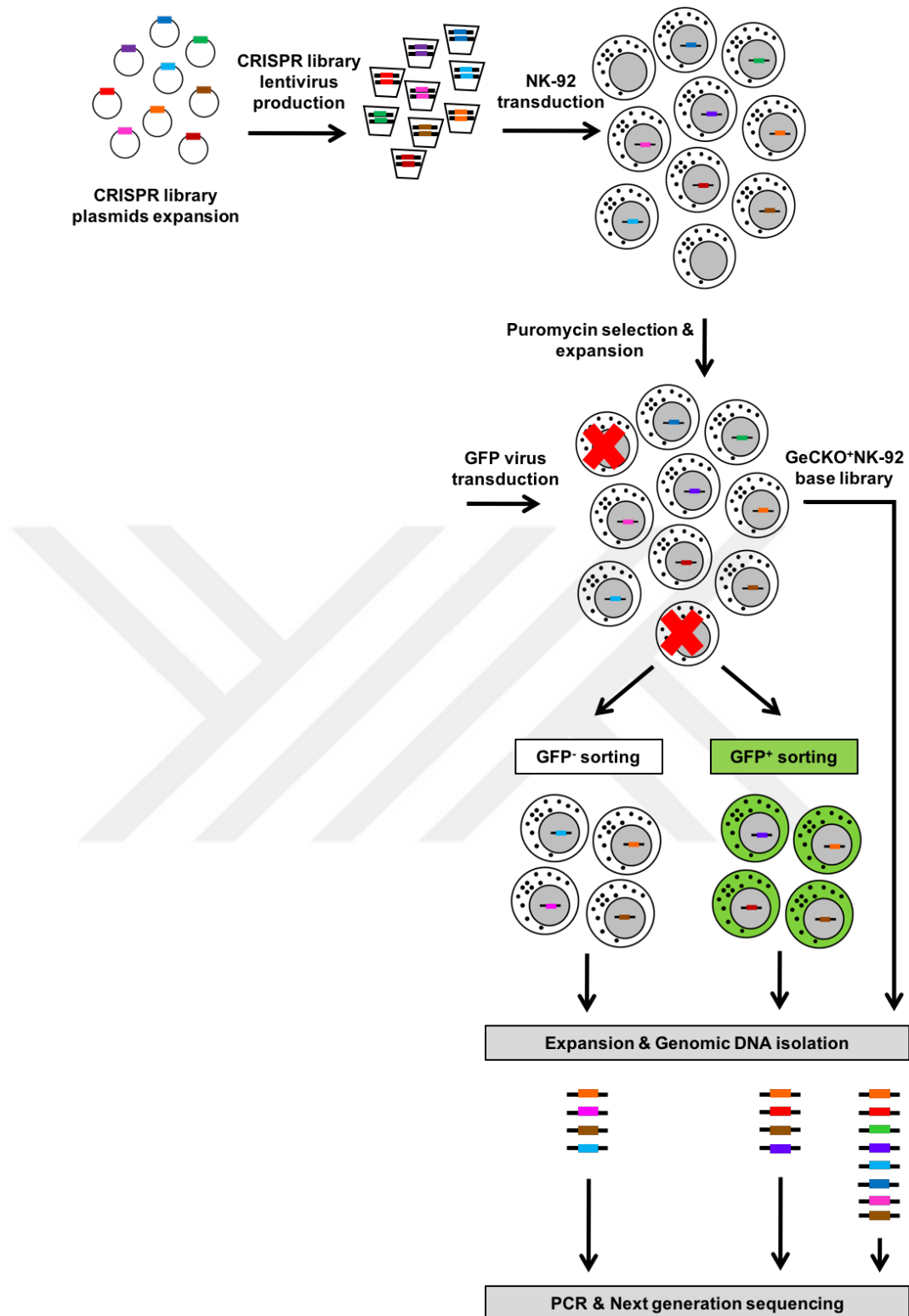


Figure 3.4. GeCKO v.2 library work flow. NK-92 cells are transduced with GeCKO library and Puromycin selection is started 24 hr post transduction. Puro-selected cells are expanded and genomic DNA is taken from this population to use as base library in NGS. LeGO-G2 viral vector for GFP expression is transduced to GeCKO⁺NK-92 cells. Next, GFP⁻ and GFP⁺ cells are sorted and further expanded for genomic DNA isolation to be used as templates for NGS. All procedure is completed for both Library A and B samples.

4. RESULTS

4.1 Optimizing Lentiviral Transduction Parameters in NK Cell Lines

Primary NK cells obtained from human PBMCs show high resistance against viral infections. NK cell lines NK-92 and YTS share this trait. The use of IKK ϵ /TBK1 small molecule inhibitor BX795 during transduction shows remarkable enhancement of gene delivery to primary NK cells (Sutlu et al., 2012) however, the use of this inhibitor with NK cell lines requires further optimization. Thus, transduction parameters such as inhibitor dose, transduction and inhibitor treatment time and MOI values all had to be investigated and optimized with the NK cell lines.

In a standard transduction experiment, cells were incubated with lentiviral vector-containing supernatant for a given time and green fluorescence protein-positive (GFP⁺) population was analyzed 3 days after transduction by flow cytometry. Below is the timeline and the map of mainly used lentiviral vector LeGO-G2 (Figure 4.1).

For flow cytometric analysis of NK-92 transductions, cells were stained with anti-CD56 antibody to gate on a live population of NK-92 cells. Samples were first gated on intact cell population on the FSC/SSC plot named as 'p1', then single cells were gated by using FSC-A/FSC-H, followed by CD56⁺ gating and finally GFP⁺ cell percentage was acquired (Figure 4.2). (On some occasions where CD56 staining was absent, cells were stained with propidium iodide (PI), then gated on PI⁺ samples).

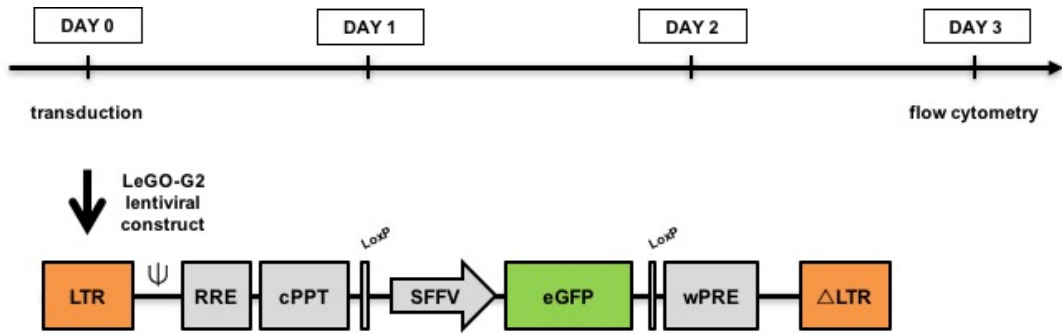


Figure 4.1. Transduction timeline and LeGO-G2 lentiviral construct. Cells were incubated with lentiviral vector containing supernatant for required amount of time, then medium was changed and the cells were left to recover for three days. Flow cytometry analysis was done on day 3 post transduction. The mainly used lentiviral vector LeGO-G2 has Long Terminal Repeats (LTRs) enclosing eGFP gene under the control of SFFV promoter. (RRE: rev response element; cPPT: central polypurine tract; SFFV: Spleen focus-forming virus; wPRE: Woodchuck hepatitis virus post-transcriptional regulatory element)

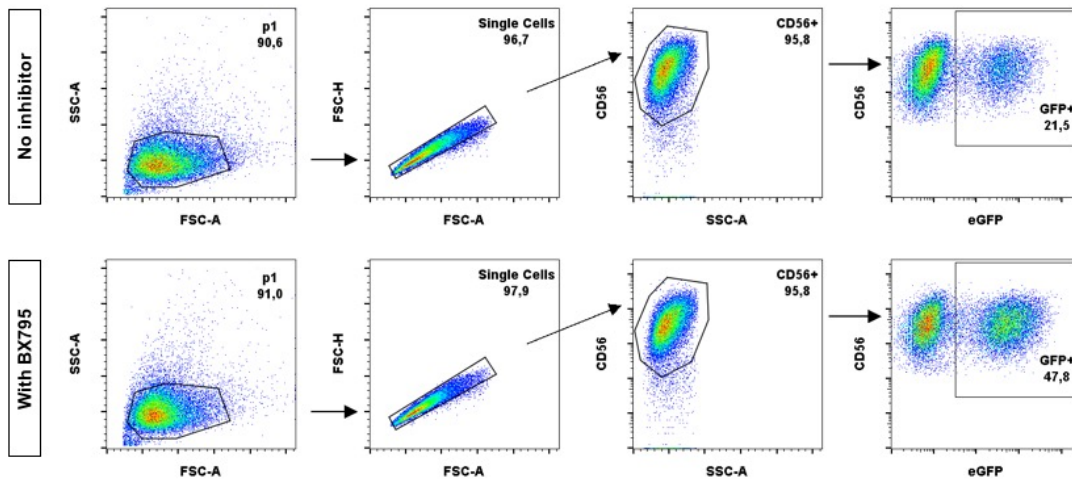


Figure 4.2. NK-92 transduction sample analysis. NK-92 cells were transduced with LeGO-G2 virus for 6 hr in the presence (6 μ M) or absence of BX795. Flow cytometry analysis was done on day 3 post transduction. One representative experiment.

4.1.1 Optimization of transduction time

Knowing that NK cells had very low transduction efficiency, it was important to understand if transduction efficiency was consistently increasing with time of exposure to viral vector. For this purpose, we tested different incubation times of NK-92 cells with

lentiviral vector containing supernatant (at MOI=20) and BX795 during that interval and checked GFP⁺ cells by flow cytometry 72 hours after transduction (Figure 4.3). The results showed that there was viral vector entry at any time point and it could take place as early as fifteen minutes of exposure. Also the effect of inhibitor was prominently observed after one hour of exposure to viral vector, which points out the role of BX795 in events triggered upon viral vector entry that take place after an hour. Still, the optimum results in terms of enhanced efficiency were observed around the 6 hour-time point so we continued to use 6 hours for regular transduction protocols unless specified differently. Furthermore, 3 and 6 μ M BX795 treatment showed comparable transduction efficiency in NK-92 cell line.

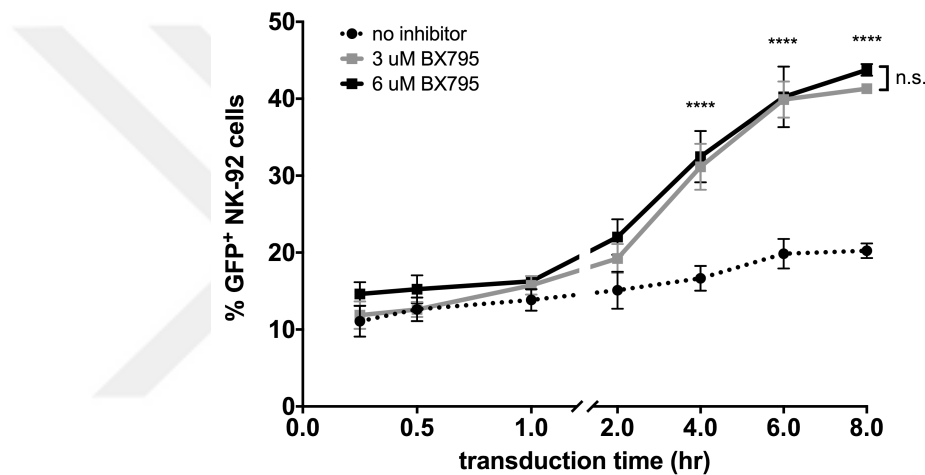


Figure 4.3. NK-92 transduction time determination. NK-92 cells were incubated with LeGO-G2 lentiviral vector containing supernatant at MOI=20 for indicated times in the presence (3 or 6 μ M) or absence of BX795. GFP percent was analyzed by flow cytometry on day 3 post transduction. Data plotted from four independent experiments, error bars indicating SEM. (2way ANOVA analysis, **** p<0.0001; n.s.: not significant)

4.1.2 MOI titration

Some easy-to-transduce cell lines such as 293FT only require MOI values ranging from 0.1 to 0.5 whereas NK cells are resistant to lentiviral transduction at those values. In order to understand the optimum viral load to be used on NK-92 cells, the effect of increasing MOI was tested by trying values ranging from 1.25 to 20 with LeGO-G2 virus for 6 hours with or without the inhibitor and GFP expression was recorded 72 hours after transduction by flow cytometry (Figure 4.4). Without the inhibitor, there was a linear increase with

increasing MOI. Increasing MOI resulted in up to 15% GFP⁺ cells without the inhibitor and above 30% with BX795 at MOI=20. The enhancing effect of BX795 was seen prominently at all MOI values. Thus, NK-92 cells were effectively transduced with lentiviral vectors at MOI=20 in the following experiments.

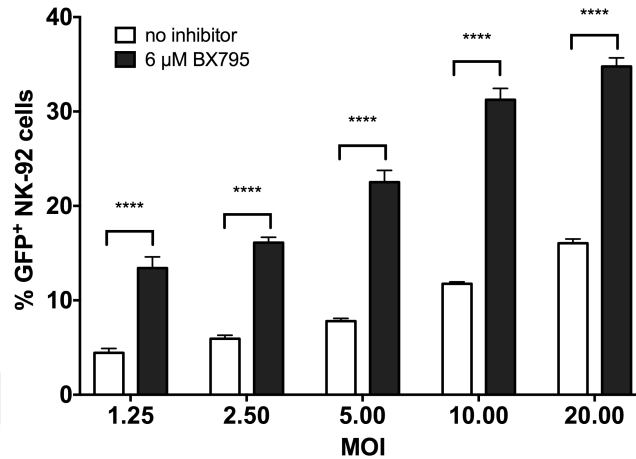


Figure 4.4. NK-92 transduction MOI titration. NK-92 cells were transduced with LeGO-G2 virus at indicated MOI in the presence (6 μM) or absence of BX795. GFP percent was analyzed by flow cytometry on day 3 post transduction. Data plotted from three independent experiments, each run in duplicates; error bars indicating SEM. (2way ANOVA analysis, **** p<0.0001)

4.1.3 BX795 dose titration and toxicity determination

Trials with 3 and 6 μM BX795 treatment during transduction showed similar effects, therefore it was crucial to see the dose-dependent effect of BX795 addition during the transduction of NK-92 cells (Figure 4.5A). Transduction without any inhibitor application (dashed line) resulted in 25% GFP⁺ NK-92 cells and a significant increase in transduction efficiency was observed with increasing doses of BX795, reaching a maximum and remaining as high as 50% between 3-10 μM concentration. Thus, using BX795 at doses 3 to 6 μM showed at least double the efficiency with NK-92 cells when added during 6 hours of transduction. Similarly, transduction efficiency of YTS cells were increased from 23% without any inhibitor (dashed line) to 40% with the addition of BX795 at doses 2 to 4 μM (Figure 4.5B).

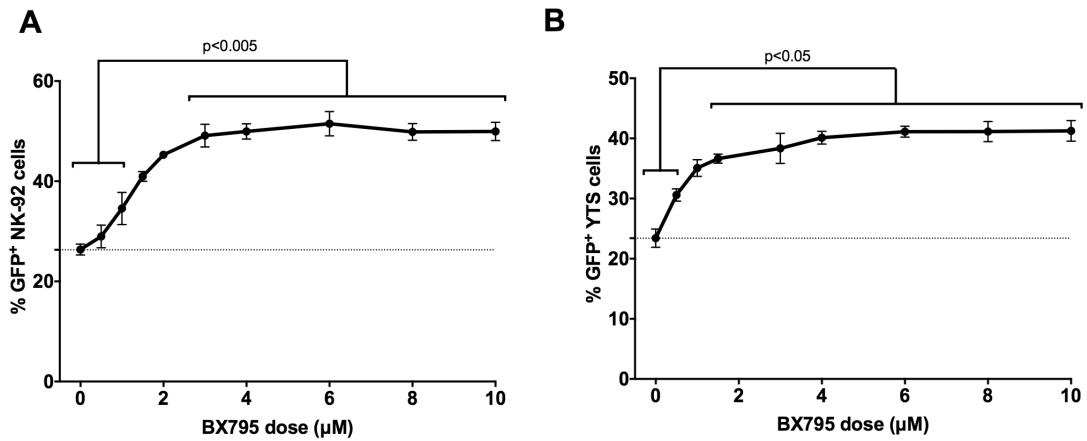


Figure 4.5. BX795 dose titration during transduction. (A) NK-92 cells or (B) YTS cells were transduced with LeGO-G2 virus at MOI=20 in the presence or absence of varying doses of BX795. GFP percent was analyzed by flow cytometry on day 3 post transduction. Data plotted from two independent experiments, each run in triplicates; error bars indicating SEM. (One-way ANOVA analysis)

BX795 presence during 6 hours of transduction became a part of the standard protocol therefore it was crucial to find out if the inhibitor caused any toxicity on cells in this period. When the same set of concentrations were used on NK-92 cells without the viral supernatant, mimicking the experimental conditions of transduction, toxicity was only at basal levels within the range of concentrations of BX795 used (Figure 4.6). Without exceeding the level of 10% death, 1.5 to 6 µM BX795 showed comparable results and could be safely used for transduction period in NK-92 cells.

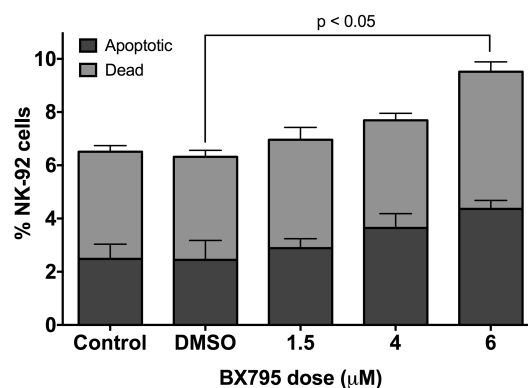


Figure 4.6. BX795 toxicity assay with Annexin V/PI staining. NK-92 cells were incubated with varying doses of BX795 for 6hr and later stained with Annexin V (apoptotic cells) and PI (dead cells). Data plotted from two independent experiments, each run in duplicates. (Multiple t-test analysis)

4.1.4 The reversibility of BX795 treatment on NK-92 cells

Next, we wanted to understand if pre-treatment of NK-92 cells with BX795 would make a difference in transduction efficiency. For this purpose, NK-92 cells were treated with 6 μ M BX795 for 6 hours, washed and transductions were set up immediately or 2, 4 and 6 hours after wash away where no further inhibitor was added and viral supernatant was kept for 6 hours. For comparison, each transduction time point had control samples with no inhibitor and inhibitor added during transduction alone. All transductions were done at MOI=20 and GFP expression was analyzed 72 hours after transduction by flow cytometry (Figure 4.7).

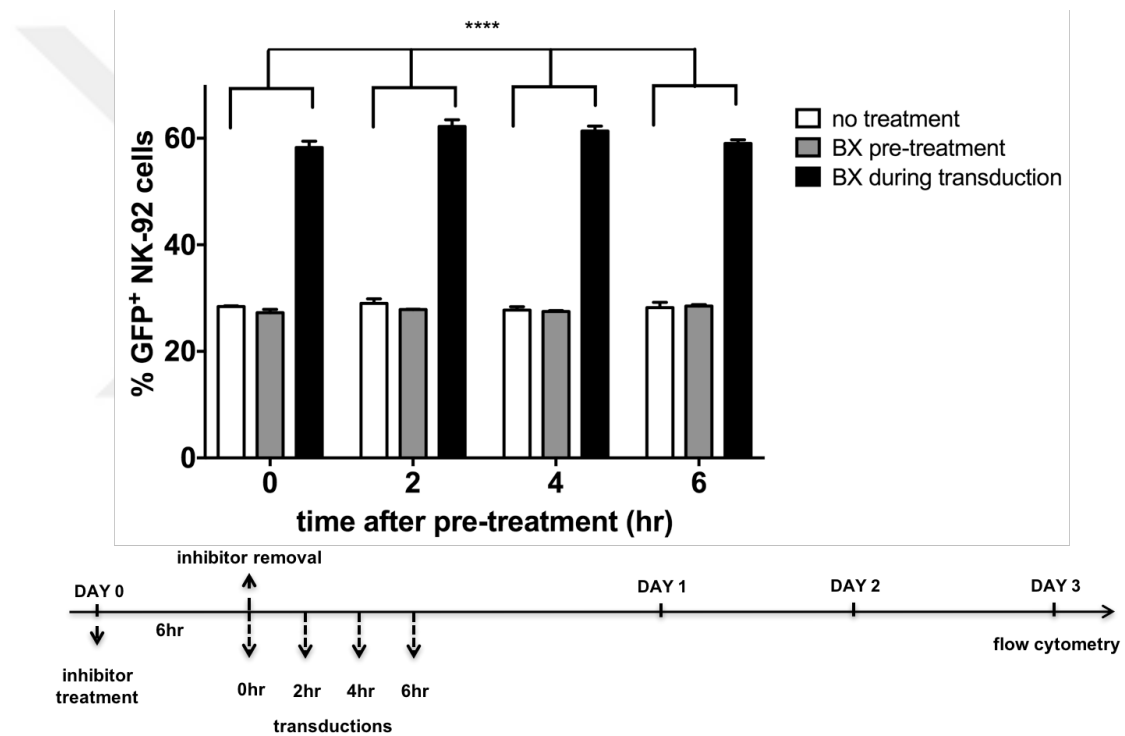


Figure 4.7. The effect of BX795 pre-treatment on NK-92 transduction efficiency. NK-92 cells were treated with 6 μ M BX795 or DMSO (control) for 6 hr and washed away. Untreated (white) or overnight-treated (grey) cells were then transduced with LeGO-G2 virus at MOI=20 at 0, 2, 4 and 6 hours after inhibitor wash-away. One set of cells were treated with 6 μ M BX795 during transduction only (black). GFP percent was analyzed by flow cytometry on day 3 post transduction. Data plotted from one representative experiment, run in duplicates. (2way ANOVA analysis, **** p<0.0001)

Strikingly, all time points showed exactly the same transduction efficiency where the effect of BX795 was completely null after wash away and pre-treatment did not enhance

any of the conditions tried. As a conclusion, it can be stated that BX795 does not have any preparative effects on the host cell and can only act once the viral vector triggers host cell anti-viral response and its effects are completely reversible upon wash away.

4.1.5 Scaling-up the transduction protocol

NK-92 transductions were generally set up in 24-well plates with maximum 1 ml total volume per well. It was necessary to address if larger transduction volume would interfere with transduction efficiency for upcoming experiments that required larger cell numbers. For this purpose, various transduction sizes were compared side by side in 24-well plates (1 ml), T25 (5 ml) and T75 (15 ml) flasks (Figure 4.8A). It was clear that all transduction volumes showed equal transduction efficiency at MOI=5 with LeGO-G2-Puro virus where untreated and BX795-treated samples showed 10% and 25% GFP-Puro⁺ cells respectively.

Next, it was important to know how many days of Puromycin selection was required with these transduction efficiencies (Figure 4.8B). It was observed that with a starting population of 10% GFP-Puro⁺ cells, selection was complete in 6 days. However, with a starting population of 25%, selection took even shorter time and by the end of 6 days both populations could be fully selected. In another setting, three different starting populations named as test1 with 9.13%, test 2 with 25.8% and test 3 with 33.6% GFP-Puro⁺ NK-92 cells were started on selection and GFP percent was analyzed three days later (Figure 4.8C). It was observed that with a starting population above 30%, test 3 resulted in complete selection in just 3 days. Thus, transduction efficiency is not dependent on volume and puromycin selection can be completed in at most one week with a starting population as low as 10% GFP-Puro⁺ cells.

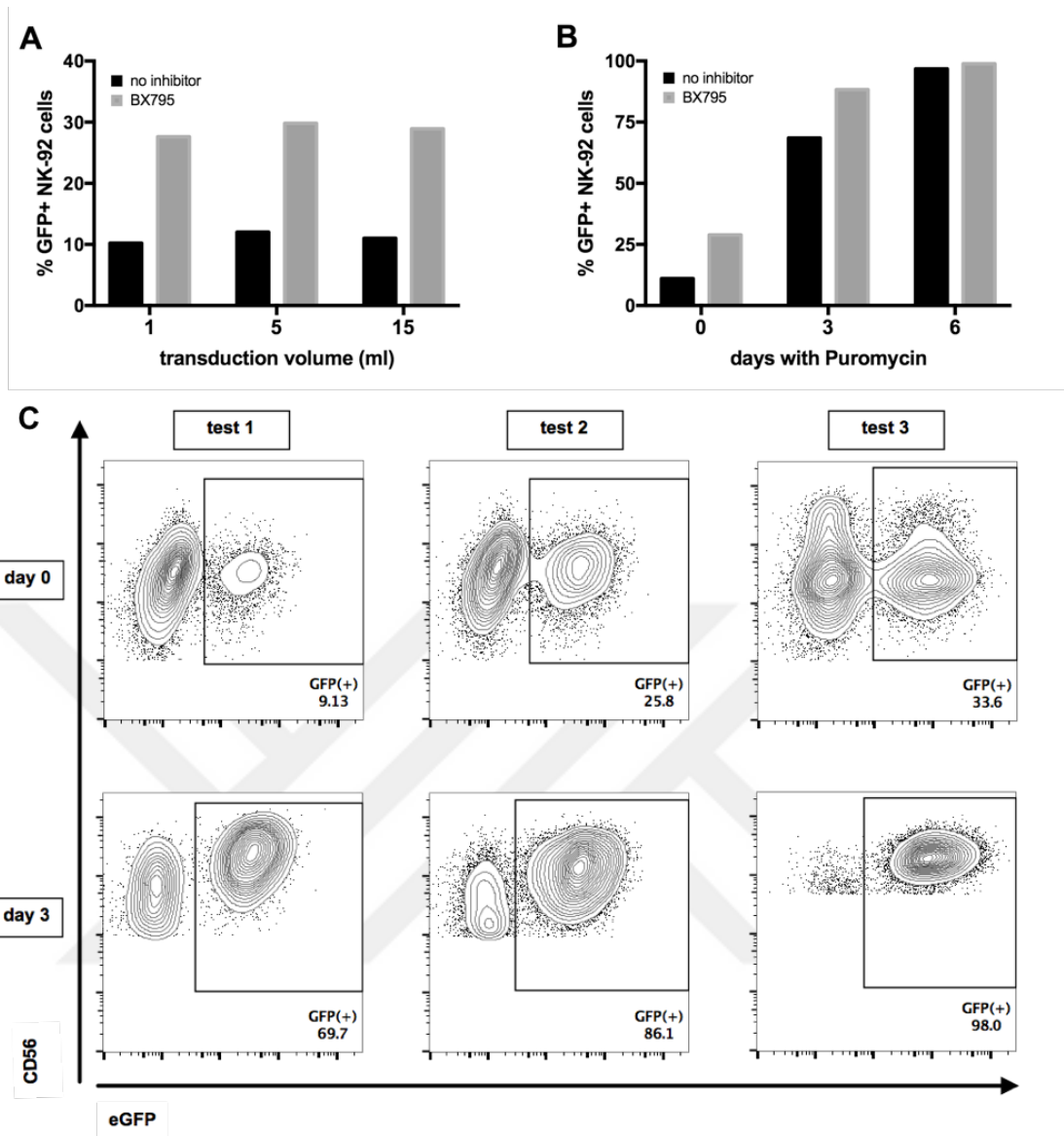


Figure 4.8. Transduction size comparison and Puromycin selection of NK-92 cells. **(A)** NK-92 cells were transduced with LeGO-G2-Puro virus at MOI=5 at indicated sizes in the presence (6 μ M) or absence of BX795. GFP percent was analyzed by flow cytometry on day 3 post transduction. **(B)** 10% (no inhibitor transduction) and 25% (BX795 transduction) GFP-Puro⁺ cells were started on Puromycin (1 μ g/ml) and GFP percent was followed by flow cytometry on days 0, 3 and 6. Data plotted from one representative experiment. **(C)** Flow cytometry plots showing Puro selection with different starting transduction efficiencies named as test1, 2 and 3.

4.1.6 Serum-free growth of NK-92 cells

For certain experiments that require analysis of phosphorylation events that are triggered during anti-viral signaling, cells are advised to be serum-starved for a period of time in order to reduce the background levels of phosphorylation. However, our preliminary experiments have proven that it is very difficult to get reliable results with serum-starvation of NK-92 cells because their viability is deeply affected by this process. To circumvent this problem, NK-92 cells were adapted to serum-free culture by gradually culturing them in media with reduced serum concentration over a period of 4 weeks. The cell culture media serum content was gradually decreased from 20% to 15%, 10%, 5% and finally serum-free culturing was possible (Chrobok et al., manuscript in preparation) (Figure 4.9A). Serum-free culturing of NK-92 cells holds a special place for applications in immunotherapy where cells to be infused to a patient cannot be grown with FBS in the context of clinical trials.

To understand if serum-free growth of NK-92 cells had a significant effect on the profile of the cells or their transduction capability, it was necessary to compare transduction of normal and serum-free-grown NK-92 cells side by side. To eliminate any effect of serum residues coming from the viral supernatant to the serum-free-grown NK-92 cells, the viral supernatant used in these experiments were purified and eluted in serum-free SCGM. Two sets of transductions with non-purified (Figure 4.9B) or purified (Figure 4.9C) LeGO-G2 virus at MOI values 2.5, 5, 10 and 20 showed comparable results for both cell types. Transductions done without the inhibitor or with 6 μ M BX795 showed overlapping GFP⁺ cell percentages for both conditions. Thus, it was evident that the use of serum-free-grown NK-92 cells did not cause any changes in transduction efficiency with non-purified or purified virus.

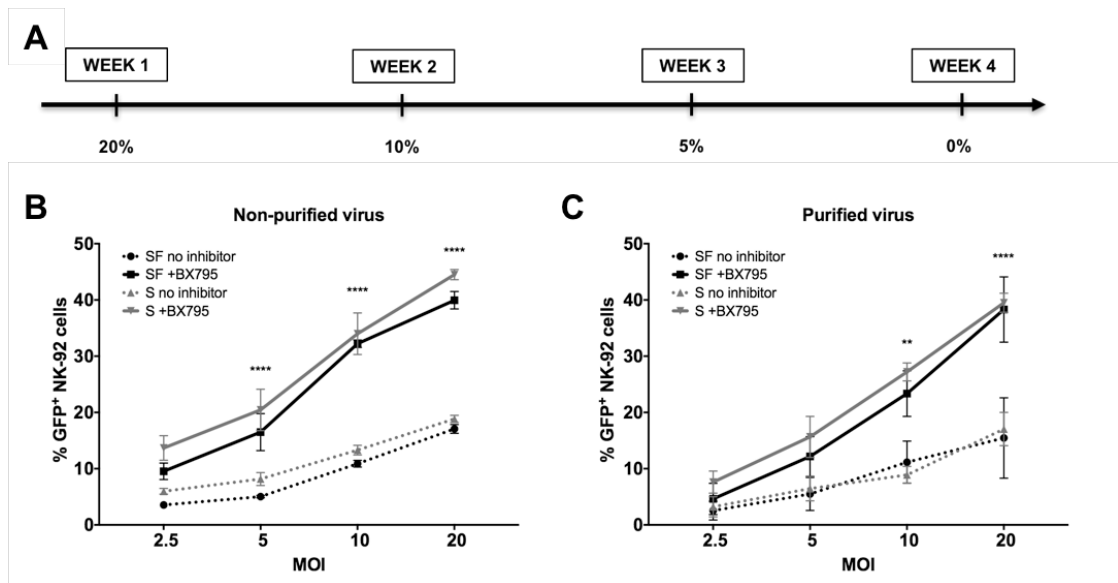


Figure 4.9. Serum-starvation and transduction comparison of normal and serum-free-grown NK-92 cells. **(A)** The cells were gradually split in media containing 20, 10, 5 or 0% FBS at indicated weeks. Normal-grown or serum-free-grown NK-92 cells were transduced with **(B)** non-purified or **(C)** purified LeGO-G2 viruses. Transductions were done in the presence (6 μ M) or absence of BX795. GFP percent was analyzed by flow cytometry on day 3 post transduction. Each graph plotted from two independent experiments, set up as duplicates; error bars with SEM. S: serum-containing normal NK-92; SF: serum-free grown NK-92. (2way ANOVA analysis, ** $p < 0.01$, *** $p < 0.001$, **** $p < 0.0001$)

We also speculated that serum-free-grown NK-92 cells could potentially have altered their cytotoxic profile. To examine this, it was tested whether serum-free NK-92 cells could degranulate against target leukemia cell line K562. When normal or serum-free NK-92 cells were co-cultured with target cell line K562 for four hours in 1:1 effector to target ratio, it was observed that serum-free NK-92 cells still had the capacity to degranulate against target cells (data not shown).

4.1.7 The role of cytokines on lentiviral transduction efficiency

IL-2 has a vital importance for the growth of NK-92 cell line because the cells are completely dependent on continuous supply or they die within 72 hours of IL-2 deprivation. Primary NK cell culturing requires additional cytokines for proliferation and expansion such as common gamma chain cytokines IL-15 and IL-21 and both of these cytokines increase transduction efficiency (Sutlu et al., 2012). On the other hand, type I

interferons (IFN α and IFN β) that are secreted in response to detection of intracellular viral components trigger an anti-viral response in the cell and reduce transduction efficiency. We wondered if selected cytokines important in NK cell culture or anti-viral response would enhance or reduce transduction efficiency in NK-92 cells when used in combination with IL-2. In order to eliminate any effects coming from viral supernatant (such as secreted factors from producer cell line 293FT), purified LeGO-G2 virus was used in these experiments. As expected, type I interferons IFN α and IFN β caused a decrease in transduction efficiency especially when used together (Figure 4.10). To our surprise, IL-12 caused an enhanced transduction efficiency in NK-92 cells where no other cytokine tested had such an effect but it was not significant when compared to IL-2 alone. IL-15 and IL-21 did not show any effect seen in primary NK cells.

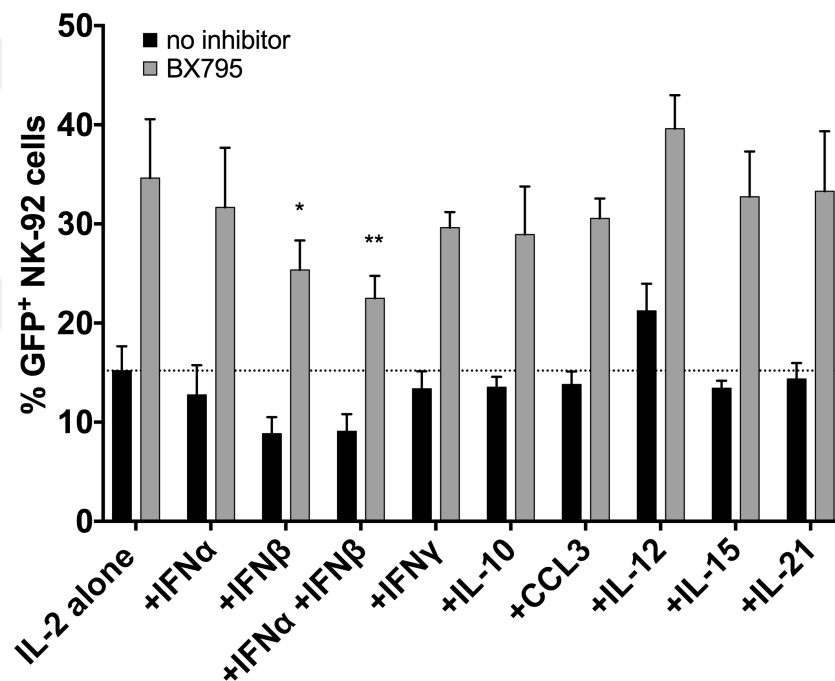


Figure 4.10. The effect of cytokines added during transduction. NK-92 cells were transduced with purified LeGO-G2 virus at MOI=10 in the presence (6 μ M) or absence of BX795 with the addition of each cytokine at 20 ng/ μ l concentration alongside 1000 U/ml IL-2. GFP percent was analyzed by flow cytometry at 72hr post transduction. Data plotted from three independent experiments, error bars indicating SD. (2way-ANOVA analysis, * p <0.05, ** p <0.01)

4.2 The Dynamics of Signals Triggered by Viral Vector Entry in NK-92 Cells

4.2.1 Intracellular elimination of viral vector

Considering the very low efficiency of lentiviral gene delivery even with MOI=20 in the absence of inhibitor in NK-92 cells, the problems could be due to low viral vector entry or intracellular elimination. It was evident that lentiviral vector entry in NK-92 cells was observed even in 15 minutes of exposure to virus with significant efficiency. In order to understand the intracellular dynamics of anti-viral response and elimination of viral vector in NK-92 cells, two types of experiments were set up.

In the first scenario, we tried six hours of exposure to lentiviral vector along with BX795 treatment for changing amounts of time. BX795 was added either at the beginning of the transduction and kept for the whole six hours or after a period of one to five hours and kept until the end of the total six hours of transduction (Figure 4.11A). At the end of six hours, viral vector and BX795 were washed away and the cells were cultured in regular growth medium. As usual, GFP⁺ cells were analyzed 72 hours after transduction and the GFP⁺ cell percentage was normalized to that of no inhibitor sample for calculating the fold enhancement in gene delivery efficiency. The results showed that there was no particular difference in transduction efficiency no matter when the inhibitor was added after viral vector exposure. This suggests that when viral vector is abundantly available in the environment, viral vector entry can take place at any time and BX795 can enhance the efficiency at all of these time points.

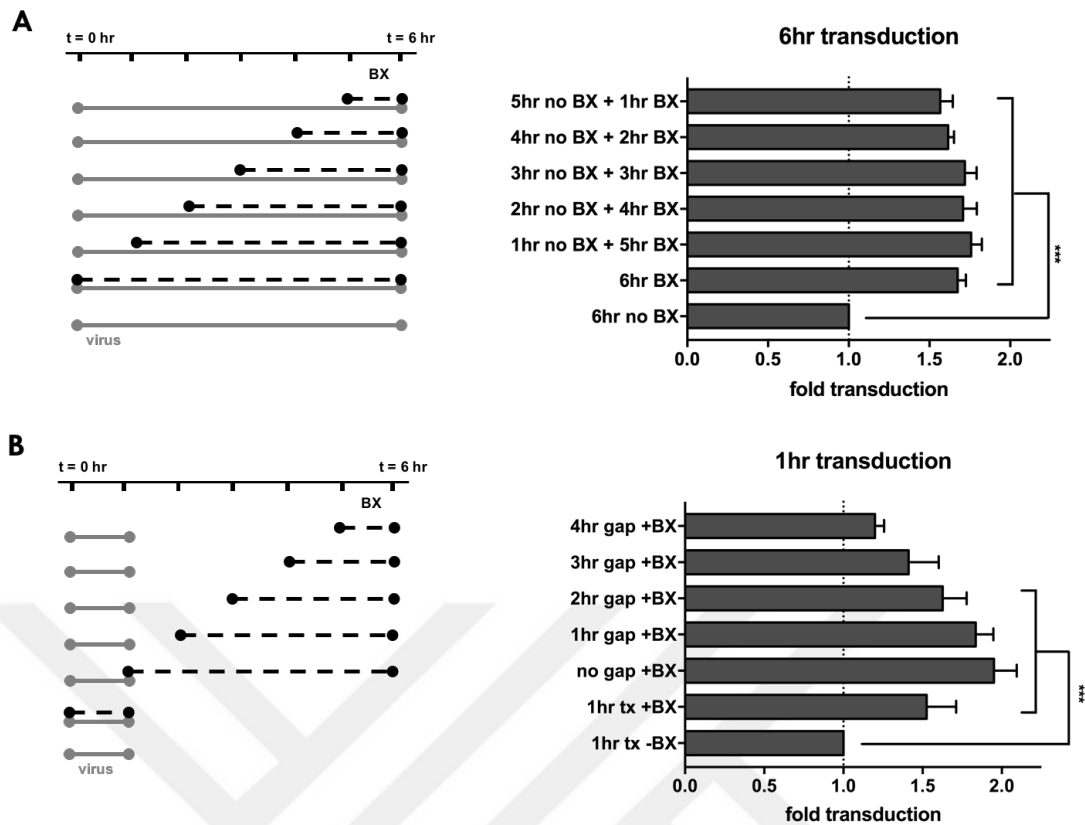


Figure 4.11. The effect of BX795 on intracellular elimination of viral vector in NK-92 cells. NK-92 cells were transduced with LeGO-G2 virus at MOI=20 (**A**) for 6 hours or (**B**) 1 hour in the presence (6 μ M) or absence of BX795 for indicated intervals. Timeline represents the 6-hour period where the grey line indicates incubation with viral vector and black dashed line indicates BX795 treatment intervals. GFP percent was analyzed by flow cytometry on day 3 post transduction. Data plotted from three independent experiments for each part, each run in duplicates, error bars indicating SD. Each transduction efficiency values was normalized to that of no inhibitor control samples to get fold transduction values. (One-way ANOVA analysis, *** $p < 0.001$)

To test the opposite scenario, we next wanted to have limited amount of viral vector exposure and see the effects of BX795 only on viral vector that was already inside the host cell (Figure 4.11B). For this purpose, the cells were incubated with viral vector containing supernatant for 1 hour (at MOI=20) and were washed. Then BX795 was added either immediately or at 1 to 4 hours after washing away the viral vector and GFP expression was analyzed 72 hours after transduction by flow cytometry. The effect of BX795 was very high (doubled when compared to control group) when added immediately after viral vector containing supernatant was washed away and incubated for 5 hours. However, if the gap between viral vector wash away and BX795 treatment was

longer, the transduction efficiency decreased, eventually reaching the basal level obtained without any inhibitor (dashed line); suggesting that BX795 acts on early events triggered by viral vector entry and prevents the intracellular elimination of viral vector.

Thus, it can be concluded that the major restriction of gene delivery by lentiviral vectors into NK-92 cells is due to intracellular elimination of viral vector and BX795 acts on early events turned on by these anti-viral signaling pathways to prevent elimination of viral vector inside the cell.

4.2.2 Analysis of signaling events triggered by viral vector entry

In order to understand which pathways were specifically turned on by the viral vector and which of those were differentially inhibited by BX795 to cause increased lentiviral gene delivery, we used immune cell signaling antibody arrays (Figure 3.2). Because many of the antibodies were specific for phosphorylated proteins, serum-free growing NK-92 cells transduced with purified LeGO-G2 virus were used for all experiments. In preliminary experiments, late time points such as 6 hours after lentiviral vector entry did not show differential expression patterns in selected signaling molecules (data not shown), therefore the priority switched to identifying early targets induced within the first two hours of lentiviral exposure.

As positive controls for phosphorylation events in the signaling array, NK-92 cells were treated with DMSO (control), IL-21 or IFN α and IFN β for 30 minutes (Figure 4.12A) where signal values were quantified and plotted in terms of Relative Fluorescence Units (RFU) and these results were normalized to that of DMSO-treated controls for fold change analysis (Figure 4.12B). It was recorded that IL-21 alone caused a 10-fold increase in STAT3 Tyr phosphorylation when compared to control and IFN α and IFN β treatments caused a 2-fold increase in STAT1 Tyr phosphorylation fitting the expectations.

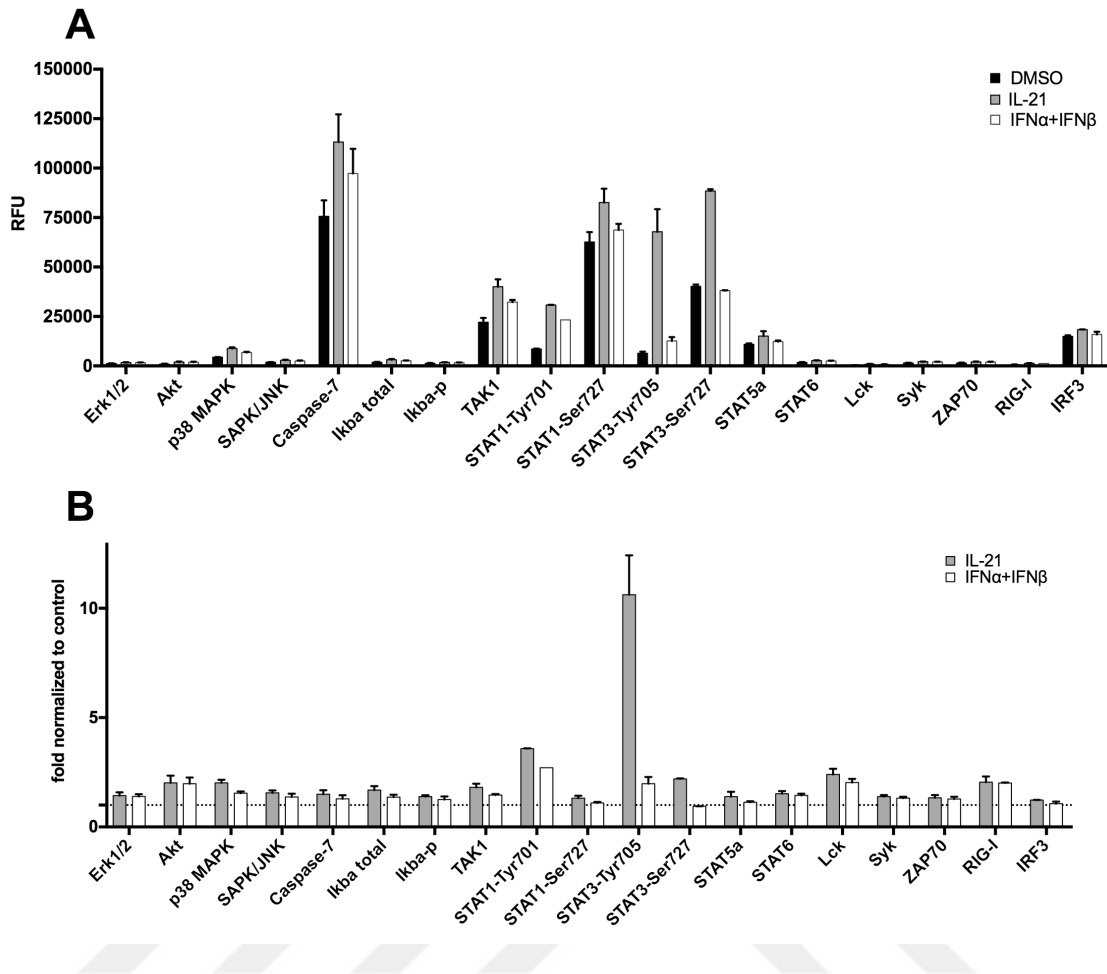


Figure 4.12. Immune cell signaling array with 30-minute IL-21 or IFN α and IFN β treatment. Serum-free NK-92 cells were treated with DMSO alone (black), 20 ng/ul IL-21 (grey) or 20 ng/ul of IFN α and IFN β each (white). **(A)** The average of two blots for each protein were plotted. RFU: relative fluorescence unit. **(B)** Each signal value was normalized to that of DMSO control for each protein. The average of two blots for each protein were plotted. Dashed line indicates the level of DMSO control sample set to 1. Error bars indicate SD.

Knowing that viral vector entry could take place as early as fifteen minutes, we tried 15, 30 and 90 minutes of exposure time and immediately lysed the cells for immune cell signaling array (Appendix Figure I1). For transduction efficiency confirmation, a fraction of cells from each group were incubated for at least 72 hours after viral vector removal and GFP expression was verified by flow cytometry. The first approach was to detect signal values directly from each blot, but the signal levels of all proteins were different. Therefore, in the next set of analysis, each sample was normalized to DMSO control of that time point (Appendix Figure I2) for accurate comparison. Expression patterns of selected proteins from the results of this set were plotted as time-course graphs in Figure

4.13. The same experiment was repeated with serum-free NK-92 cells and purified LeGO-G2 with exactly the same parameters but this time IL-2 was included during transduction period and 15-minute time point was excluded. Again, the signal values were plotted (Appendix Figure I3) and the values were further analyzed by calculating fold induction by normalizing to DMSO control of their relative time points (Appendix Figure I4). The average of these two independent experiments were plotted for 30- and 90-minute time-points as shown in Figure 4.14.

For all transductions in general, it was evident that 15 minutes did not cause any changes in expression level or phosphorylation status of selected proteins. We noted that BX795 treatment alone caused a decrease in STAT1, STAT3 and STAT5a Tyr phosphorylations as well as p38 and SAPK/JNK when compared to DMSO control of that time-point. This effect of BX795 was observed at all time points, showing the role of BX795 independent of viral vector presence inside the cells (Figure 4.13).

We observed that the earliest detectable change in the levels of p38, SAPK/JNK, TAK-1 and STAT1 begins 30 minutes after viral vector incubation and increases at the 90-minute time-point. This pattern was fitting to the model of MAPK signaling pathways, where the signal starts from MAP3Ks (such as TAK-1), phosphorylating MAPKs (such as p38 and JNK) that in turn phosphorylate Ser residues of STAT1 and STAT3. Looking at the time-course graphs combined for selected proteins from the first experiment, there were some early and late responders to viral vector in the cell. Some early signaling molecules that were phosphorylated in response to the intracellular virus included Lck and Syk, whereas late increases were seen in p38, TAK-1 and STAT1 Ser phosphorylation. These observations were all true for combination of two independent experiments shown in Figure 4.14, for the 90-minute time-point specifically when virus was present. The only difference between the two experiments was the addition of IL-2 in the latter; marking a change in the levels of Lck dramatically when present. This effect was due to the position of Lck in the IL-2 receptor β tails that induced other signals independent of the virus or inhibitor presence (Hatakeyama et al., 1991).

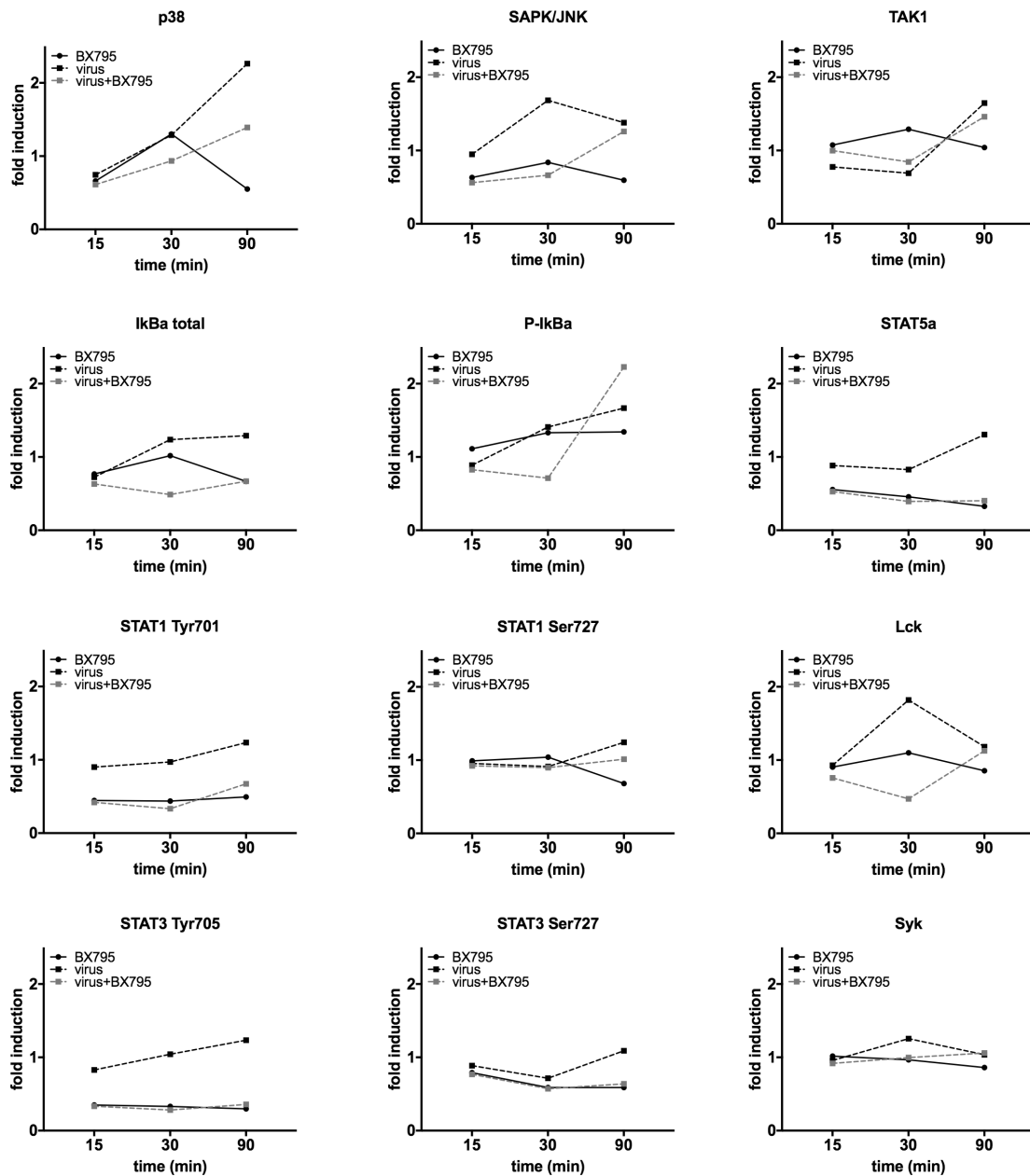


Figure 4.13. Time-course expression levels of selected proteins from immune cell signaling array. Serum-free NK-92 cells were treated with BX795 alone (black line), virus alone (black dashed line) and virus with BX795 (grey dashed line) for 15, 30 or 90 minutes and each signal was normalized to that of DMSO control for each time point.

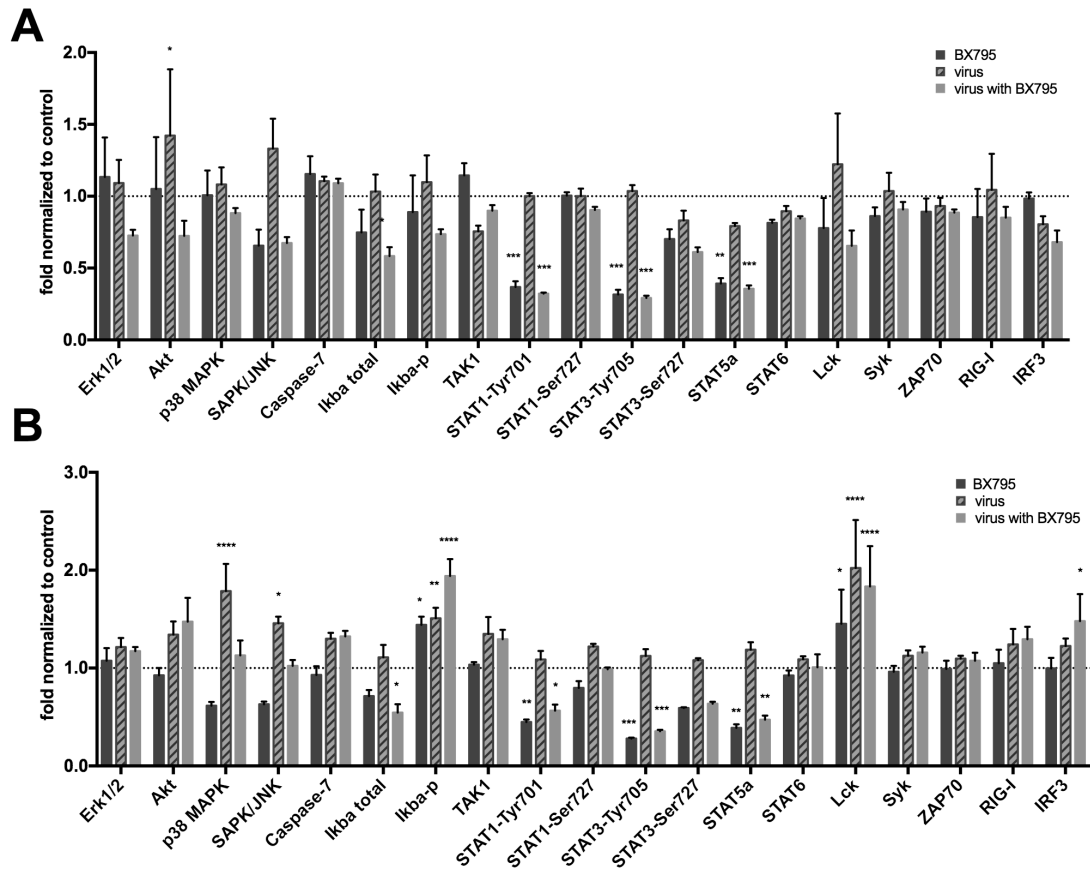


Figure 4.14. Immune cell signaling array with 30-90 minute-transductions normalized to control (average of two independent experiments). Serum-free NK-92 cells were incubated with DMSO alone, 6 μ M BX795 alone (dark grey), viral vector at MOI=20 (striped) or viral vector with 6 μ M BX795 (light grey) for (A) 30 or (B) 90 minutes and each signal value was normalized to that of DMSO control for each time point. The average of two blots from two independent experiments for each protein were plotted. Dashed line indicates the level of DMSO control sample. Error bars indicate SEM. (2way-ANOVA analysis: * $p < 0.05$, ** $p < 0.01$, *** $p < 0.001$, **** $p < 0.0001$)

The inhibitory effect of BX795 on STAT phosphorylation was also observed with intracellular flow cytometry for STAT3-Ser727 phosphorylation and the results were correlated with the immune cell signaling array (Figure 4.15). Cells stained with intracellular STAT3-P-Ser727 showed that there was an increase in Ser phosphorylation in a time-dependent manner and this phosphorylation was inhibited by BX795 treatment alone that was parallel to the results seen before in the immune cell signaling array. Total RIG-I and Phospho-IRF7 peaked at 90 minutes with virus, and IRF7 Ser phosphorylation was also inhibited by BX795 treatment alone. Taken together, these observations suggest that viral vector triggers STAT3 Ser phosphorylation that is dependent on MAPK

pathways in NK-92 cells and BX795 alone can inhibit these events that interfere with anti-viral signaling.

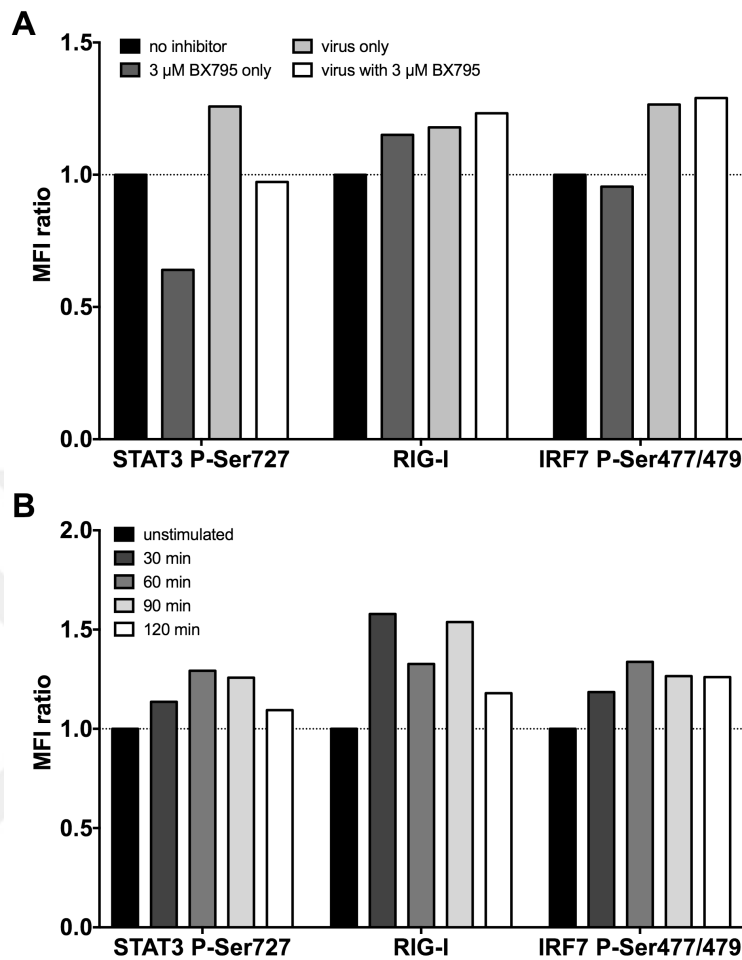


Figure 4.15. Intracellular flow cytometry with STAT3 P-Ser727, RIG-I and IRF7 P-Ser 477/479 antibodies. **(A)** NK-92 cells were treated with 3 μ M BX795 alone, transduced with LeGO-G2 virus alone or transduced with LeGO-G2 virus in the presence of 3 μ M BX795 for 120 minutes. **(B)** NK-92 cells were transduced with LeGO-G2 virus alone (at MOI=20) for 30, 60, 90 or 120 minutes and stained intracellularly with STAT3 P-Ser727, RIG-I and IRF7 P-Ser 477/479 antibodies. MFI value of each sample was normalized to that of unstimulated sample to get MFI ratio. One representative experiment.

4.3 Targeting Candidate Genes in 293FT and NK-92 Cell Lines by CRISPR/Cas9-Mediated Genome Editing

4.3.1 Targeting genes in the 293FT cell line

293FT cells were chosen for the first trial with CRISPRs targeting *DDX58*, *IFIH1*, *TBK1* and *TRIM5 α* genes with the pspCas9(BB) backbone delivered by transfection. Each CRISPR was designed to disrupt the start codon of the corresponding genes, therefore altering gene expression. Additionally, HDR was aimed with 100 bp-long ssODN design containing 5' and 3' homology arms spanning the upstream and downstream of the transcription start site. A 7 bp-long spacer region contained the altered sequence changing the ATG-containing sequence into a restriction enzyme recognition site (EcoRI or Sall) that was not found anywhere else in the region of interest. The restriction enzyme recognition site was 6 bp long and one more base was inserted to ensure frameshift if correct insertion could occur. (All CRISPR design schemes with annotations can be found in Appendix H.)

293FT cells were first co-transfected with CRISPR/Cas9 plasmid (pspCas9(BB)-2A-Puro) and ssODNs for HDR for each gene individually. Puromycin selection was started 24 hours post-transfection and the cells were kept in Puromycin (1 μ g/ml) for 3 consecutive days. Then Puromycin was removed and the cells were set up in 96-well plates for growth of single cell clones. In a course of four weeks following transfection, single cell clones were expanded and genomic DNA was isolated. For each gene, the region of interest could be amplified by PCR and the PCR product could be digested with the corresponding restriction enzyme to select clones with successful HDR. This process known as restriction fragment length polymorphism (RFLP) helped identify single cell clones with desired mutations. In summary, the transfections led to the following results:

target	PCR product size (bp)	restriction enzyme	digest product size (bp)	# of single cell clones	# of single cell clones with HDR	# of single cell clones with other mutations
DDX58	572	EcoRI	108 + 464	19	2	2
IFIH1	527	Sall	110 + 417	23	4	3
TBK1	506	EcoRI	180 + 326	16	5	7
TRIM5 α	546	EcoRI	192 + 354	19	8	2

Table 4.1. 293FT CRISPR/Cas9-modified single cell clones.

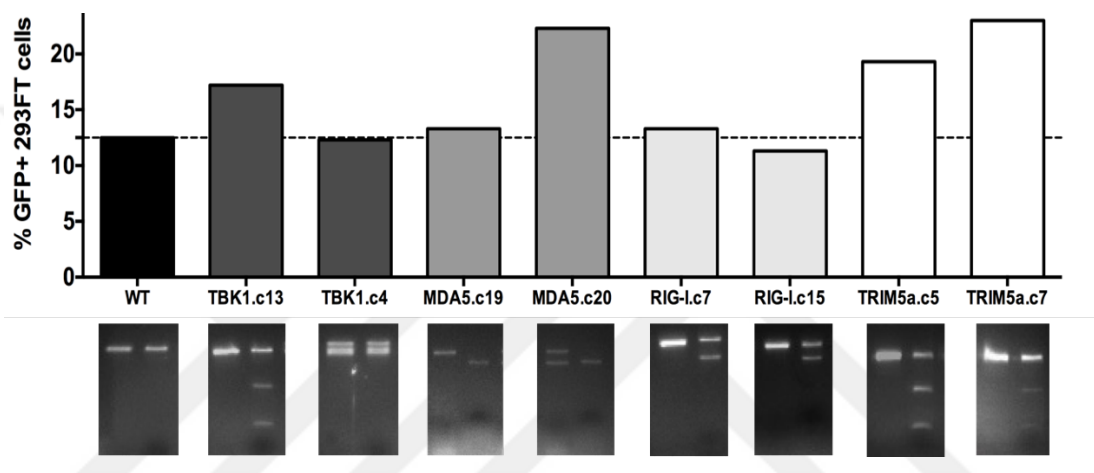


Figure 4.16. RFLP and transduction of 293FT CRISPR/Cas9-modified single cell clones. For each single cell clone, PCR product (left lane) and corresponding restriction digest result (right lane) from gel electrophoresis were depicted below clone name and number. Each clone was then subjected to LeGO-G2 transduction (MOI=0.1) and GFP percentage was analyzed by flow cytometry on day 3 post transduction. Dashed line indicates baseline transduction value of WT sample. One representative experiment.

RFLP results for selected clones (Figure 4.16) showed that most clones with HDR were heterozygous mutants and one allele was either still WT or contained other mutations. TBK1.c4 and MDA5.c20 showed multiple bands in PCR, suggesting homozygous mutations whereas all other clones showed one undigested intact PCR product and one digested product, suggesting one allele successfully altered with HDR. Regardless, two single cell clones with successful genome editing for each target were selected for further analysis with LeGO-G2 transduction. Aiming to see potential alterations in lentiviral gene delivery, a low MOI value (MOI=0.1) was selected. Due to the easily-transduced nature of 293FT cells, transduction resulted in 12.5% GFP⁺ WT cells and some, especially one

MDA5 clone and both TRIM5 α clones showed remarkable differences in GFP percentage, reaching up to 20%. Taken together, it was concluded that among all targets TRIM5 α participated in lentiviral gene delivery and that its disruption enhanced transduction in 293FT cells.

The selected clones being heterozygous raised question marks about the remaining gene expression in these cells. Consequently, it was decided to switch to the lentiviral CRISPR constructs (target sequences cloned into lentiCRISPRv2 vector, collectively referred to as lentiCRISPR constructs from here on) to potentially disrupt gene expression in all cells transduced with the corresponding lentiCRISPR virus. (sgRNA target sequences for these constructs were retrieved from GeCKO v.2 Library as explained in Section 3.2.3 and were different from sgRNA sequences used in transfection experiments.) The anti-viral signaling pathways differ from cell to cell, therefore it was necessary to check how an easily-transduced cell line such as 293FT would respond to transductions after alteration of 20 candidate genes playing roles in distinct pathways. These selected target genes are: *TBK1*, *JAK3*, *MAVS*, *SYK*, *LCK*, *MAP3K7 (TAK1)*, *IRF3*, *IRF7*, *IRF9*, *TLR3*, *TLR7*, *MAPK8 (JNK)*, *TMEM173 (STING)*, *MAPK14 (p38 α)*, *TRIM5 α* , *TRIM25*, *TRIM28*, *DDX58 (RIG-I)*, *IFIH1 (MDA5)* and *PIK3CA (PI3K)*.

293FT cells were transduced with the lentiCRISPR viruses one by one where Cas9⁺ cells were selected with Puromycin starting 72 hours post transduction. Single cell assays were not set up in this case because all transduced and Puro-selected cells were expected have constant lentiCRISPR expression, therefore disrupting all alleles found in the genome. After complete selection, lentiCRISPR⁺ cells were subjected to LeGO-G2 transduction first at MOI value 0.2 to compare differences in lentiviral gene delivery efficiency. As expected, WT cells were 20% GFP⁺ whereas some of the lentiCRISPR⁺ cells, namely TRIM5 α -lentiCRISPR⁺ and to some extent MAVS-lentiCRISPR⁺ cells, showed higher results than the baseline (Figure 4.17A). The transduction of 293FT cells change dramatically with the number of infectious particles per cell, hence selected cell lines were further transduced with LeGO-G2 at MOI 0.1, 0.2 and 0.4 to test whether the differences in GFP expression would be affected by limiting or extra infectious particles in the environment (Figure 4.17B). Strikingly, TRIM5 α -lentiCRISPR⁺ cells showed the highest efficiency at every MOI level tested. The cell lines that showed no effect in transduction at any MOI were similar with the previous experiment. Thus, it was clear

that different anti-viral signaling pathways were triggered depending on cell type and TRIM5 α played a major role in lentiviral gene delivery in non-immune cell line 293FT.

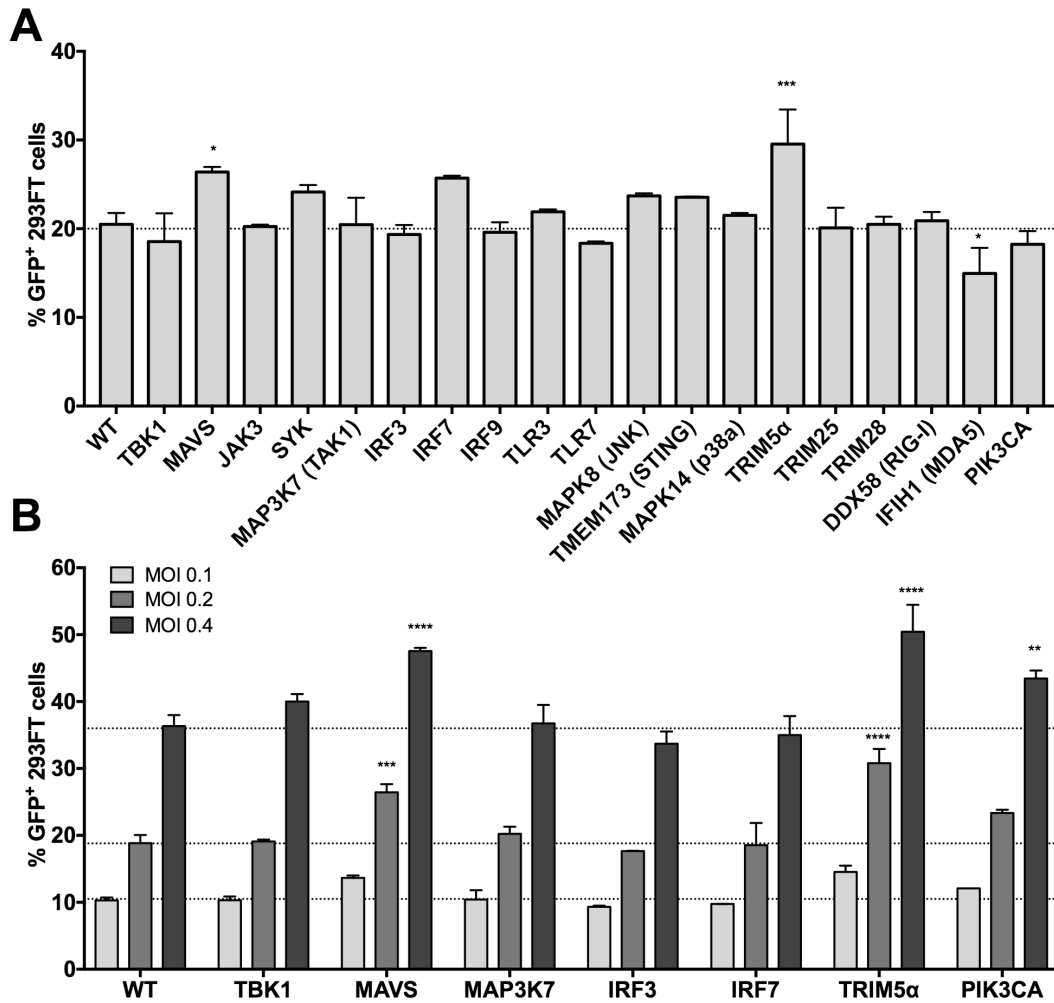


Figure 4.17. 293FT lentiCRISPR-transduced cell lines show changes in lentiviral gene delivery. **(A)** 293FT cells were first transduced with corresponding lentiCRISPR viruses for 16 hours. Three days later, all cells were started on Puromycin selection. After complete Puro selection, LeGO-G2 virus transductions were carried out (at MOI=0.2). **(B)** Selected 293FT lentiCRISPR⁺ cell lines were transduced with LeGO-G2 (at MOI=0.1; 0.2; 0.4). GFP percent was analyzed by flow cytometry on day 3 post transduction. Data plotted from one representative experiment in each part, each run in duplicates, error bars indicating SD. Dashed line indicates baseline for transduction at each MOI. (2way-ANOVA analysis: * p<0.05, ** p<0.01, *** p<0.001, **** p<0.0001)

4.3.2 Targeting genes in the NK-92 cell line

It was well assessed that certain genes play roles in anti-viral signaling in NK cells that could potentially interfere with lentiviral gene delivery, therefore CRISPR/Cas9 system was utilized for potentially creating knock-out cell lines. For this purpose, the same 20 genes were selected for CRISPR/Cas9-mediated genome editing and the cells were transduced with the lentiCRISPR viruses one by one where lentiCRISPR⁺ cells were selected with Puromycin starting 72 hours post transduction. After the course of a week-long selection, lentiCRISPR⁺ cells were subjected to LeGO-G2 transduction to compare differences in lentiviral gene delivery efficiency. With two independent transductions done 3 days apart, it was striking to see that some gene disruptions caused significant increases in transduction efficiency both in the absence and presence of BX795 (Figure 4.18A).

To our surprise, the highest impact was seen with the TRIM25-lentiCRISPR⁺ NK-92 cells, followed by PI3K-, JNK-, SYK- and STING-, TRIM28-, DDX58- and MDA5-lentiCRISPR⁺ cells. Endosomal RNA sensors TLR3 and TLR7 and their corresponding transcription factors IRF3 and IRF7 showed a decrease in transduction efficiency upon genome editing when compared to others, as did MAPK14- lentiCRISPR⁺ NK-92 cells. The GFP level of all transduced samples showed steady values when checked with flow cytometry on days 2, 3 and 6 post transduction (data not shown). To confirm the downregulation of genes targeted in lentiCRISPR⁺ NK-92 cells; qRT-PCR was carried out with 12 out of 20 candidate genes. All 12 lentiCRISPR⁺ NK-92 cells showed decreased expression when normalized to actin and WT NK-92 expression levels (Figure 4.18B). Thus, it was clear that lentiviral vectors induced signaling from cytoplasmic RNA sensors RIG-I and MDA5 more dominantly than the endosomal RNA receptors TLR3 and TLR7; and the role of TRIM25 in the signaling of RIG-I was particularly effective in this pathway in NK-92 cells.

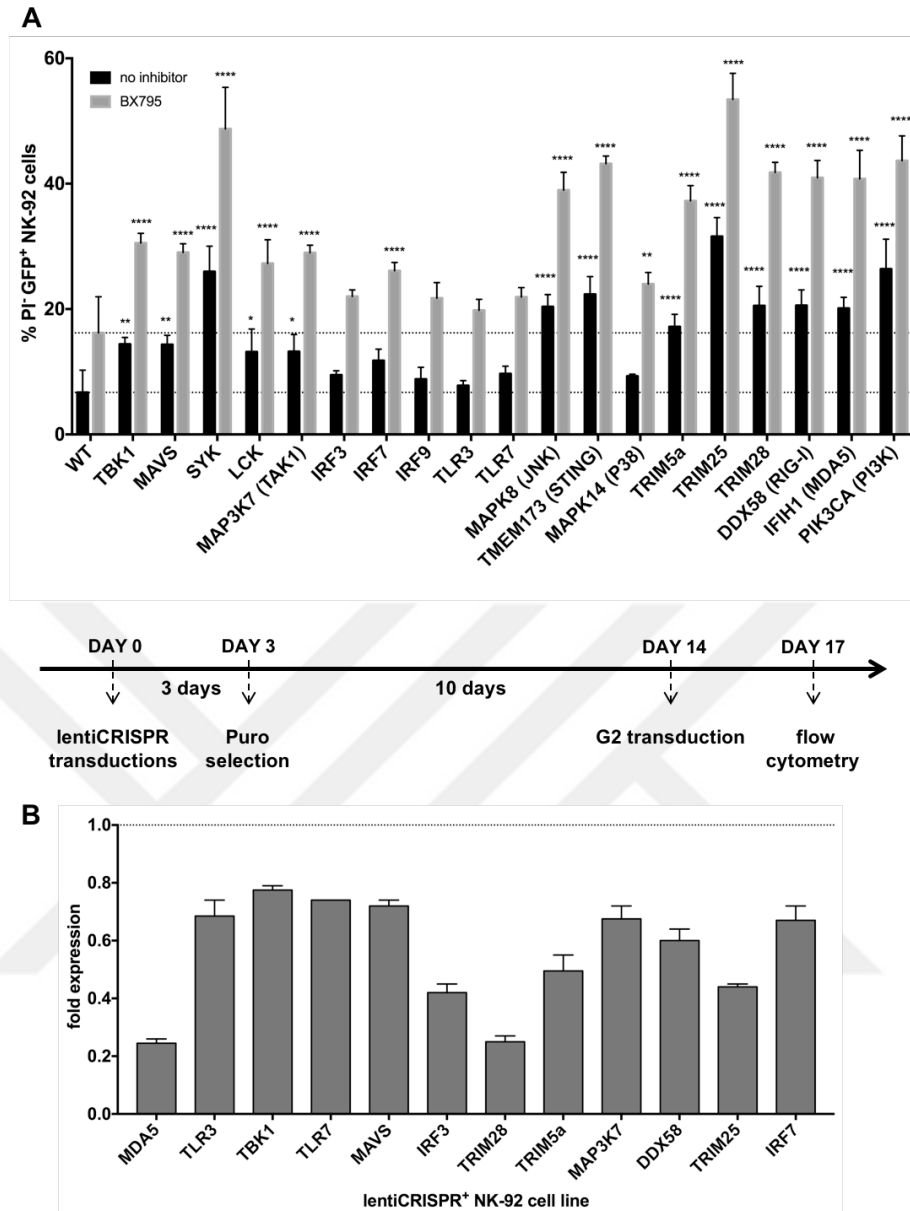


Figure 4.18. NK-92 lentiCRISPR-transduced cell lines show changes in lentiviral gene delivery. **(A)** NK-92 cells were first transduced with corresponding lentiCRISPR viruses in the presence of 3 μ M BX795 for 6 hours. Three days later, all cells were started on Puromycin selection. On day 10 and day 13 of Puro selection, two independent LeGO-G2 virus transductions were carried out (at MOI=10) in the presence (3 μ M) or absence of BX795. GFP percent was analyzed by flow cytometry on day 3 post transduction. Data plotted from two independent experiments for each part, each run in duplicates, error bars with SD. Dashed line indicates baseline for transduction. Statistical analysis made with multiple annova with comparisons of each value to WT sample's no inhibitor or BX795 counterpart. (**** $p < 0.0001$) **(B)** qRT-PCR analysis was done with total RNA isolated from 12 of the NK-92 lentiCRISPR-transduced and Puro- selected cell lines. Expression values were quantified by $2^{(-\text{ddCt})}$ calculations made with β -actin selected as reference gene and then all values were normalized to that of WT NK-92 cells. Average of duplicates were plotted for each sample with error bars indicating SD.

Focusing on RIG-I signaling could potentially provide answers about lentiviral gene delivery in NK cells therefore genomic DNA sequence analysis were carried out with DDX58-lentiCRISPR⁺ NK-92 cells. Genomic DNA isolates were used in PCR with primers spanning the binding site of CRISPR and the start codon of the *DDX58* gene. (DDX58-lentiCRISPR binding site with annotations can be found in Appendix H.) The sequencing of PCR products revealed that lentiCRISPR was successful in genome editing, with NHEJ outcomes ranging from 1 bp to 134 bp deletions in the target region (Figure 4.19). All alterations were found to be upstream of PAM sequence (on the reverse strand) at the theoretical site of DSB. This set of sequences reflected a small fraction of altered cells in the transduced pool of NK-92 cells, which overall should have various mutant or truncated versions of the RIG-I protein. Strikingly, a single nucleotide polymorphism (SNP) from C to T was detected downstream of transcription start site even in the WT PCR products independent of lentiCRISPR, causing an Arg to Cys mutation in the 7th amino acid, that could potentially alter the structure and function of the protein and create a heterogeneous population (Hu et al., 2010). The position of this amino acid is strategically significant, because the N-terminus of the protein contains the CARD required for MAVS signaling therefore affecting the rest of the anti-viral response.

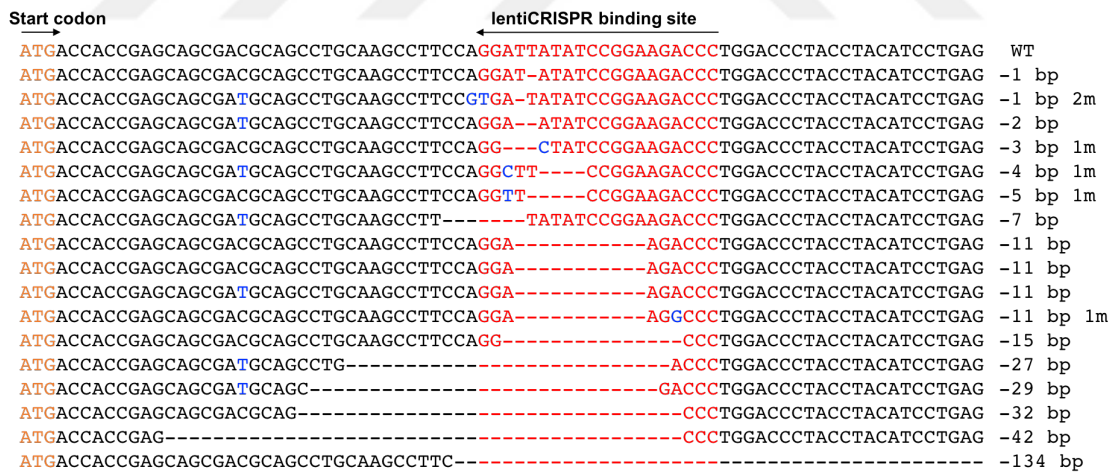


Figure 4.19. Sequencing of DDX58-lentiCRISPR⁺ NK-92 genomic DNA pool containing the CRISPR binding site. Start codon of DDX58 (orange) and lentiCRISPR binding site (red) are indicated on figure. LentiCRISPR binding site and PAM sequence are in the reverse strand. Mutations (m) are shown with blue.

Taken together, these results indicated that i) the lentiCRISPR constructs were reliable in genome editing resulting in NHEJ, ii) potential DSB site 3 bp upstream of PAM sequence was the hotspot for mutations and, iii) certain SNPs in RIG-I could be one of the reasons behind the low efficiency of lentiviral gene delivery in the NK-92 cell line and perhaps in human primary NK cells.

4.4 Preliminary Results for Future Directions

4.4.1 A p38 inhibitor: a twisted player in anti-viral signaling

The MAPK p38 was a promising candidate for increasing transduction efficiency because p38 phosphorylation was upregulated in the presence of viral vectors and downregulated in the presence of BX795 treatment. To understand the role of p38 in lentiviral transduction, we tested a known potent p38 α inhibitor, VX745, and observed the effects in NK-92 cells. To our surprise, the addition of VX745 during transduction of NK-92 cells caused a markedly lower transduction efficiency than the DMSO controls (Figure 4.20A). This trend was the same with all four doses tried during transduction and no toxicity was observed at any concentration. Interestingly, BX795 alone could increase the transduction efficiency from 13% to 40% but when VX745 was added along with BX795, the efficiency decreased to 25%. This showed that blocking p38 α with a potent inhibitor caused some other pathways to play more dominant anti-viral roles when the lentiviral vector was inside the host cell, correlated with findings with a variety of WT viruses.

Alternatively, the addition of VX745 once viral vector was internalized also showed inhibition of viral gene delivery. Although the experiment was set up in the same way as before (Figure 4.11B) we observed lower transduction efficiencies when compared to DMSO controls at all time points (Figure 4.20B). BX795 caused a 3-fold induction in transduction efficiency when added during transduction as expected. These findings

indicate that blocking p38 pathways after viral vector exposure caused a marked reduction in viral gene delivery in NK-92 cells.

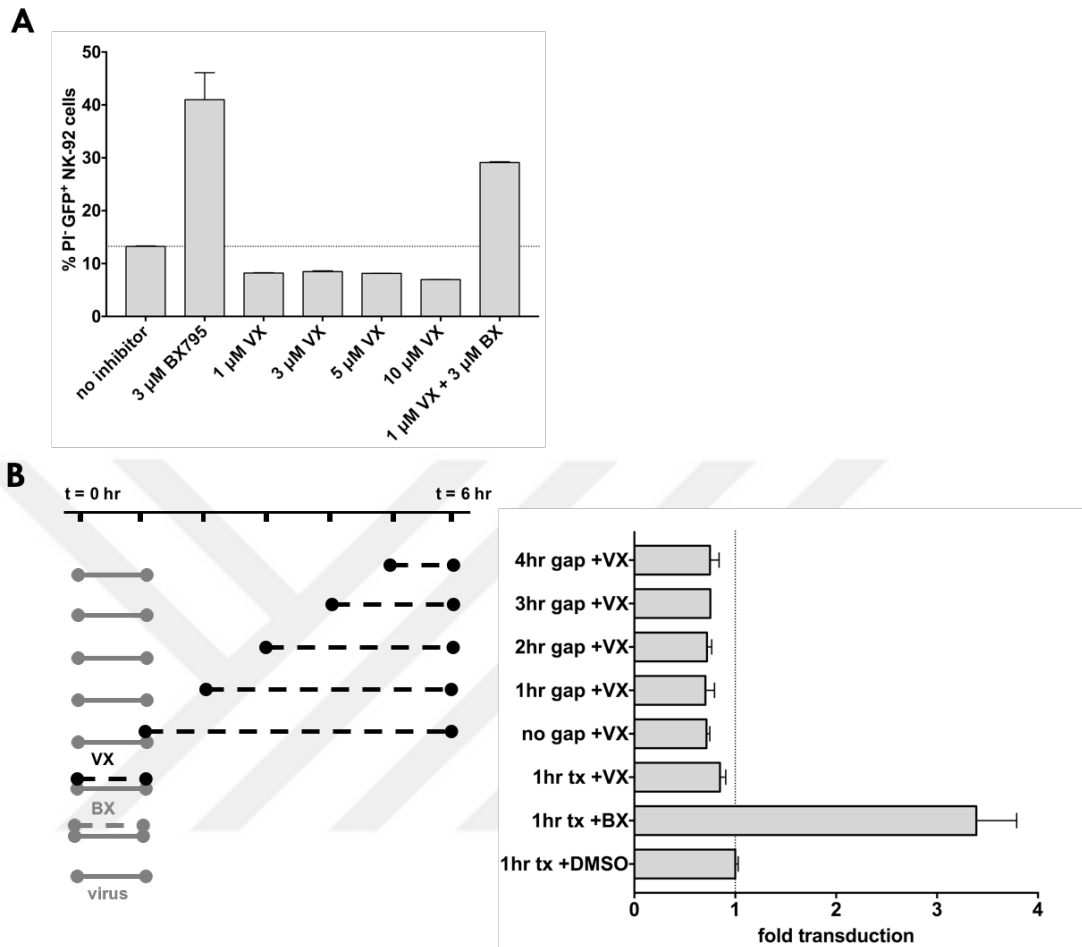


Figure 4.20. The role of p38 α inhibitor VX745 when added during transduction of NK-92 cells. NK-92 cells were transduced with LeGO-G2 virus (at MOI=10) **(A)** for 6 hours or **(B)** for 1 hour in the absence of any inhibitors, with BX795 or VX745 at indicated concentrations. GFP percent was analyzed by flow cytometry on day 3 post transduction. (GFP percentages were normalized to DMSO control in part B to get fold transduction values.) Data plotted from one representative experiment for each part, run in duplicates, error bars indicating SD. Dashed line represents baseline for transduction.

4.4.2 Genome editing using the GeCKO library in NK-92 cells

4.4.2.1 Transduction, selection and expansion of GeCKO⁺NK-92 cells

Finding out candidate genes playing pivotal roles in lentiviral gene delivery in NK cells has been a crucial task throughout this study where single gene silencing and knock-out approaches were tried. Notably, a wider perspective could be useful in understanding the big picture, making more sense about the crosstalk between previously unlinked pathways and leading to the discovery of novel actors in antiviral signaling pathways. Therefore, GeCKO library approach was used to obtain a complete knock-out library of NK-92 cells. The complete work flow for GeCKO experiments was summarized in Figure 3.3.

In essence, NK-92 cells are first transduced with GeCKO Library A and B viruses separately where the lentiviral lentiCRISPRv2 construct contains a target-specific sgRNA sequence and Cas9-Puro^R enclosed within the LTRs. This part of the construct gets integrated into the host cell's genome where target-specific CRISPR/Cas9 would be expressed constantly, causing the disruption of its target gene. By obtaining a GeCKO⁺ NK-92 cell population with the right transduction efficiency, we ensure that each and every construct will be found in the genomic DNA isolate from these pools which can be named as "base library A and B". By completing two PCR set ups summarized in Figure 3.2, the part that contains the target-specific sgRNA sequence will be amplified from each transduced pool. Hypothetically speaking, if a gene X causes resistance against lentiviral gene delivery in NK cells, the cells with gene X knock-out would have higher efficiency when a secondary transduction occurs. By making this secondary transduction with the GFP-virus LeGO-G2, we aimed to further isolate GFP⁻ and GFP⁺ populations and compare their genomic DNA make-up to the base libraries. Coming back to the example, if gene X-targeting sgRNA sequence was found in the GFP⁺ population but not in the GFP⁻ population, it would prove the hypothesis that gene X is involved in antiviral resistance. In order to achieve reliable results with the complexity of GeCKO approach, each step had to be planned and carefully compiled. The timeline of events can be summarized in the chart below:

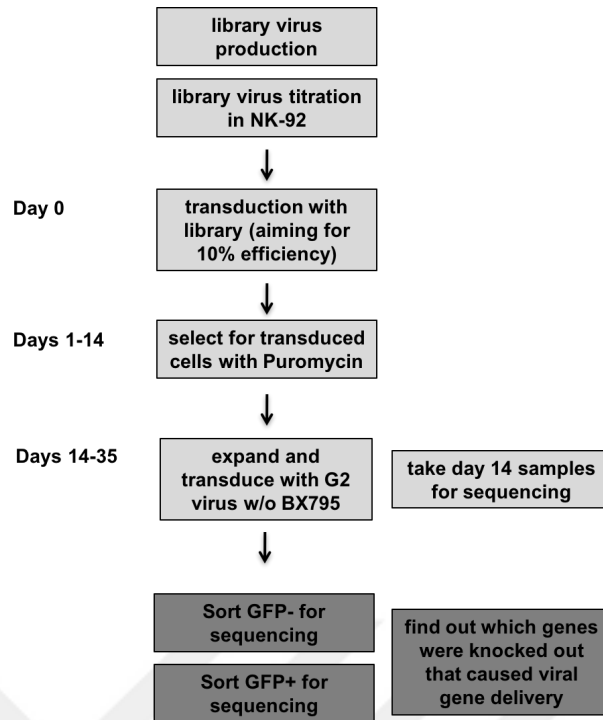


Figure 4.21. GeCKO library timeline.

Briefly, GeCKO Library A and B virus productions were followed as the regular protocol and titration of these productions were completed in NK-92 cells. Transduction of NK-92 cells were aimed at 10-20% GeCKO⁺ cells in order to assure one construct entry per cell, that would result in one gene knock-out per transduced cell. Starting with 10⁷ cells per transduction with each Library, transductions were done in the presence of 3 μM BX795 for 6 hours in 15ml volume (knowing that scaling-up the transduction protocol would not cause any changes in transduction efficiency). 24 hours after the transduction, Puromycin selection was started to enrich the GeCKO⁺ population. Selection and expansion of GeCKO-LibA⁺-NK-92 and GeCKO-LibB⁺-NK-92 cells took 14 days. At the end of this timeline, 40x10⁶ cells from each population (Library A or B) were taken for genomic DNA isolation. This expansion was crucial to have each and every construct represented at least 100X in the genomic DNA pool that would be used as sequencing baseline.

4.4.2.2 Transduction of GeCKO⁺NK-92 populations with LeGO-G2

On day 14 of Puromycin selection, 10⁷ cells from each GeCKO-LibA⁺-NK-92 and GeCKO-LibB⁺-NK-92 cells were subjected to LeGO-G2 transduction in the absence of

any inhibitor, at MOI=10 for 6 hours. GFP expression of control or GeCKO⁺ NK-92 cells were assessed by flow cytometry 48 and 72 hours following transduction (Figure 4.22). Surprisingly, GeCKO-LibA⁺-NK-92 and GeCKO-LibB⁺-NK-92 cells showed almost 43% and 45% transduction respectively whereas control transduction was down at 26%. This could potentially mean that disrupting certain genes would make a difference in lentiviral gene delivery, therefore GFP⁺ and GFP⁻ populations in both transductions were FACS-sorted and expanded further. 18 days after sorting (21 days after LeGO-G2 transduction), GFP expression of each population was checked again by flow cytometry (Figure 4.23). Notably, all populations showed stable GFP expression, therefore genomic DNA isolation was completed from 20x10⁶ cells from each GFP⁻ and GFP⁺ population.

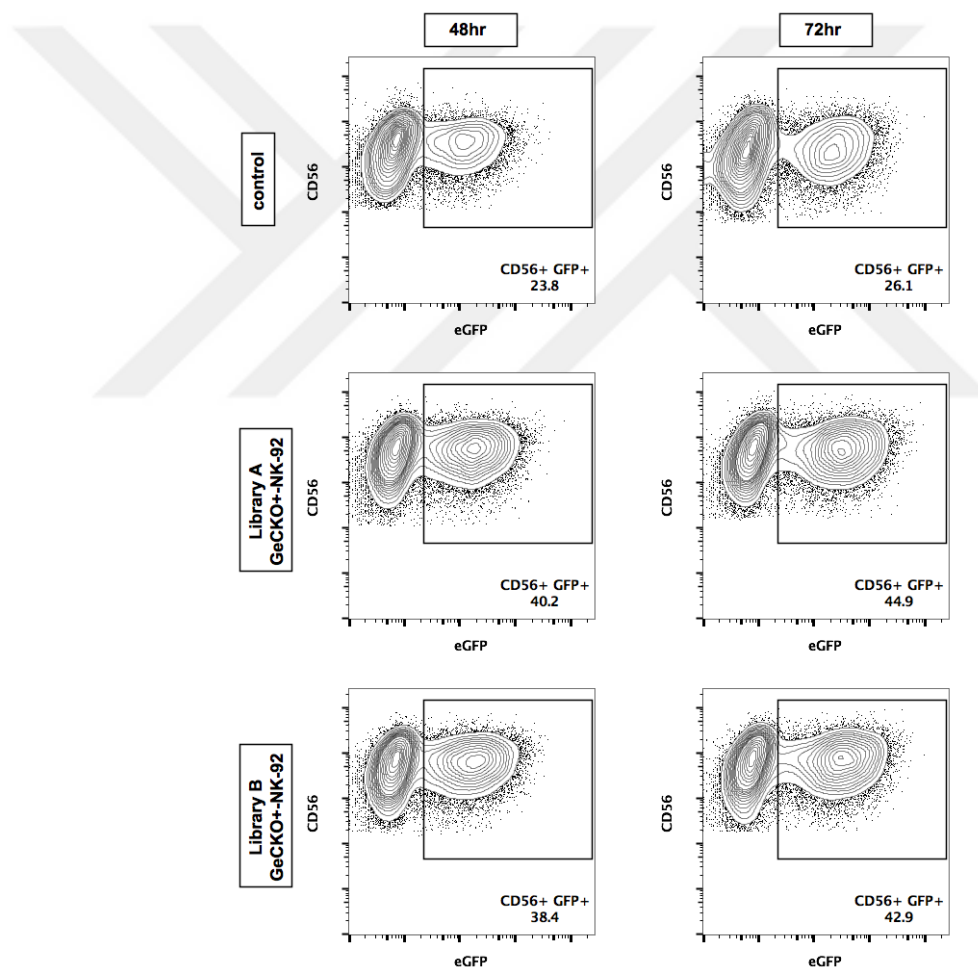


Figure 4.22. LeGO-G2 transduction of GeCKO⁺ NK-92 cells. WT NK-92, GeCKO-LibA⁺-NK-92 and GeCKO-LibB⁺-NK-92 cells were transduced with LeGO-G2 virus at MOI=10 for 6 hours. GFP expression was assessed 48 and 72 hours after transduction.

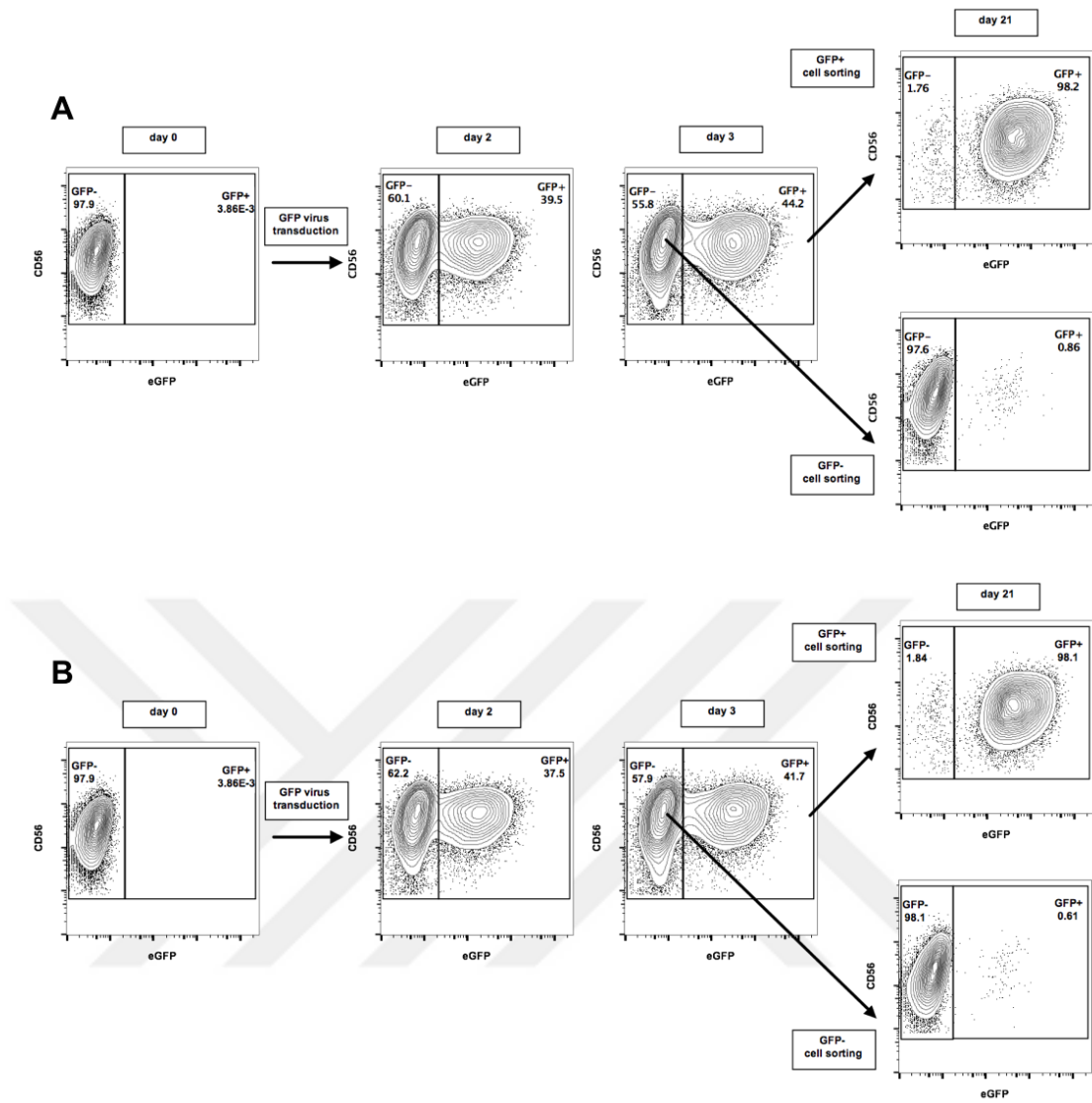


Figure 4.23. GFP expression of sorted GeCKO⁺ NK-92 cells. GFP⁺ and GFP⁻ populations of **(A)** GeCKO-LibA⁺-NK-92 and **(B)** GeCKO-LibB⁺-NK-92 cells 18 days after sorting (21 days after LeGO-G2 transduction).

5. DISCUSSION

Current gene therapy trials rely on genetic modification of immune cells using viral vectors. The use of lentiviral vectors provides efficient genetic modification with the advantages of integrating gene-of-interest into host cell genome. The potential approaches to genetic modification of NK cells open new doors in fighting autoimmune diseases and a variety of cancers (Alici & Sutlu, 2009; Carlsten & Childs, 2015; Childs & Berg, 2013). However, both primary NK cells and NK-92 cells are resistant to lentiviral gene delivery compared to other members of the hematopoietic system and the use of IKK ϵ /TBK1 small molecule inhibitor BX795 during transduction shows remarkable enhancement in primary NK cells (Sutlu et al., 2012). The roles of specific PRRs were suspected to be significant in this process (Kajaste-Rudnitski & Naldini, 2015); however, there were no previous reports suggesting the involvement of any known innate immune response mechanism related to lentiviral transduction in NK cells. HIV-1 is naturally packed with virulent factors that play various roles in blocking anti-viral signaling pathways of the host system (Rustagi & Gale, 2014). Using one or more of these factors as examples, the host system can be manipulated to provide highly efficient lentiviral gene delivery in NK cells. Small molecule inhibitors especially with reversible effects and low toxicity are among the main candidates for this purpose.

The current study aiming to identify specific roles of the small molecule inhibitor BX795 in lentiviral gene delivery in NK cells examined transduction dynamics and signaling events related to viral vector transduction. BX795 was shown to be the inhibitor of

IKK ϵ /TBK1-mediated phosphorylation of IRF3 in macrophages upon signaling of LPS or poly (I:C) treatment (Clark et al., 2009). Regarding the use of BX795 to enhance lentiviral gene delivery, all previous data relied on information retrieved from primary NK cell transductions (Sutlu et al., 2012). It is difficult to get sufficient amount of primary NK cells for comprehensive analysis of intracellular dynamics of lentiviral gene delivery. Thus, transduction parameters such as inhibitor dose, transduction and inhibitor treatment time and MOI values all needed to be optimized with the NK cell lines.

NK-92 cells were previously reported to have transduction efficiencies ranging from 20 to 90% with different protocols that require consecutive transductions and various viral loads (Imamura et al., 2014; Micucci et al., 2006; Nagashima et al., 1998; Sutlu et al., 2012). Here, we wanted to obtain an optimal transduction protocol for ease of application throughout this study. Our results demonstrated that transduction time and viral load could only be increased to a certain extent and the restrictive factors were still present in all conditions, preventing the cells to become fully transduced. Transduction time determination experiments showed that increasing viral vector exposure time had a directly proportional effect on the transduction efficiency in NK-92 cells. Surprisingly, viral vector exposure as short as 15 minutes could be enough for viral vector entry into the host cells and 6 hours of exposure was optimal in standard transduction experiments. By using BX795 at two different doses during these transduction times, it was conclusive that both concentrations showed enhanced lentiviral gene delivery starting from 1 hour of exposure to lentiviral vector. Before that time point, there was no significant difference observed between control sample and the samples treated with BX795. This information provided clues about the requirement for BX795 in early signaling events taking place upon viral vector internalization.

Transduction of NK-92 cells at various MOI values indicated an increase in transduction efficiency with increasing viral load. Working with very high-titer lentiviral vectors, we were able to try MOI levels ranging from 1.25 to 20. Interestingly, the level reached without inhibitor at the highest MOI was almost the equivalent of the level reached with BX795 treatment at the lowest MOI value. This showed that BX795 could potentially be used with 10-fold less viral particles and still result in higher transduction efficiency. In the clinical setting, it would be highly preferable to use as few viral particles as possible to rule out the possibility of more than one lentiviral vector integrating in the host genome, potentially creating unpredicted gene disruption.

The dose-dependent effect of BX795 during lentiviral transduction and its related toxicity in primary NK cells were shown before (Sutlu et al., 2012). In this study, it was demonstrated that both NK-92 and YTS cell lines act in parallel to primary NK cells, showing a dose-dependent increase in transduction efficiency when exposed to the inhibitor BX795 during transduction. It was clearly seen that using doses of 3 to 6 μM BX795 in NK-92 cells and 1.5 to 3 μM in YTS cells were enough to induce significant increases in transduction efficiency. Additionally, the use of BX795 at these concentrations during transduction did not cause any toxicity in NK-92 cells. Collectively, these data supported the reliability of BX795 treatment in lentiviral gene delivery in terms of host cell viability.

For small-scale experiments, 24-well plates were optimal for transduction with small amount of cells and total volume requirement. However, for experiments that use millions of cells per condition, the transduction protocol needed to be scaled-up. Our results showed equally efficient transduction in all sizes tried. Puromycin selection was essential for lentiCRISPR and GeCKO library experiments. It was clear that a starting population of 30% GFP-Puro^R-positive cells could reach up to 100% in less than a week. This was easy to assess with a fluorescent marker where GFP- Puro^R-positive cells could be analyzed by flow cytometry. However, there was not a fluorescent marker for follow up with lentiCRISPR experiments and the required starting population was 10-20% Puro^R-positive cells. By the help of these optimization experiments, we could estimate the minimum time required for complete selection and expansion of cells in lentiCRISPR transductions.

In the context of signaling experiments, the use of serum-starved cells was advised for phosphorylation events to be detected accurately. However, NK-92 cells were dramatically affected by short-term serum-deprivation. In an attempt to grow NK-92 cells without serum, we deprived serum gradually over the course of four weeks and eventually obtained healthy cells living in serum-free media. These experiments also became one part of another project run in collaboration with Dr. Adil Duru's and Dr. Evren Alici's groups and is currently being prepared for publication, showing the growth and profile of serum-free-grown NK-92 cells for potential clinical applications (Chrobok et al., manuscript in preparation). The signaling events that were triggered upon lentiviral gene delivery required comparable transduction of serum-free growing NK-92 cells to their regularly cultured counter parts. For this purpose, the two cell types were transduced with

either regular lentiviral supernatant collected from the culture of 293FT cells or with column-purified virus to eliminate any factors coming from the 293FT culture interfering with serum-free growing cells. To our surprise, both transductions showed equally comparable results in regular and serum-deprived NK-92 cells; thus, the use of serum-free growing cells for signaling experiments was completely reliable.

Involvement of common γ -chain cytokines, especially IL-2, -12, -15, -18 and -21 in clinical expansion of primary NK cells as well as NK-92 cells affect many features ranging from cytotoxic profile to enhancement of immune responses have been demonstrated both *in vitro* and *in vivo* (Adib-Conquy et al., 2014; Ferlazzo, Pack, et al., 2004; Gregoire et al., 2007; Imamura et al., 2014; Klingemann & Martinson, 2004; Konstantinidis et al., 2005; Krzewski & Strominger, 2008; Sahn et al., 2012). Additionally, stimulation of primary NK cells with IL-2, -15 and -21 prior to transduction was shown to increase lentiviral gene delivery (Micucci et al., 2006; Sutlu et al., 2012). However, this was not the case with NK-92 when we tested the effect of these cytokines added alongside IL-2. Surprisingly, only IL-12 showed an enhancement in transduction efficiency both in the absence and presence of BX795, correlated with previous findings (Micucci et al., 2006). NK-92 cells are dependent on IL-2 for survival and their culture contains excessive amount of IL-2 that could potentially limit the amount of available common γ -chain receptor required for the signaling of IL-15 and -21. As expected, type I interferons caused a decrease in lentiviral gene delivery. Overall, standard transduction experiments did not require any additional treatment with cytokines to enhance lentiviral gene delivery in NK-92 cells.

Lentiviral gene delivery dynamics were intriguing to investigate because it was evident that viral vector internalization was a requirement for BX795-mediated enhancement of transduction. Our results demonstrated that viral vector entry could take place any time during 6 hours of transduction and BX795 addition at any point of this time scale resulted in at least a 2-fold enhancement. We knew that BX795 treatment did not have preparative effects on the host cell but it was clear that it could act on cells that had already taken up viral particles. This effect could not be assessed fully unless viral vector entry was limited to a time frame. The exact requirement for BX795 in any of the events leading to lentiviral RNA reverse-transcription, cDNA synthesis or integration was still unknown. In the 1-hour-transduction scenario, limited amount of viral vector exposure showed that BX795 treatment was increasing the efficiency of gene delivery for vectors already inside the cell

where no new entry could take place. Furthermore, this effect of BX795 was vanishing as the gap between viral vector exposure and inhibitor treatment was extending. Overall, these data suggested that BX795 prevented early elimination of viral vector, probably increasing the level of integration by dampening first stages of anti-viral response.

Knowing that BX795 acted on early events upon lentiviral vector entry, it was appealing to see which signaling pathways in particular were affected by the presence of the inhibitor. To test this, lentiviral vector alone, BX795 alone and both of them together were incubated with NK-92 cells and the pathways were analyzed by the immune cell signaling array. After testing time points ranging from 15 minutes to 12 hours, we determined that phosphorylation events for these specific signaling molecules could be detected up to 2 hours of lentiviral vector exposure. It was aimed to see differential gene expression patterns in transduced cells with or without the inhibitor however, there were no differences detected with transduced cells in 15 minutes when compared to control. Interestingly, the effect of BX795 alone on other signaling molecules in the absence of lentiviral vector could be followed starting from 15 minutes. These events were most likely due to the off-target binding of BX795 to kinases other than its major target IKK ϵ /TBK1. STAT1, STAT3 and STAT5 Tyr phosphorylations that are dependent on JAKs were significantly downregulated by the presence of BX795 even in 15 minutes. However, STAT1 and STAT3 Ser phosphorylations were not affected in the same manner. Looking at the longer time points revealed that BX795 alone could also cause reduced phosphorylation of p38, JNK and I κ B α as well as STAT1 and STAT3 Ser phosphorylations that are known to be downstream of MAPK signaling (Decker & Kovarik, 2000; Goh et al., 1999; Lim & Cao, 1999). This was also in parallel with intracellular flow cytometry results showing similar downregulation in STAT3 P-Ser727 in 2 hours of treatment with the inhibitor whereas lentiviral vector could increase this phosphorylation in a time-course trend, peaking at 90 minutes of exposure.

When we examined the signals activated in cells transduced by only the lentiviral vector, it was clearly seen that there was a time-dependent increase in p38 and JNK phosphorylation, correlated with previous findings in WT HIV (Lee et al., 2011; Muthumani et al., 2004, 2005, 2008) and other RNA virus infections (Börgeling et al., 2014; Mikkelsen et al., 2009; Poeck et al., 2010). To our knowledge, there were no previous studies showing the effect of lentiviral gene delivery in NK cells inducing p38 phosphorylation *in vitro*. Furthermore, p38 was suggested to be induced by poly (I:C)

triggering, an RNA-virus genome mimetic, in NK cells (Pisegna et al., 2004). Taken together, these observations suggested that the presence of lentiviral vectors could induce MAPK signaling and BX795 could have adverse effects on MAPKs that in turn regulate Ser phosphorylation of STATs important in immune cell signaling.

The nature of RNA signaling was controversial where total RIG-I and IRF3 amounts did not seem to be altered significantly upon lentiviral transduction at any time point tested. Total RIG-I expression in NK-92 cells could already be high prior to lentiviral transduction therefore there could not be any further increase observed. BX795 treatment was shown to inhibit IRF3 phosphorylation in some contexts where cytoplasmic RNA and DNA sensors induced TBK1-driven anti-viral responses (Devhare et al., 2016; K. Yang et al., 2015; S. Yang et al., 2016). Surprisingly, one study in macrophages showed that using BX795 treatment before poly (I:C) stimulation abrogated the TLR response and elevated RLR response (Hotz et al., 2015). When checked with intracellular staining, RIG-I expression was increased to only 1.5-fold compared to unstimulated control and BX795 treatment did not cause any changes in this pattern. Similarly, P-IRF7 detection was eminent with lentiviral vector entry regardless of BX795 presence. These findings suggested that IRF7 signaling might not be under direct influence of BX795 however the experiments need repeating before further conclusions.

Based on previous knowledge, TLR3 signaling can induce NF- κ B and IRF3 and to some extent MAPKs and AP-1 whereas TLR7/8 signaling is known to induce IRF7 in a MyD88-dependent fashion (O'Neill et al., 2013). APC-independent activation of NK cells through dsRNA sensing by TLR3 was shown previously (Schmidt et al., 2004). The stimulation of NK cells with dsRNA signaling was also reported to activate TLR3 pathways that involved p38 and IRF3 (Pisegna et al., 2004). In the same study, it was assessed by RT-PCR analysis that freshly isolated NK cells as well as YTS and NK-92 cell lines expressed adequate levels of TLR3 without any prior stimulation. This finding was correlated with increased cytotoxicity in dsRNA-stimulated in primary NK cells and NK-92 cell line. p38 phosphorylation was also correlated with dsRNA exposure time, hypothesized to be related to TLR3 signaling in primary NK cells and NK-92 cell line where TLR3^{low} NKL cell line did not show this response. MAPK family members ERK, JNK and p38 were also reported to play roles in NK cell cytotoxicity (Trotta et al., 2000). These data collectively point to specific roles of p38 and JNK in NK cells that can be

linked to the presence of danger signals and result in increased cytotoxicity against targets but it remains to be tested.

Another group showed that primary NK cells express almost no TLR7/8 and predominantly get activated by poly (I:C) triggering through TLR3 whereas TLR7/8-induced activation requires further cytokine signals provided by other immune cells in the host system (Gorski et al., 2006). However, a later study showed that poly (I:C) triggering induced RLR-mediated IFN γ response in human NK cells rather than TLR3 and required activation by cytokines produced by DCs (Perrot et al., 2010). Activation of primary NK cells by HIV-1 ssRNA was also shown to induce TLR-mediated responses in crosstalk with DCs (Alter et al., 2007; Sivori et al., 2004). Overall, the expression of TLRs and their mechanisms of activation rely on the complex immune microenvironment *in vivo* (Adib-Conquy et al., 2014). Hence, it was crucial to see which pathway, TLR- or RLR-mediated signaling, had the leading role in lentiviral gene delivery in NK-92 cells. Therefore, we aimed to create single gene knock-out cell lines with CRISPR/Cas9-mediated genome editing.

First, it was interesting to see how the selected gene disruptions would affect the success of lentiviral gene delivery in easy-to-transduce cell line 293FT. The constructs designed to target the start codon of selected genes *DDX58 (RIG-I)*, *IFIH1 (MDA5)*, *TBK1* and *TRIM5 α* by transient expression of CRISPR/Cas9 plasmids were all successful in generating cells with at least one allele mutated at target site. The targeted genome editing was achieved by HDR by introduction of ssODNs with homology arms in both 5' and 3' regions spanning the CRISPR binding site but the start codon was replaced with a restriction enzyme recognition site for selecting single cell clones with RFLP method. We showed that CRISPR/Cas9-mediated genome editing is a powerful tool, working with high efficiency by transfection method where CRISPR/Cas9 complex can only be found in the cell for a restricted amount of time and ssODN can be utilized for successful HDR in 293FT cells. Single cell clones needed to be identified in this context because not all transfected cells ended up having HDR and mutant clones were to be used in further experiments (summarized in Table 4.1).

Among selected clones, *TRIM5 α* mutants were the ones showing the most anticipated difference in transduction with lentiviral vector compared to WT. *TRIM5 α* was one of the most effective members of tripartite motif family proteins that induced NF- κ B and

AP-1 in HEK293 cells and TAK-1 signaling was essential for this induction (Pertel et al., 2011; Uchil et al., 2013). One out of two *MDA5*-mutant single cell clones also showed an increase in transduction but the verification of these mutants required further experiments.

To further assess the roles of candidate genes in anti-viral signaling, the usual suspects list was increased to 20 genes and 20 different lentiviral CRISPR/Cas9 constructs were cloned and produced as lentiviral vectors (from then on referred to as lentiCRISPRs for ease of use). NK cells have very low transfection efficiency, therefore all constructs were required to be in lentiviral vector system. To first address if constructs were functional, they were transduced one by one to 293FT cells. The constructs had Puro^R to select for successfully transduced cells and once selection was complete, all cells were expected have target site mutated in all alleles. To screen the effect of each gene on lentiviral gene delivery in 293FT cells, a low MOI (0.2) transduction was set up. The results showed significant increase in TRIM5 α - and to some extent in MAVS-lentiCRISPR⁺ samples. This effect could be due to limited amount of infectious particles in the transduction environment, therefore different MOI values were tested for selected high-ranking and non-effective samples. For all transductions tried, TRIM5 α -lentiCRISPR⁺ samples showed the highest transduction efficiency when compared to WT. The verification of these results at protein expression level remain to be tested.

When the set up was switched to NK-92 cells, more candidates showed differential results fitting the expectations coming from signaling data. We tested NK-92 transductions with LeGO-G2 lentiviral vector with or without BX795 to follow if any of the gene disruptions would result in an indifferent response to BX795. To our surprise, all conditions tested showed an increase in transduction in the presence of BX795, even in TBK1-targeting sample, suggesting either incomplete alteration of the target gene or off-target binding of the inhibitor as seen in the immune cell signaling array. Convincingly, the highest impact in transduction was seen with the TRIM25-lentiCRISPR⁺ samples. This effect could further support the roles of RLRs in anti-viral signaling where TRIM25 is responsible for ubiquitination of RIG-I (Gack et al., 2007). RIG-I- and *MDA5*-lentiCRISPR⁺ cells were among the highest-ranking samples in transduction, showing important roles of cytosolic RNA sensing. At the same level, TRIM28-lentiCRISPR⁺ samples showed an effect in transduction efficiency, probably due to the roles of TRIM28 in integration of reverse-transcription products (Allouch et al., 2011). Among these samples, *MDA5*- and

TRIM28-lentiCRISPR⁺ ones showed 80% reduction in their corresponding gene expression when checked at mRNA level whereas RIG-I- and TRIM25-lentiCRISPR⁺ samples showed 40% reduction. These data suggested that the genes were altered in all 12 lentiCRISPR⁺ cell lines however there could still be truncated or mutated proteins transcribed from these genes.

SYK-, JNK-, STING- and PI3K-lentiCRISPR⁺ samples also showed significantly higher lentiviral gene delivery in NK-92 cells, fitting the expectations coming from immune cell signaling data. PI3K is involved with many of the important signaling events in NK cells including IL-15 and Akt pathways (Ali et al., 2015). Surprisingly, endosomal RNA sensors TLR3 and TLR7 failed to enhance transduction as much as RIG-I and MDA5 after lentiCRISPR targeting. Interestingly, STING targeting seemed to cause a higher impact in efficiency than TLRs. It might suggest that reverse transcription products of lentiviral vector could still induce signals through cytoplasmic DNA sensors (Altfeld & Gale Jr, 2015). Overall, these data could potentially show a more dominant role for cytoplasmic RNA/DNA sensors rather than TLRs in initiating the anti-viral state of NK-92 cells upon lentiviral transduction.

Interestingly, two major candidates selected from signaling experiments, JNK and p38, showed opposite effects upon lentiCRISPR targeting. JNK-lentiCRISPR⁺ samples were significantly more prominent in lentiviral gene delivery; on the contrary, p38-lentiCRISPR⁺ samples showed almost no difference. Danger signals associated with viral invasion cause the activation of TAK-1 through TRIM5 α upon capsid binding or nucleic acid sensing by endosomal TLRs and these could further activate MAPKs p38 and JNK in NK-92 cells. Previous studies with HIV-1 showed abrogation of infection by JNK inhibitors (Lee et al., 2011; Muthumani et al., 2004); however, our findings pointed the opposite in potential knock-down of JNK but the levels of knock-down still need to be tested. JNK is important for STAT3 Ser phosphorylation (Lim & Cao, 1999) that was found to be upregulated upon lentiviral vector internalization in our experiments. Apparently, MAPKs play essential roles in NK cell signaling dynamics but there are many other factors influencing the balance of these signals.

Among all candidate genes targeted, RIG-I seemed to have the highest potential for causing adverse effects in abrogation of lentiviral gene delivery in NK-92 cells. Therefore, we sequenced the PCR products spanning the *DDX58* genomic DNA region

containing the potential DSB site. Astonishingly, among the sequenced products, many showed variations in the potential cut site of Cas9, 3 bp upstream of PAM sequence. Ranging from 1 to 134 bp, most samples showed deletions and a few had mutations but no insertions were observed. It was crucial to see a variety of mutations in the population due to the risk of clonal selection. If a certain mutation had caused selective advantage, all clones would be descendants of the same mutant, therefore limiting the outcome of following experiments. The most surprising finding was the discovery of an SNP a few nucleotides downstream of transcription start site, causing a major alteration in the amino acid sequence from Arg to Cys in the 7th position. This SNP was also identified in one study showing differential anti-viral responses in DCs due to the change in RIG-I protein structure right at the CARDS, impacting the downstream signaling (Hu et al., 2010). Thus, it would be very appealing to see the genotype of transduced NK-92 cells and compare the lentiviral gene delivery associated with RIG-I polymorphism in the population.

The curious case of p38 induction led to the investigation of the effects of a new inhibitor, VX745, that could potentially change the dynamics of lentiviral gene delivery. VX745 was used in many studies for complete inhibition of p38 α including clinical trials in autoimmune disease rheumatoid arthritis to dampen inflammation (Gaestel et al., 2009). We hypothesized that blocking p38 would cause an increase in lentiviral gene delivery in NK-92 cells since the results of signaling array showed an upregulation of p38 phosphorylation upon viral exposure and downregulation when BX795 was present. Surprisingly, the results conveyed reduced transduction efficiency in NK-92 cells when VX745 was used during or hours after exposure to lentiviral vector. Preliminary results were intriguing and further experiments are required to reach a conclusion about the specific role of this inhibitor in anti-viral signaling in NK cells.

Observing the effect of one gene knock-out/knock-down at a time is useful and necessary for identification of candidate players in anti-viral immunity of NK cells. However, genome-wide screens provide a different perspective and help one understand the very complex network of signaling pathways contributing to the anti-viral state. Therefore, it was illuminating for us to apply a genome-wide screen with GeCKO library in NK-92 cells to see the effects of pathways contributing to the elimination of viral vectors. Preliminary data provided us remarkable results where GeCKO-LibA⁺- and GeCKO-LibB⁺-NK-92 cells showed almost double the efficiency when transduced with the LeGO-G2 vector, almost mimicking the effect of BX795 in the absence of the inhibitor.

Based on our findings, we propose a role for BX795 interfering with the responses downstream of RLRs and TLRs in a complex network. Additionally, we think that the lentiviral vector entry induces as RLR-dominated response with specific roles of TRIM25 in NK-92 cells. The cytokines and danger signals obtained from the culture are expected to influence the intracellular dynamics of lentiviral vector signaling through the activation of MAPKs p38 and JNK in this process. Overall, our model can be summarized in Figure 5.1.

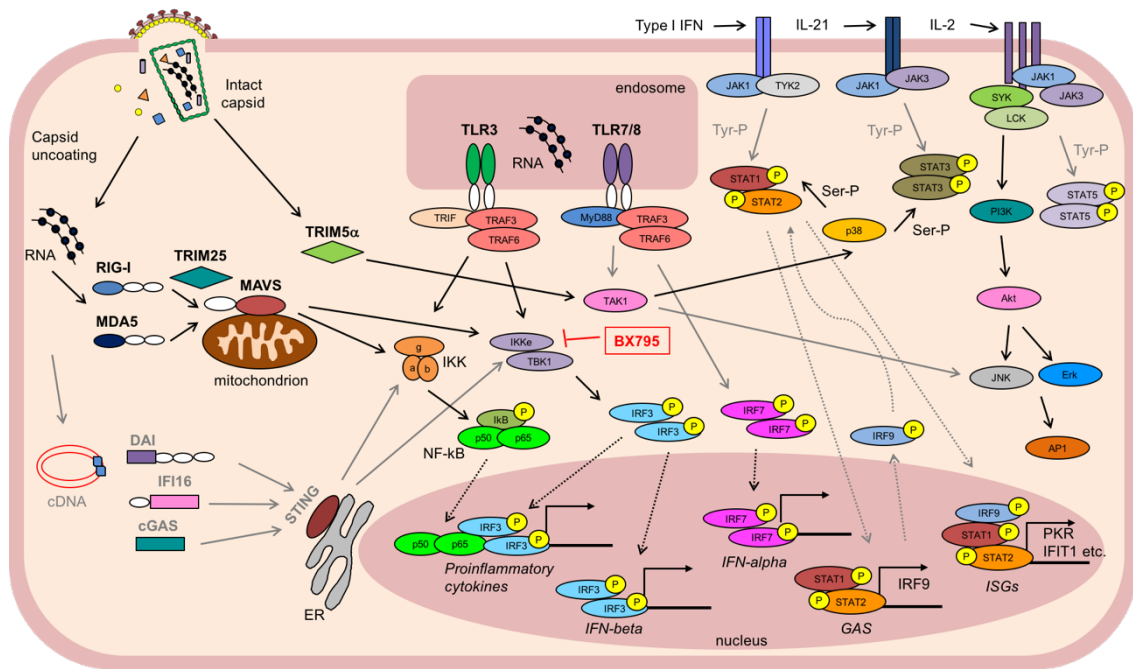


Figure 5.1. Proposed model for signaling events triggered upon lentiviral vector delivery in NK cells. BX795, the small molecule inhibitor of TBK1/IKK ϵ , could increase transduction efficiency in NK cells by potentially blocking signals received from RLRs and TLR3, with additional effects on MAPK signaling. It is possible that some signaling events (annotated with black arrows) such as dsRNA signaling are more dominant in NK cells over others (annotated with grey) but their individual contributions remain to be tested.

6. CONCLUSION

This study is an extensive effort in investigating the roles of candidate genes in anti-viral signaling pathways that are causing resistance to lentiviral gene delivery in human NK cells. The use of small molecule inhibitor BX795 has significantly altered the transduction efficiency of NK cells and the update of current lentiviral transductions is valuable for future uses in immunotherapy. The optimization of transduction methods and better understanding of responses to lentiviral gene delivery may provide answers for all gene therapy trials with applications ranging from stem cells to other members of the lymphocytic lineage. Regarding further applications, other studies in our lab have used optimized transduction protocols with BX795 to generate genetically-modified NK-92 cells retargeted against specific tumor antigens.

Our aim in characterizing novel pathways to target with small molecule inhibitors has led us to the identification of primarily TRIM5 α in 293FT and RIG-I and TRIM25 in NK-92 cells that gave rise to an anti-viral response upon lentiviral gene delivery. Overcoming signaling events in 293FT that interfere with lentiviral vector production could be useful in generation of higher-titer vectors. The identification of RIG-I pathway as the main resistance behind lentiviral gene delivery in NK cells could potentially open new doors in gene therapy applications. The induction of MAPKs in NK-92 cells in the presence of lentiviral vectors requires further analysis to find the specific roles of the pathways leading to p38 and JNK phosphorylation. If RIG-I and p38 pathways are intertwined, this would be a novel finding that impacts our understanding of the response of NK cell to lentiviral vectors.

REFERENCES

- Ablasser, A., Bauernfeind, F., Hartmann, G., Latz, E., Fitzgerald, K. A., & Hornung, V. (2009). RIG-I-dependent sensing of poly(dA:dT) through the induction of an RNA polymerase III-transcribed RNA intermediate. *Nature Immunology*, *10*(10), 1065–1072. <http://doi.org/10.1038/ni.1779>
- Adib-Conquy, M., Scott-Algara, D., Cavaillon, J.-M., & Souza-Fonseca-Guimaraes, F. (2014). TLR-mediated activation of NK cells and their role in bacterial/viral immune responses in mammals. *Immunology and Cell Biology*, *92*(3), 256–62. <http://doi.org/10.1038/icb.2013.99>
- Ali, A. K., Nandagopal, N., & Lee, S. H. (2015). IL-15-PI3K-AKT-mTOR: A critical pathway in the life journey of Natural Killer cells. *Frontiers in Immunology*, *6*, 1–22. <http://doi.org/10.3389/fimmu.2015.00355>
- Alici, E., & Sutlu, T. (2009). Natural killer cell-based immunotherapy in cancer: Current insights and future prospects. *Journal of Internal Medicine*, *266*(2), 154–181. <http://doi.org/10.1111/j.1365-2796.2009.02121.x>
- Allouch, A., Di Primio, C., Alpi, E., Lusic, M., Arosio, D., Giacca, M., & Cereseto, A. (2011). The TRIM family protein KAP1 inhibits HIV-1 integration. *Cell Host and Microbe*, *9*(6), 484–495. <http://doi.org/10.1016/j.chom.2011.05.004>
- Alter, G., Suscovich, T. J., Teigen, N., Meier, A., Streeck, H., Brander, C., & Altfeld, M. (2007). Single-stranded RNA derived from HIV-1 serves as a potent activator of NK cells. *Journal of Immunology*, *178*(12), 7658–66. <http://doi.org/10.1093/imm/178/12/7658>
- Altfeld, M., & Gale Jr, M. (2015). Innate immunity against HIV-1 infection. *Nature Immunology*, *16*(6), 554–562. <http://doi.org/10.1038/ni.3157>

- Altwater, B., Landmeier, S., Pscherer, S., Temme, J., Schweer, K., Kailayangiri, S., ... Rossig, C. (2009). 2B4 (CD244) signaling by recombinant antigen-specific chimeric receptors costimulates natural killer cell activation to leukemia and neuroblastoma cells. *Clinical Cancer Research*, *15*(15), 4857–4866. <http://doi.org/10.1158/1078-0432.CCR-08-2810>
- Ansorge, S., Lanthier, S., Transfiguracion, J., Durocher, Y., Henry, O., & Kamen, A. (2009). Development of a scalable process for high-yield lentiviral vector production by transient transfection of HEK293 suspension cultures. *Journal of Gene Medicine*, *11*(10), 868–876. <http://doi.org/10.1002/jgm.1370>
- Arai, S., Meagher, R., Swearingen, M., Myint, H., Rich, E., Martinson, J., & Klingemann, H. (2008). Infusion of the allogeneic cell line NK-92 in patients with advanced renal cell cancer or melanoma: a phase I trial. *Cytotherapy*, *10*(6), 625–32. <http://doi.org/10.1080/14653240802301872>
- Baginska, J., Viry, E., Paggetti, J., Medves, S., Berchem, G., Moussay, E., & Janji, B. (2013). The critical role of the tumor microenvironment in shaping natural killer cell-mediated anti-tumor immunity. *Frontiers in Immunology*. <http://doi.org/10.3389/fimmu.2013.00490>
- Baker, A. H. (2007). Adenovirus toxicity and tropism in vivo: not as simple as A,B,C (or D,E,F). *Molecular Therapy: The Journal of the American Society of Gene Therapy*, *15*(12), 2061–2062. <http://doi.org/10.1038/sj.mt.6300349>
- Bernardini, G., Antonangeli, F., Bonanni, V., & Santoni, A. (2016). Dysregulation of Chemokine/Chemokine Receptor Axes and NK Cell Tissue Localization during Diseases. *Frontiers in Immunology*, *7*, 1–9. <http://doi.org/10.3389/fimmu.2016.00402>
- Berson, J. F., Long, D., Doranz, B. J., Rucker, J., Jirik, F. R., & Doms, R. W. (1996). A seven-transmembrane domain receptor involved in fusion and entry of T-cell-tropic human immunodeficiency virus type 1 strains. *Journal of Virology*, *70*(9), 6288–95. [http://doi.org/0022-538X/96/\\$04.0010](http://doi.org/0022-538X/96/$04.0010)
- Binstadt, B. A., Brumbaugh, K. M., Dick, C. J., Scharenberg, A. M., Williams, B. L., Colonna, M., ... Leibson, P. J. (1996). Sequential involvement of Lck and SHP-1 with MHC-recognizing receptors on NK cells inhibits FcR-initiated tyrosine kinase activation. *Immunity*, *5*(6), 629–638. [http://doi.org/10.1016/S1074-7613\(00\)80276-9](http://doi.org/10.1016/S1074-7613(00)80276-9)
- Binyamin, L., Alpaugh, R. K., Hughes, T. L., Lutz, C. T., Campbell, K. S., & Weiner, L. M. (2008). Blocking NK cell inhibitory self-recognition promotes antibody-dependent cellular cytotoxicity in a model of anti-lymphoma therapy. *Journal of Immunology*, *180*(9), 6392–401. <http://doi.org/10.4049/jimmunol.180.9.6392>
- Boehme, K. W., Guerrero, M., & Compton, T. (2006). Human cytomegalovirus envelope glycoproteins B and H are necessary for TLR2 activation in permissive cells. *Journal of Immunology*, *177*(10), 7094–7102. <http://doi.org/177/10/7094>

- Boissel, L., Betancur-Boissel, M., Lu, W., Krause, D. S., Van Etten, R. a, Wels, W. S., & Klingemann, H. (2013). Retargeting NK-92 cells by means of CD19- and CD20-specific chimeric antigen receptors compares favorably with antibody-dependent cellular cytotoxicity. *Oncoimmunology*, 2(10), e26527. <http://doi.org/10.4161/onci.26527>
- Boissel, L., Betancur, M., Lu, W., Wels, W. S., Marino, T., Van Etten, R. A., & Klingemann, H. (2012). Comparison of mRNA and lentiviral based transfection of natural killer cells with chimeric antigen receptors recognizing lymphoid antigens. *Leukemia & Lymphoma*, 53(5), 958–965. <http://doi.org/10.3109/10428194.2011.634048>
- Boissel, L., Betancur, M., Wels, W. S., Tuncer, H., & Klingemann, H. (2009). Transfection with mRNA for CD19 specific chimeric antigen receptor restores NK cell mediated killing of CLL cells. *Leukemia Research*, 33(9), 1255–1259. <http://doi.org/10.1016/j.leukres.2008.11.024>
- Borg, C., Jalil, A., Laderach, D., Maruyama, K., Wakasugi, H., Charrier, S., ... Zitvogel, L. (2004). NK cell activation by dendritic cells (DCs) requires the formation of a synapse leading to IL-12 polarization in DCs. *Blood*, 104(10), 3267–3275. <http://doi.org/10.1182/blood-2004-01-0380>
- Börgeling, Y., Schmolke, M., Viemann, D., Nordhoff, C., Roth, J., & Ludwig, S. (2014). Inhibition of p38 mitogen-activated protein kinase impairs influenza virus-induced primary and secondary host gene responses and protects mice from lethal H5N1 infection. *Journal of Biological Chemistry*, 289(1), 13–27. <http://doi.org/10.1074/jbc.M113.469239>
- Breckpot, K., Escors, D., Arce, F., Lopes, L., Karwacz, K., Van Lint, S., ... Collins, M. (2010). HIV-1 lentiviral vector immunogenicity is mediated by Toll-like receptor 3 (TLR3) and TLR7. *Journal of Virology*, 84(11), 5627–36. <http://doi.org/10.1128/JVI.00014-10>
- Brilot, F., Strowig, T., Roberts, S. M., Arrey, F., & Münz, C. (2007). NK cell survival mediated through the regulatory synapse with human DCs requires IL-15Ralpha. *Journal of Clinical Investigation*, 117(11), 3316–3329. <http://doi.org/10.1172/JCI31751>
- Bruns, A. M., & Horvath, C. M. (2015). LGP2 synergy with MDA5 in RLR-mediated RNA recognition and antiviral signaling. *Cytokine*, 74, 198–206. <http://doi.org/10.1016/j.cyto.2015.02.010>
- Bruns, A. M., Leser, G. P., Lamb, R. A., & Horvath, C. M. (2014). The Innate Immune Sensor LGP2 Activates Antiviral Signaling by Regulating MDA5-RNA Interaction and Filament Assembly. *Molecular Cell*, 55(5), 771–781. <http://doi.org/10.1016/j.molcel.2014.07.003>
- Bryceson, Y. T., March, M. E., Ljunggren, H., & Long, E. O. (2006). Activation, coactivation, and costimulation of resting human natural killer cells. *Immunological Reviews*, 214, 73–91. <http://doi.org/10.1111/j.1600-065X.2006.00457.x>

- Bukrinsky, M. I., Haggerty, S., Dempsey, M. P., Sharova, N., Adzhubel, A., Spitz, L., ... Stevenson, M. (1993). A nuclear localization signal within HIV-1 matrix protein that governs infection of non-dividing cells. *Nature*, *365*(6447), 666–9. <http://doi.org/10.1038/365666a0>
- Campbell, J. J., Qin, S., Unutmaz, D., Soler, D., Murphy, K. E., Hodge, M. R., ... Butcher, E. C. (2001). Unique Subpopulations of CD56+ NK and NK-T Peripheral Blood Lymphocytes Identified by Chemokine Receptor Expression Repertoire. *Journal of Immunology*, *166*, 6477–6482. <http://doi.org/10.4049/jimmunol.166.11.6477>
- Carlsten, M., & Childs, R. (2015). Genetic manipulation of NK cells for cancer immunotherapy: techniques and clinical implications. *Frontiers in Immunology*, *6*, 1–9. <http://doi.org/10.3389/fimmu.2015.00266>
- Cavazzana-Calvo, M., Hacein-Bey, S., de Saint Basile, G., Gross, F., Yvon, E., Nusbaum, P., ... Fischer, A. (2000). Gene Therapy of Human Severe Combined Immunodeficiency (SCID)-X1 Disease. *Science*, *288*(2000), 669–672. <http://doi.org/10.1126/science.288.5466.669>
- Chan, A., Hong, D.-L., Atzberger, A., Kollnberger, S., Filer, A. D., Buckley, C. D., ... Bowness, P. (2007). CD56bright human NK cells differentiate into CD56dim cells: role of contact with peripheral fibroblasts. *Journal of Immunology*, *179*, 89–94. <http://doi.org/10.4049/jimmunol.179.1.89>
- Chang, Y. H., Connolly, J., Shimasaki, N., Mimura, K., Kono, K., & Campana, D. (2013). A chimeric receptor with NKG2D specificity enhances natural killer cell activation and killing of tumor cells. *Cancer Research*, *73*(6), 1777–1786. <http://doi.org/10.1158/0008-5472.CAN-12-3558>
- Chen, J., Nikolaitchik, O., Singh, J., Wright, A., Bencsics, C. E., Coffin, J. M., ... Hu, W.-S. (2009). High efficiency of HIV-1 genomic RNA packaging and heterozygote formation revealed by single virion analysis. *Proceedings of the National Academy of Sciences of the United States of America*, *106*(32), 13535–40. <http://doi.org/10.1073/pnas.0906822106>
- Chen, J., Rahman, S. A., Nikolaitchik, O. A., Grunwald, D., Sardo, L., Burdick, R. C., ... Hu, W.-S. (2016). HIV-1 RNA genome dimerizes on the plasma membrane in the presence of Gag protein. *Proceedings of the National Academy of Sciences of the United States of America*, *113*(2), E201–8. <http://doi.org/10.1073/pnas.1518572113>
- Chen, X., Han, J., Chu, J., Zhang, L., Zhang, J., Chen, C., ... Yu, J. (2016). A combinational therapy of EGFR-CAR NK cells and oncolytic herpes simplex virus 1 for breast cancer brain metastases. *Oncotarget*, *7*(19), 27764–77. <http://doi.org/10.18632/oncotarget.8526>
- Childs, R. W., & Berg, M. (2013). Bringing natural killer cells to the clinic: ex vivo manipulation. *ASH Education Program Book*, *2013*, 234–246. <http://doi.org/10.1182/asheducation-2013.1.234>
- Chiu, Y. H., MacMillan, J. B., & Chen, Z. J. (2009). RNA Polymerase III Detects Cytosolic DNA and Induces Type I Interferons through the RIG-I Pathway. *Cell*, *138*(3), 576–591. <http://doi.org/10.1016/j.cell.2009.06.015>

- Chu, J., Deng, Y., Benson, D. M., He, S., Hughes, T., Zhang, J., ... Yu, J. (2014). CS1-specific chimeric antigen receptor (CAR)-engineered natural killer cells enhance in vitro and in vivo antitumor activity against human multiple myeloma. *Leukemia*, 28(4), 917–27. <http://doi.org/10.1038/leu.2013.279>
- Clark, K., Plater, L., Peggie, M., & Cohen, P. (2009). Use of the pharmacological inhibitor BX795 to study the regulation and physiological roles of TBK1 and I κ B Kinase epsilon: A distinct upstream kinase mediates ser-172 phosphorylation and activation. *Journal of Biological Chemistry*, 284(21), 14136–14146. <http://doi.org/10.1074/jbc.M109.000414>
- Cyranoski, D. (2016). CRISPR gene editing tested in a person. *Nature*, 539(7630), 479. <http://doi.org/10.1038/nature.2016.20988>
- Dambuza, I. M., & Brown, G. D. (2015). C-type lectins in immunity: Recent developments. *Current Opinion in Immunology*, 32, 21–27. <http://doi.org/10.1016/j.coi.2014.12.002>
- Daya, S., & Berns, K. I. (2008). Gene therapy using adeno-associated virus vectors. *Clinical Microbiology Reviews*, 21(4), 583–593. <http://doi.org/10.1128/CMR.00008-08>
- De Maria, A., Bozzano, F., Cantoni, C., & Moretta, L. (2011). Revisiting human natural killer cell subset function revealed cytolytic CD56(dim)CD16+ NK cells as rapid producers of abundant IFN-gamma on activation. *Proceedings of the National Academy of Sciences of the United States of America*, 108(2), 728–32. <http://doi.org/10.1073/pnas.1012356108>
- Decker, T., & Kovarik, P. (2000). Serine phosphorylation of STATs. *Oncogene*, 19(21), 2628–37. <http://doi.org/10.1038/sj.onc.1203481>
- Dempsey, A., & Bowie, A. G. (2015). Innate immune recognition of DNA: A recent history. *Virology*, 479–480, 146–52. <http://doi.org/10.1016/j.virol.2015.03.013>
- DePolo, N. J., Reed, J. D., Sheridan, P. L., Townsend, K., Sauter, S. L., Jolly, D. J., & Dubensky, T. W. (2000). VSV-G pseudotyped lentiviral vector particles produced in human cells are inactivated by human serum. *Molecular Therapy: The Journal of the American Society of Gene Therapy*, 2(3), 218–22. <http://doi.org/10.1006/mthe.2000.0116>
- Dever, D. P., Bak, R. O., Reinisch, A., Camarena, J., Washington, G., Nicolas, C. E., ... Porteus, M. H. (2016). CRISPR/Cas9 β -globin gene targeting in human haematopoietic stem cells. *Nature*, 539(7629), 384–89. <http://doi.org/10.1038/nature20134>
- Devhare, P. B., Desai, S., & Lole, K. S. (2016). Innate immune responses in human hepatocyte-derived cell lines alter genotype 1 hepatitis E virus replication efficiencies. *Scientific Reports*, 6, 26827. <http://doi.org/10.1038/srep26827>
- Dolganiuc, A., Oak, S., Kodys, K., Golenbock, D. T., Finberg, R. W., Kurt-Jones, E., & Szabo, G. (2004). Hepatitis C core and nonstructural 3 proteins trigger toll-like receptor 2-mediated pathways and inflammatory activation. *Gastroenterology*, 127(5), 1513–1524. <http://doi.org/10.1053/j.gastro.2004.08.067>

- Dull, T., Zufferey, R., Kelly, M., Mandel, R. J., Nguyen, M., Trono, D., & Naldini, L. (1998). A third-generation lentivirus vector with a conditional packaging system. *Journal of Virology*, *72*(11), 8463–71. <http://doi.org/98440501>
- Esser, R., Müller, T., Stefes, D., Kloess, S., Seidel, D., Gillies, S. D., ... Wels, W. S. (2012). NK cells engineered to express a GD 2-specific antigen receptor display built-in ADCC-like activity against tumour cells of neuroectodermal origin. *Journal of Cellular and Molecular Medicine*, *16*(3), 569–581. <http://doi.org/10.1111/j.1582-4934.2011.01343.x>
- Feng, Y., Broder, C. C., Kennedy, P. E., & Berger, E. A. (2011). Pillars article: HIV-1 entry cofactor: functional cDNA cloning of a seven-transmembrane, G protein-coupled receptor. *Science*. 1996. 272: 872-877. *Journal of Immunology*, *186*(11), 6076–81. <http://doi.org/10.1126/science.272.5263.872>.
- Ferlazzo, G., Pack, M., Thomas, D., Paludan, C., Schmid, D., Strowig, T., ... Münz, C. (2004). Distinct roles of IL-12 and IL-15 in human natural killer cell activation by dendritic cells from secondary lymphoid organs. *Proceedings of the National Academy of Sciences of the United States of America*, *101*, 16606–16611. <http://doi.org/10.1073/pnas.0407522101>
- Ferlazzo, G., Thomas, D., Lin, S., Goodman, K., Morandi, B., Muller, W. A., ... Münz, C. (2004). The abundant NK cells in human secondary lymphoid tissues require activation to express killer cell Ig-Like receptors and become cytolytic. *Journal of Immunology*, *172*(3), 1455–1462. <http://doi.org/10.4049/jimmunol.172.3.1455>
- Fernandes-Alnemri, T., Yu, J.-W., Datta, P., Wu, J., & Alnemri, E. S. (2009). AIM2 activates the inflammasome and cell death in response to cytoplasmic DNA. *Nature*, *458*(7237), 509–513. <http://doi.org/10.1038/nature07710>
- Figueiredo, C., Seltsam, A., & Blasczyk, R. (2009). Permanent silencing of NKG2A expression for cell-based therapeutics. *Journal of Molecular Medicine*, *87*(2), 199–210. <http://doi.org/10.1007/s00109-008-0417-0>
- Fitzgerald, K. a., McWhirter, S. M., Faia, K. L., Rowe, D. C., Latz, E., Golenbock, D. T., ... Maniatis, T. (2003). IKK ϵ and TBK1 are essential components of the IRF3 signaling pathway. *Nature Immunology*, *4*(5), 491–496. <http://doi.org/10.1038/ni921>
- Gack, M. U., Shin, Y. C., Joo, C.-H., Urano, T., Liang, C., Sun, L., ... Jung, J. U. (2007). TRIM25 RING-finger E3 ubiquitin ligase is essential for RIG-I-mediated antiviral activity. *Nature*, *446*(7138), 916–920. <http://doi.org/10.1038/nature05732>
- Gaestel, M., Kotlyarov, A., & Kracht, M. (2009). Targeting innate immunity protein kinase signalling in inflammation. *Nature Reviews Drug Discovery*, *8*, 480–99. <http://doi.org/10.1038/nrd2829>
- Gallay, P., Hope, T., Chin, D., & Trono, D. (1997). HIV-1 infection of nondividing cells through the recognition of integrase by the importin/karyopherin pathway. *Proceedings of the National Academy of Sciences of the United States of America*, *94*(18), 9825–30. <http://doi.org/10.1073/pnas.94.18.9825>

- Genovese, P., Schirotti, G., Escobar, G., Di Tomaso, T., Firrito, C., Calabria, A., ... Naldini, L. (2014). Targeted genome editing in human repopulating haematopoietic stem cells. *Nature*, *510*(7504), 235–40. <http://doi.org/10.1038/nature13420>
- Genßler, S., Burger, M. C., Zhang, C., Oelsner, S., Mildenerger, I., Wagner, M., ... Wels, W. S. (2016). Dual targeting of glioblastoma with chimeric antigen receptor-engineered natural killer cells overcomes heterogeneity of target antigen expression and enhances antitumor activity and survival. *Oncoimmunology*, *5*(4), e1119354. <http://doi.org/10.1080/2162402X.2015.1119354>
- Georgel, P., Jiang, Z., Kunz, S., Janssen, E., Mols, J., Hoebe, K., ... Beutler, B. (2007). Vesicular stomatitis virus glycoprotein G activates a specific antiviral Toll-like receptor 4-dependent pathway. *Virology*, *362*(2), 304–313. <http://doi.org/10.1016/j.virol.2006.12.032>
- Gerosa, F., Gobbi, A., Zorzi, P., Burg, S., Briere, F., Carra, G., & Trinchieri, G. (2005). The Reciprocal Interaction of NK Cells with Plasmacytoid or Myeloid Dendritic Cells Profoundly Affects Innate Resistance Functions. *Journal of Immunology*, *174*(2), 727–734. <http://doi.org/10.4049/jimmunol.174.2.727>
- Gill, D. R., Pringle, I. A., & Hyde, S. C. (2009). Progress and prospects: the design and production of plasmid vectors. *Gene Therapy*, *16*(2), 165–71. <http://doi.org/10.1038/gt.2008.183>
- Goh, K. C., Haque, S. J., & Williams, B. R. (1999). p38 MAP kinase is required for STAT1 serine phosphorylation and transcriptional activation induced by interferons. *The EMBO Journal*, *18*(20), 5601–8. <http://doi.org/10.1093/emboj/18.20.5601>
- Gong, J. H., Maki, G., & Klingemann, H. G. (1994). CHARACTERIZATION OF A HUMAN CELL-LINE (NK-92) WITH PHENOTYPICAL AND FUNCTIONAL-CHARACTERISTICS OF ACTIVATED NATURAL-KILLER-CELLS. *Leukemia*, *8*(4), 652–658.
- Gorski, K. S., Waller, E. L., Bjornton-Severson, J., Hanten, J. A., Riter, C. L., Kieper, W. C., ... Alkan, S. S. (2006). Distinct indirect pathways govern human NK-cell activation by TLR-7 and TLR-8 agonists. *International Immunology*, *18*(7), 1115–1126. <http://doi.org/10.1093/intimm/dxl046>
- Gregoire, C., Chasson, L., Luci, C., Tomasello, E., Geissmann, F., Vivier, E., & Walzer, T. (2007). The trafficking of natural killer cells. *Immunological Reviews*, *220*, 169–182. <http://doi.org/IMR563> [pii]n10.1111/j.1600-065X.2007.00563.x
- Han, J., Chu, J., Keung Chan, W., Zhang, J., Wang, Y., Cohen, J. B., ... Yu, J. (2015). CAR-Engineered NK Cells Targeting Wild-Type EGFR and EGFRvIII Enhance Killing of Glioblastoma and Patient-Derived Glioblastoma Stem Cells. *Scientific Reports*, *5*, 11483. <http://doi.org/10.1038/srep11483>
- Hasmim, M., Messai, Y., Ziani, L., Thiery, J., Bouhris, J. H., Noman, M. Z., & Chouaib, S. (2015). Critical role of tumor microenvironment in shaping NK cell functions: Implication of hypoxic stress. *Frontiers in Immunology*, *6*, 1–9. <http://doi.org/10.3389/fimmu.2015.00482>

- Hatakeyama, M., Kono, T., Kobayashi, N., Kawahara, A., Levin, S. D., Perlmutter, R. M., & Taniguchi, T. (1991). Interaction of the IL-2 receptor with the src-family kinase p56lck: identification of novel intermolecular association. *Science*, *252*(5012), 1523–8.
- Herberman, R., Nunn, M. E., & Lavrin, D. H. (1975). Natural cytotoxic reactivity of mouse lymphoid cells against syngeneic acid allogeneic tumors. I. Distribution of reactivity and specificity. *International Journal of Cancer. Journal International Du Cancer*, *16*(2), 216–229. <http://doi.org/10.1002/ijc.2910160204>
- Hirano, S., Nishimasu, H., Ishitani, R., & Nureki, O. (2016). Structural Basis for the Altered PAM Specificities of Engineered CRISPR-Cas9. *Molecular Cell*, *61*(6), 886–894. <http://doi.org/10.1016/j.molcel.2016.02.018>
- Hornung, V., Ablasser, A., Charrel-Dennis, M., Bauernfeind, F., Horvath, G., Caffrey, D. R., ... Fitzgerald, K. A. (2009). AIM2 recognizes cytosolic dsDNA and forms a caspase-1-activating inflammasome with ASC. *Nature*, *458*(7237), 514–518. <http://doi.org/10.1038/nature07725>
- Hornung, V., Hartmann, R., Ablasser, A., & Hopfner, K.-P. (2014). OAS proteins and cGAS: unifying concepts in sensing and responding to cytosolic nucleic acids. *Nature Reviews Immunology*, *14*(8), 521–8. <http://doi.org/10.1038/nri3719>
- Hotz, C., Roetzer, L. C., Huber, T., Sailer, A., Oberson, A., Treinies, M., ... Bourquin, C. (2015). TLR and RLR Signaling Are Reprogrammed in Opposite Directions after Detection of Viral Infection. *Journal of Immunology*, *195*, 4387–95. <http://doi.org/10.4049/jimmunol.1500079>
- Houghton, B. C., Booth, C., & Thrasher, A. J. (2015). Lentivirus technologies for modulation of the immune system. *Current Opinion in Pharmacology*, *24*, 119–127. <http://doi.org/10.1016/j.coph.2015.08.007>
- Hrecka, K., Hao, C., Gierszewska, M., Swanson, S. K., Kesik-Brodacka, M., Srivastava, S., ... Skowronski, J. (2011). Vpx relieves inhibition of HIV-1 infection of macrophages mediated by the SAMHD1 protein. *Nature*, *474*(7353), 658–661. <http://doi.org/10.1038/nature10195>
- Hu, J., Nistal-Villán, E., Voho, A., Ganee, A., Kumar, M., Ding, Y., ... Wetmur, J. G. (2010). A common polymorphism in the caspase recruitment domain of RIG-I modifies the innate immune response of human dendritic cells. *Journal of Immunology*, *185*(1), 424–32. <http://doi.org/10.4049/jimmunol.0903291>
- Ibraheem, D., Elaissari, A., & Fessi, H. (2014). Gene therapy and DNA delivery systems. *International Journal of Pharmaceutics*, *459*(1–2), 70–83. <http://doi.org/10.1016/j.ijpharm.2013.11.041>
- Imamura, M., Shook, D., Kamiya, T., Shimasaki, N., Chai, S. M. H., Coustan-Smith, E., ... Campana, D. (2014). Autonomous growth and increased cytotoxicity of natural killer cells expressing membrane-bound interleukin-15. *Blood*, *124*(7), 1081–1088. <http://doi.org/10.1182/blood-2014-02-556837>

- Jakobsen, M. R., Bak, R. O., Andersen, A., Berg, R. K., Jensen, S. B., Jin, T., ... Paludan, S. R. (2013). IFI16 senses DNA forms of the lentiviral replication cycle and controls HIV-1 replication. *Proceedings of the National Academy of Sciences of the United States of America*, *110*(48), E4571-80. <http://doi.org/10.1073/pnas.1311669110>
- James, A. M., Cohen, A. D., & Campbell, K. S. (2013). Combination immune therapies to enhance anti-tumor responses by NK cells. *Frontiers in Immunology*, *4*, 1–12. <http://doi.org/10.3389/fimmu.2013.00481>
- Jiang, H., Zhang, W., Shang, P., Zhang, H., Fu, W., Ye, F., ... Hou, J. (2014). Transfection of chimeric anti-CD138 gene enhances natural killer cell activation and killing of multiple myeloma cells. *Molecular Oncology*, *8*(2), 297–310. <http://doi.org/10.1016/j.molonc.2013.12.001>
- Jiang, W., Zhang, C., Tian, Z., & Zhang, J. (2014). HIL-15 gene-modified human natural killer cells (NKL-IL15) augments the anti-human hepatocellular carcinoma effect in vivo. *Immunobiology*, *219*(7), 547–553. <http://doi.org/10.1016/j.imbio.2014.03.007>
- Jiang, W., Zhang, J., & Tian, Z. (2008). Functional characterization of interleukin-15 gene transduction into the human natural killer cell line NKL. *Cytotherapy*, *10*(3), 265–74. <http://doi.org/10.1080/14653240801965156>
- Jinushi, M., Takehara, T., Tatsumi, T., Hiramatsu, N., Sakamori, R., Yamaguchi, S., & Hayashi, N. (2005). Impairment of natural killer cell and dendritic cell functions by the soluble form of MHC class I-related chain A in advanced human hepatocellular carcinomas. *Journal of Hepatology*, *43*(6), 1013–1020.
- Kai Chan, Y., & Gack, M. U. (2016). Viral evasion of intracellular DNA and RNA sensing. *Nature Reviews Microbiology*, *14*(6), 360–373. <http://doi.org/10.1038/nrmicro.2016.45>
- Kajaste-Rudnitski, A., & Naldini, L. (2015). Cellular innate immunity and restriction of viral infection—implications for lentiviral gene therapy in human hematopoietic cells. *Human Gene Therapy*, *4*, 201–9.
- Kanneganti, T.-D. (2010). Central roles of NLRs and inflammasomes in viral infection. *Nature Reviews Immunology*, *10*(10), 688–98. <http://doi.org/10.1016/j.pestbp.2011.02.012>
- Kärre, K. (2002). NK cells, MHC class I molecules and the missing self. *Scandinavian Journal of Immunology*. <http://doi.org/10.1046/j.1365-3083.2002.01053.x>
- Kärre, K. (2008). Natural killer cell recognition of missing self. *Nature Immunology*, *9*(5), 477–480. <http://doi.org/10.1038/ni0508-477>
- Kato, H., Takeuchi, O., Sato, S., Yoneyama, M., Yamamoto, M., Matsui, K., ... Akira, S. (2006). Differential roles of MDA5 and RIG-I helicases in the recognition of RNA viruses. *Nature*, *441*(7089), 101–105. <http://doi.org/10.1038/nature04734>
- Kiessling, R., Klein, E., & Wigzell, H. (1975). “Natural” killer cells in the mouse. *European Journal of Immunology*, *5*, 112–117. <http://doi.org/10.1002/eji.1830050208>

- Kleinstiver, B. P., Prew, M. S., Tsai, S. Q., Topkar, V. V., Nguyen, N. T., Zheng, Z., ... Joung, J. K. (2015). Engineered CRISPR-Cas9 nucleases with altered PAM specificities. *Nature*, *523*(7561), 481–485. <http://doi.org/10.1038/nature14592>
- Klingemann, H., Boissel, L., & Toneguzzo, F. (2016). Natural Killer Cells for Immunotherapy – Advantages of the NK-92 Cell Line over Blood NK Cells. *Frontiers in Immunology*, *7*, 1–7. <http://doi.org/10.3389/fimmu.2016.00091>
- Klingemann, H., & Martinson, J. (2004). Ex vivo expansion of natural killer cells for clinical applications. *Cytotherapy*, *6*(1), 15–22. <http://doi.org/10.1080/14653240310004548>
- Kobayashi, E., Kishi, H., Ozawa, T., Hamana, H., Nakagawa, H., Jin, A., ... Muraguchi, A. (2014). A chimeric antigen receptor for TRAIL-receptor 1 induces apoptosis in various types of tumor cells. *Biochemical and Biophysical Research Communications*, *453*(4), 798–803. <http://doi.org/10.1016/j.bbrc.2014.10.024>
- Konjević, G., Mirjačić Martinović, K., Vuletić, A., Jović, V., Jurisić, V., Babović, N., & Spužić, I. (2007). Low expression of CD161 and NKG2D activating NK receptor is associated with impaired NK cell cytotoxicity in metastatic melanoma patients. *Clinical and Experimental Metastasis*, *24*(1), 1–11. <http://doi.org/10.1007/s10585-006-9043-9>
- Konstantinidis, K. V., Alici, E., Aints, A., Christensson, B., Ljunggren, H. G., & Dilber, M. S. (2005). Targeting IL-2 to the endoplasmic reticulum confines autocrine growth stimulation to NK-92 cells. *Experimental Hematology*, *33*(2), 159–164. <http://doi.org/10.1016/j.exphem.2004.11.003>
- Kruschinski, A., Moosmann, A., Poschke, I., Norell, H., Chmielewski, M., Seliger, B., ... Charo, J. (2008). Engineering antigen-specific primary human NK cells against HER-2 positive carcinomas. *Proceedings of the National Academy of Sciences of the United States of America*, *105*(45), 17481–6. <http://doi.org/10.1073/pnas.0804788105>
- Krzewski, K., & Strominger, J. L. (2008). The Killer's Kiss: The many functions of NK cell immunological synapses. *Current Opinion in Cell Biology*, *20*(5), 597–605. <http://doi.org/10.1016/j.ceb.2008.05.006>
- Kustikova, O. S., Wahlers, A., Ku, K., Sta, B., Zander, A. R., Baum, C., & Fehse, B. (2003). Dose finding with retroviral vectors: correlation of retroviral vector copy numbers in single cells with gene transfer efficiency in a cell population. *Blood*, *102*(12), 3934–3937. <http://doi.org/10.1182/blood-2003-05-1424>
- Laguet, N., Sobhian, B., Casartelli, N., Ringeard, M., Chable-Bessia, C., Ségéral, E., ... Benkirane, M. (2011). SAMHD1 is the dendritic- and myeloid-cell-specific HIV-1 restriction factor counteracted by Vpx. *Nature*, *474*(7353), 654–7. <http://doi.org/10.1038/nature10117>
- Lahouassa, H., Daddacha, W., Hofmann, H., Ayinde, D., Logue, E. C., Dragin, L., ... Margottin-Goguet, F. (2012). SAMHD1 restricts the replication of human immunodeficiency virus type 1 by depleting the intracellular pool of deoxynucleoside triphosphates. *Nature Immunology*, *13*(3), 223–228. <http://doi.org/10.1038/ni.2236>

- Lai, J., Bernhard, O. K., Turville, S. G., Harman, A. N., Wilkinson, J., & Cunningham, A. L. (2009). Oligomerization of the macrophage mannose receptor enhances gp120-mediated binding of HIV-1. *Journal of Biological Chemistry*, 284(17), 11027–11038. <http://doi.org/10.1074/jbc.M809698200>
- Lascano, J., Uchil, P. D., Mothes, W., & Luban, J. (2016). TRIM5 Retroviral Restriction Activity Correlates with the Ability To Induce Innate Immune Signaling. *Journal of Virology*, 90(1), 308–16. <http://doi.org/10.1128/JVI.02496-15>
- Lee, J. M., Yoon, S. H., Kim, H.-S., Kim, S. Y., Sohn, H.-J., Oh, S.-T., ... Kim, T.-G. (2010). Direct and indirect antitumor effects by human peripheral blood lymphocytes expressing both chimeric immune receptor and interleukin-2 in ovarian cancer xenograft model. *Cancer Gene Therapy*, 17(10), 742–750. <http://doi.org/10.1038/cgt.2010.30>
- Lee, M.-H., Padmashali, R., & Andreadis, S. T. (2011). JNK1 is required for lentivirus entry and gene transfer. *Journal of Virology*, 85(6), 2657–2665. <http://doi.org/10.1128/JVI.01765-10>
- Leoni, V., Gianni, T., Salvioli, S., & Campadelli-Fiume, G. (2012). Herpes Simplex Virus Glycoproteins gH/gL and gB Bind Toll-Like Receptor 2, and Soluble gH/gL Is Sufficient To Activate NF- κ B. *Journal of Virology*, 86(12), 6555–6562. <http://doi.org/10.1128/JVI.00295-12>
- Lévy, C., Verhoeven, E., & Cosset, F.-L. (2015). Surface engineering of lentiviral vectors for gene transfer into gene therapy target cells. *Current Opinion in Pharmacology*, 24, 79–85. <http://doi.org/10.1016/j.coph.2015.08.003>
- Li, L., Liu, L. N., Feller, S., Allen, C., Shivakumar, R., Fratantoni, J., ... Peshwa, M. (2010). Expression of chimeric antigen receptors in natural killer cells with a regulatory-compliant non-viral method. *Cancer Gene Therapy*, 17(3), 147–154. <http://doi.org/10.1038/cgt.2009.61>
- Li, M., Kao, E., Gao, X., Sandig, H., Limmer, K., Pavon-Eternod, M., ... David, M. (2012). Codon-usage-based inhibition of HIV protein synthesis by human schlafen 11. *Nature*, 491(7422), 125–8. <http://doi.org/10.1038/nature11433>
- Lim, C. P., & Cao, X. (1999). Serine phosphorylation and negative regulation of Stat3 by JNK. *Journal of Biological Chemistry*, 274(43), 31055–31061. <http://doi.org/10.1074/jbc.274.43.31055>
- Liu, C., Perilla, J. R., Ning, J., Lu, M., Hou, G., Ramalho, R., ... Zhang, P. (2016). Cyclophilin A stabilizes the HIV-1 capsid through a novel non-canonical binding site. *Nature Communications*, 7, 10714. <http://doi.org/10.1038/ncomms10714>
- Liu, H., Yang, B., Sun, T., Lin, L., Hu, Y., Deng, M., ... Jiao, S. (2015). Specific growth inhibition of ErbB2-expressing human breast cancer cells by genetically modified NK-92 cells. *Oncology Reports*, 33(1), 95–102. <http://doi.org/10.3892/or.2014.3548>
- Ljunggren, H. G., & Kärre, K. (1990). In search of the “missing self”: MHC molecules and NK cell recognition. *Immunology Today*, 11(C), 237–244. [http://doi.org/10.1016/0167-5699\(90\)90097-S](http://doi.org/10.1016/0167-5699(90)90097-S)

- Lundqvist, A., Abrams, S. I., Schrupp, D. S., Alvarez, G., Suffredini, D., Berg, M., & Childs, R. (2006). Bortezomib and depsipeptide sensitize tumors to tumor necrosis factor-related apoptosis-inducing ligand: A novel method to potentiate natural killer cell tumor cytotoxicity. *Cancer Research*, *66*(14), 7317–7325. <http://doi.org/10.1158/0008-5472.CAN-06-0680>
- Lysakova-Devine, T., & O'Farrelly, C. (2014). Tissue-specific NK cell populations and their origin. *Journal of Leukocyte Biology*, *96*(6), 981–990. <http://doi.org/10.1189/jlb.1RU0514-241R>
- Malathi, K., Dong, B., Gale, M. J., & Silverman, R. H. (2007). Small self-RNA generated by RNase L amplifies antiviral innate immunity. *Nature*, *448*(7155), 816–819. <http://doi.org/10.1038/nature06042>
- Malim, M. H., Hauber, J., Le, S. Y., Maizel, J. V., & Cullen, B. R. (1989). The HIV-1 rev trans-activator acts through a structured target sequence to activate nuclear export of unspliced viral mRNA. *Nature*, *338*(6212), 254–257. <http://doi.org/10.1038/338254a0>
- Medvedev, a E., Johnsen, a C., Haux, J., Steinkjer, B., Egeberg, K., Lynch, D. H., ... Espevik, T. (1997). Regulation of Fas and Fas-ligand expression in NK cells by cytokines and the involvement of Fas-ligand in NK/LAK cell-mediated cytotoxicity. *Cytokine*, *9*(6), 394–404. <http://doi.org/10.1006/cyto.1996.0181>
- Melchjorsen, J. (2013). Learning from the messengers: Innate sensing of viruses and cytokine regulation of immunity-clues for treatments and vaccines. *Viruses*, *5*(2), 470–527. <http://doi.org/10.3390/v5020470>
- Merten, O.-W., Charrier, S., Laroudie, N., Fauchille, S., Dugué, C., Jenny, C., ... Galy, A. (2011). Large-scale manufacture and characterization of a lentiviral vector produced for clinical ex vivo gene therapy application. *Human Gene Therapy*, *22*(3), 343–56. <http://doi.org/10.1089/hum.2010.060>
- Merten, O.-W., Hebben, M., & Bovolenta, C. (2016). Production of lentiviral vectors. *Molecular Therapy. Methods & Clinical Development*, *3*, 16017. <http://doi.org/10.1038/mtm.2016.17>
- Micucci, F., Zingoni, A., Piccoli, M., Frati, L., Santoni, A., & Galandrini, R. (2006). High-efficient lentiviral vector-mediated gene transfer into primary human NK cells. *Experimental Hematology*, *34*, 1344–1352. <http://doi.org/10.1016/j.exphem.2006.06.001>
- Mikkelsen, S. S., Jensen, S. B., Chiliveru, S., Melchjorsen, J., Julkunen, I., Gaestel, M., ... Paludan, S. R. (2009). RIG-I-mediated activation of p38 MAPK is essential for viral induction of interferon and activation of dendritic cells. Dependence on TRAF2 and TAK1. *Journal of Biological Chemistry*, *284*(16), 10774–10782. <http://doi.org/10.1074/jbc.M807272200>
- Moretta, a, Marcenaro, E., Parolini, S., Ferlazzo, G., & Moretta, L. (2008). NK cells at the interface between innate and adaptive immunity. *Cell Death and Differentiation*, *15*, 226–233. <http://doi.org/10.1038/sj.cdd.4402170>

- Müller, T., Uherek, C., Maki, G., Chow, K. U., Schimpf, A., Klingemann, H. G., ... Wels, W. S. (2008). Expression of a CD20-specific chimeric antigen receptor enhances cytotoxic activity of NK cells and overcomes NK-resistance of lymphoma and leukemia cells. *Cancer Immunology, Immunotherapy*, 57(3), 411–423. <http://doi.org/10.1007/s00262-007-0383-3>
- Muthumani, K., Choo, A. Y., Hwang, D. S., Premkumar, A., Dayes, N. S., Harris, C., ... Weiner, D. B. (2005). HIV-1 Nef-induced FasL induction and bystander killing requires p38 MAPK activation. *Blood*, 106(6), 2059–2068. <http://doi.org/10.1182/blood-2005-03-0932>
- Muthumani, K., Choo, A. Y., Shedlock, D. J., Laddy, D. J., Sundaram, S. G., Hirao, L., ... Weiner, D. B. (2008). Human immunodeficiency virus type 1 Nef induces programmed death 1 expression through a p38 mitogen-activated protein kinase-dependent mechanism. *Journal of Virology*, 82(23), 11536–11544. <http://doi.org/10.1128/JVI.00485-08>
- Muthumani, K., Wadsworth, S. a, Dayes, N. S., Hwang, D. S., Choo, A. Y., Abeysinghe, H. R., ... Weiner, D. B. (2004). Suppression of HIV-1 viral replication and cellular pathogenesis by a novel p38/JNK kinase inhibitor. *AIDS*, 18(5), 739–48. <http://doi.org/10.1097/01.aids.0000111456.61782.18>
- Nagashima, S., Mailliard, R., Kashii, Y., Reichert, T. E., Herberman, R. B., Robbins, P., & Whiteside, T. L. (1998). Stable transduction of the interleukin-2 gene into human natural killer cell lines and their phenotypic and functional characterization in vitro and in vivo. *Blood*, 91(10), 3850–61. [http://doi.org/0006-4971/98/9110-0013\\$3.00/0](http://doi.org/0006-4971/98/9110-0013$3.00/0)
- Nallagatla, S. R., Hwang, J., Toroney, R., Zheng, X., Cameron, C. E., & Bevilacqua, P. C. (2007). 5'-triphosphate-dependent activation of PKR by RNAs with short stem-loops. *Science*, 318(5855), 1455–1458. <http://doi.org/10.1126/science.1147347>
- O'Callaghan, C. (2000). Molecular basis of human natural killer cell recognition of HLA-E (human leucocyte antigen-E) and its relevance to clearance of pathogen-infected and tumour cells. *Clinical Science*, 99, 9–17. <http://doi.org/10.1042/CS19990334>
- O'Neill, L. A. J., Golenbock, D., & Bowie, A. G. (2013). The history of Toll-like receptors - redefining innate immunity. *Nature Reviews Immunology*, 13(6), 453–60. <http://doi.org/10.1038/nri3446>
- Orange, J. S., & Ballas, Z. K. (2006). Natural killer cells in human health and disease. *Clinical Immunology*. <http://doi.org/10.1016/j.clim.2005.10.011>
- Otto, E., Jones-Trower, a, Vanin, E. F., Stambaugh, K., Mueller, S. N., Anderson, W. F., & McGarrity, G. J. (1994). Characterization of a replication-competent retrovirus resulting from recombination of packaging and vector sequences. *Human Gene Therapy*, 5(5), 567–75. <http://doi.org/10.1089/hum.1994.5.5-567>
- Pan, H., Xie, J., Ye, F., & Gao, S.-J. (2006). Modulation of Kaposi's sarcoma-associated herpesvirus infection and replication by MEK/ERK, JNK, and p38 multiple mitogen-activated protein kinase pathways during primary infection. *Journal of Virology*, 80(11), 5371–82. <http://doi.org/10.1128/JVI.02299-05>

- Panne, D., Maniatis, T., & Harrison, S. C. (2007). An atomic model of the interferon-beta enhanceosome. *Cell*, *129*(6), 1111–23. <http://doi.org/10.1016/j.cell.2007.05.019>
- Paun, A., & Pitha, P. M. (2007). The IRF family, revisited. *Biochimie*, *89*, 744–53. <http://doi.org/10.1016/j.pestbp.2011.02.012>.
- Perrot, I., Deaudeau, F., Massacrier, C., Hughes, N., Garrone, P., Durand, I., ... Caux, C. (2010). TLR3 and Rig-like receptor on myeloid dendritic cells and Rig-like receptor on human NK cells are both mandatory for production of IFN-gamma in response to double-stranded RNA. *Journal of Immunology*, *185*(4), 2080–2088. <http://doi.org/10.4049/jimmunol.1000532>
- Pertel, T., Hausmann, S., Morger, D., Zuger, S., Guerra, J., Lascano, J., ... Luban, J. (2011). TRIM5 is an innate immune sensor for the retrovirus capsid lattice. *Nature*, *472*(7343), 361–365. <http://doi.org/10.1038/nature09976>
- Pesce, S., Moretta, L., Moretta, A., & Marcenaro, E. (2016). Human NK Cell Subsets Redistribution in Pathological Conditions: A Role for CCR7 Receptor. *Frontiers in Immunology*, *7*, 1–10. <http://doi.org/10.3389/fimmu.2016.00414>
- Pichlmair, A., Lassnig, C., Eberle, C., Górna, M. W., Baumann, C. L., Burkard, T. R., ... Superti-Furga, G. (2011). IFIT1 is an antiviral protein that recognizes 5'-triphosphate RNA. *Nature Immunology*, *12*(7), 624–30. <http://doi.org/10.1038/ni.2048>
- Pisegna, S., Pirozzi, G., Piccoli, M., Frati, L., Santoni, A., & Palmieri, G. (2004). p38 MAPK activation controls the TLR3-mediated up-regulation of cytotoxicity and cytokine production in human NK cells. *Blood*, *104*(13), 4157–4164. <http://doi.org/10.1182/blood-2004-05-1860>.
- Poeck, H., Bscheider, M., Gross, O., Finger, K., Roth, S., Rebsamen, M., ... Ruland, J. (2010). Recognition of RNA virus by RIG-I results in activation of CARD9 and inflammasome signaling for interleukin 1 beta production. *Nature Immunology*, *11*(1), 63–9. <http://doi.org/10.1038/ni.1824>
- Popov, S., Rexach, M., Ratner, L., Blobel, G., & Bukrinsky, M. (1998). Viral protein R regulates docking of the HIV-1 preintegration complex to the nuclear pore complex. *Journal of Biological Chemistry*, *273*(21), 13347–13352. <http://doi.org/10.1074/jbc.273.21.13347>
- Ramezani, A., & Hawley, R. G. (2010). Strategies to insulate lentiviral vector-expressed transgenes. *Methods in Molecular Biology*, *614*, 77–100. http://doi.org/10.1007/978-1-60761-533-0_5.
- Ran, F. A., Hsu, P. D., Wright, J., Agarwala, V., Scott, D. A., & Zhang, F. (2013). Genome engineering using the CRISPR-Cas9 system. *Nature Protocols*, *8*(11), 2281–308. <http://doi.org/10.1038/nprot.2013.143>
- Raulet, D. H., & Guerra, N. (2009). Oncogenic stress sensed by the immune system: role of natural killer cell receptors. *Nature Reviews Immunology*, *9*(8), 568–580. <http://doi.org/10.1038/nri2604>

- Real, G., Monteiro, F., Burger, C., & Alves, P. M. (2011). Improvement of lentiviral transfer vectors using cis-acting regulatory elements for increased gene expression. *Applied Microbiology and Biotechnology*, *91*(6), 1581–1591. <http://doi.org/10.1007/s00253-011-3392-2>
- Romanski, A., Uherek, C., Bug, G., Seifried, E., Klingemann, H., Wels, W. S., ... Tonn, T. (2016). CD19-CAR engineered NK-92 cells are sufficient to overcome NK cell resistance in B-cell malignancies. *Journal of Cellular and Molecular Medicine*, *20*(7), 1287–1294. <http://doi.org/10.1111/jcmm.12810>
- Rustagi, A., & Gale, M. (2014). Innate Antiviral Immune Signaling, Viral Evasion and Modulation by HIV-1. *Journal of Molecular Biology*, *426*(6), 1161–1177. <http://doi.org/10.1016/j.jmb.2013.12.003>
- Sahm, C., Schönfeld, K., & Wels, W. S. (2012). Expression of IL-15 in NK cells results in rapid enrichment and selective cytotoxicity of gene-modified effectors that carry a tumor-specific antigen receptor. *Cancer Immunology, Immunotherapy : CII*, *61*(9), 1451–61. <http://doi.org/10.1007/s00262-012-1212-x>
- Sakuma, T., Barry, M. A., & Ikeda, Y. (2012). Lentiviral vectors: basic to translational. *Biochemical Journal*, *443*, 603–618. <http://doi.org/10.1042/BJ20120146>
- Sander, J. D., & Joung, J. K. (2014). CRISPR-Cas systems for editing, regulating and targeting genomes. *Nature Biotechnology*, *32*(4), 347–55. <http://doi.org/10.1038/nbt.2842>
- Sanjana, N. E., Shalem, O., & Zhang, F. (2014). Improved vectors and genome-wide libraries for CRISPR screening. *Nature Methods*, *11*(8), 783–784. <http://doi.org/10.1038/nmeth.3047>
- Satoh, T., Kato, H., Kumagai, Y., Yoneyama, M., Sato, S., Matsushita, K., ... Takeuchi, O. (2010). LGP2 is a positive regulator of RIG-I- and MDA5-mediated antiviral responses. *Proceedings of the National Academy of Sciences of the United States of America*, *107*(4), 1512–7. <http://doi.org/10.1073/pnas.0912986107>
- Schirrmann, T., & Pecher, G. (2002). Human natural killer cell line modified with a chimeric immunoglobulin T-cell receptor gene leads to tumor growth inhibition in vivo. *Cancer Gene Therapy*, *9*(4), 390–398. <http://doi.org/10.1038/sj.cgt.7700453>
- Schirrmann, T., & Pecher, G. (2005). Specific targeting of CD33+ leukemia cells by a natural killer cell line modified with a chimeric receptor. *Leukemia Research*, *29*(3), 301–306. <http://doi.org/10.1016/j.leukres.2004.07.005>
- Schmidt, K. N., Leung, B., Kwong, M., Zarembek, K. a, Satyal, S., Navas, T. a, ... Godowski, P. J. (2004). APC-independent activation of NK cells by the Toll-like receptor 3 agonist double-stranded RNA. *Journal of Immunology*, *172*, 138–143. <http://doi.org/10.4049/jimmunol.172.1.138>
- Schönfeld, K., Sahm, C., Zhang, C., Naundorf, S., Brendel, C., Odendahl, M., ... Wels, W. S. (2015). Selective inhibition of tumor growth by clonal NK cells expressing an ErbB2/HER2-specific chimeric antigen receptor. *Molecular Therapy : The Journal of the American Society of Gene Therapy*, *23*(2), 330–8. <http://doi.org/10.1038/mt.2014.219>

- Shalem, O., Sanjana, N. E., Hartenian, E., Shi, X., Scott, D. A., Heckl, D., ... Doench, J. G. (2014). Genome-scale CRISPR-Cas9 knockout screening in human cells. *Science*, *343*(6166), 84–87. <http://doi.org/10.1126/science.1247005>.
- Sheu, J., Beltzer, J., Fury, B., Wilczek, K., Tobin, S., Falconer, D., ... Bauer, G. (2015). Large-scale production of lentiviral vector in a closed system hollow fiber bioreactor. *Molecular Therapy. Methods & Clinical Development*, *2*, 15020. <http://doi.org/10.1038/mtm.2015.20>
- Shimasaki, N., Fujisaki, H., Cho, D., Masselli, M., Lockey, T., Eldridge, P., ... Campana, D. (2012). A clinically adaptable method to enhance the cytotoxicity of natural killer cells against B-cell malignancies. *Cytotherapy*, *14*(7), 830–40. <http://doi.org/10.3109/14653249.2012.671519>
- Sivori, S., Falco, M., Della Chiesa, M., Carlomagno, S., Vitale, M., Moretta, L., & Moretta, A. (2004). CpG and double-stranded RNA trigger human NK cells by Toll-like receptors: induction of cytokine release and cytotoxicity against tumors and dendritic cells. *Proceedings of the National Academy of Sciences of the United States of America*, *101*(27), 10116–21. <http://doi.org/10.1073/pnas.0403744101>
- Sliwkowski, M. X., & Mellman, I. (2013). Antibody therapeutics in cancer. *Science*, *341*(6151), 1192–8. <http://doi.org/10.1126/science.1241145>
- Smyth, M. J., Hayakawa, Y., Takeda, K., & Yagita, H. (2002). New aspects of natural-killer-cell surveillance and therapy of cancer. *Nature Reviews Cancer*, *2*(11), 850–61. <http://doi.org/10.1038/nrc928>
- Stavrou, S., & Ross, S. R. (2015). APOBEC3 Proteins in Viral Immunity. *Journal of Immunology*, *195*, 4565–4570. <http://doi.org/10.4049/jimmunol.1501504>
- Suck, G., Odendahl, M., Nowakowska, P., Seidl, C., Wels, W. S., Klingemann, H. G., & Tonn, T. (2015). NK-92 : an “off-the-shelf therapeutic” for adoptive natural killer cell-based cancer immunotherapy. *Cancer Immunology, Immunotherapy*. <http://doi.org/10.1007/s00262-015-1761-x>
- Sun, L., Wu, J., Du, F., Chen, X., & Chen, Z. J. (2013). Cyclic GMP-AMP Synthase Is a Cytosolic DNA Sensor That Activates the Type I Interferon Pathway. *Science*, *339*, 786–791. <http://doi.org/10.1126/science.1229963>
- Sundquist, W. I., & Kräusslich, H. G. (2012). HIV-1 assembly, budding, and maturation. *Cold Spring Harbor Perspectives in Medicine*, *2*(7), 1–24. <http://doi.org/10.1101/cshperspect.a006924>
- Sutlu, T., Nyström, S., Gilljam, M., Stellan, B., Applequist, S. E., & Alici, E. (2012). Inhibition of Intracellular Antiviral Defense Mechanisms Augments Lentiviral Transduction of Human Natural Killer Cells: Implications for Gene Therapy. *Human Gene Therapy*, *23*, 1090–1100. <http://doi.org/10.1089/hum.2012.080>
- Takaoka, A., Wang, Z., Choi, M. K., Yanai, H., Negishi, H., Ban, T., ... Taniguchi, T. (2007). DAI (DLM-1/ZBP1) is a cytosolic DNA sensor and an activator of innate immune response. *Nature*, *448*(7152), 501–505. <http://doi.org/10.1038/nature06013>

- Takeuchi, O., & Akira, S. (2010). Pattern Recognition Receptors and Inflammation. *Cell*, *140*(6), 805-20. <http://doi.org/10.1016/j.cell.2010.01.022>
- Tonn, T., Schwabe, D., Klingemann, H. G., Becker, S., Esser, R., Koehl, U., ... Bug, G. (2013). Treatment of patients with advanced cancer with the natural killer cell line NK-92. *Cytotherapy*, *15*(12), 1563–1570. <http://doi.org/10.1016/j.jcyt.2013.06.017>
- Trotta, R., Fettucciari, K., Azzoni, L., Abebe, B., Puorro, K. a., Eisenlohr, L. C., & Perussia, B. (2000). Differential Role of p38 and c-Jun N-Terminal Kinase 1 Mitogen-Activated Protein Kinases in NK Cell Cytotoxicity. *Journal of Immunology*, *165*(4), 1782–1789. <http://doi.org/10.4049/jimmunol.165.4.1782>
- Turville, S. G., Santos, J. J., Frank, I., Cameron, P. U., Wilkinson, J., Miranda-Saksena, M., ... Cunningham, A. L. (2004). Immunodeficiency virus uptake, turnover, and 2-phase transfer in human dendritic cells. *Blood*, *103*(6), 2170–2179. <http://doi.org/10.1182/blood-2003-09-3129>
- Uchil, P. D., Hinz, A., Siegel, S., Coenen-Stass, A., Pertel, T., Luban, J., & Mothes, W. (2013). TRIM protein-mediated regulation of inflammatory and innate immune signaling and its association with antiretroviral activity. *Journal of Virology*, *87*(1), 257–72. <http://doi.org/10.1128/JVI.01804-12>
- Van Maele, B., De Rijck, J., De Clercq, E., & Debyser, Z. (2003). Impact of the central polypurine tract on the kinetics of human immunodeficiency virus type 1 vector transduction. *Journal of Virology*, *77*(8), 4685–94. <http://doi.org/10.1128/JVI.77.8.4685-4694.2003>
- Voskoboinik, I., Smyth, M. J., & Trapani, J. A. (2006). Perforin-mediated target-cell death and immune homeostasis. *Nature Reviews Immunology*, *6*(12), 940–952. <http://doi.org/10.1038/nri1983>
- Weber, K., Bartsch, U., Stocking, C., & Fehse, B. (2008). A multicolor panel of novel lentiviral “gene ontology” (LeGO) vectors for functional gene analysis. *Molecular Therapy: The Journal of the American Society of Gene Therapy*, *16*(4), 698–706. <http://doi.org/10.1038/mt.2008.6>
- Wu, B., Peisley, A., Richards, C., Yao, H., Zeng, X., Lin, C., ... Hur, S. (2013). Structural basis for dsRNA recognition, filament formation, and antiviral signal activation by MDA5. *Cell*, *152*(1–2), 276–289. <http://doi.org/10.1016/j.cell.2012.11.048>
- Yang, B., Liu, H., Shi, W., Wang, Z., Sun, S., Zhang, G., ... Jiao, S. (2013). Blocking transforming growth factor- β signaling pathway augments antitumor effect of adoptive NK-92 cell therapy. *International Immunopharmacology*, *17*(2), 198–204. <http://doi.org/10.1016/j.intimp.2013.06.003>
- Yang, K., Wang, J., Wu, M., Li, M., Wang, Y., & Huang, X. (2015). Mesenchymal stem cells detect and defend against gammaherpesvirus infection via the cGAS-STING pathway. *Scientific Reports*, *5*, 7820. <http://doi.org/10.1038/srep07820>
- Yang, S., Zhan, Y., Zhou, Y., Jiang, Y., Zheng, X., Yu, L., ... Tong, G. (2016). Interferon regulatory factor 3 is a key regulation factor for inducing the expression of SAMHD1 in antiviral innate immunity. *Scientific Reports*, *6*, 1–16. <http://doi.org/10.1038/srep29665>

- Yildiz, S., Alpdundar, E., Gungor, B., Kahraman, T., Bayyurt, B., Gursel, I., & Gursel, M. (2015). Enhanced immunostimulatory activity of cyclic dinucleotides on mouse cells when complexed with a cell-penetrating peptide or combined with CpG. *European Journal of Immunology*, *45*(4), 1170–1179. <http://doi.org/10.1002/eji.201445133>
- Yin, H., Kanasty, R. L., Eltoukhy, A. a, Vegas, A. J., Dorkin, J. R., & Anderson, D. G. (2014). Non-viral vectors for gene-based therapy. *Nature Reviews Genetics*, *15*(8), 541–555. <http://doi.org/10.1038/nrg3763>
- Yoneyama, M., Kikuchi, M., Matsumoto, K., Imaizumi, T., Miyagishi, M., Taira, K., ... Fujita, T. (2005). Shared and Unique Functions of the DExD/H-Box Helicases RIG-I, MDA5, and LGP2 in Antiviral Innate Immunity. *Journal of Immunology*, *175*(5), 2851–2858. <http://doi.org/10.4049/jimmunol.175.5.2851>
- Zetsche, B., Gootenberg, J. S., Abudayyeh, O. O., Slaymaker, I. M., Makarova, K. S., Essletzbichler, P., ... Zhang, F. (2015). Cpf1 Is a Single RNA-Guided Endonuclease of a Class 2 CRISPR-Cas System. *Cell*, *163*(3), 759–771. <http://doi.org/10.1016/j.cell.2015.09.038>
- Zhang, C., Burger, M. C., Jennewein, L., Genßler, S., Schönfeld, K., Zeiner, P., ... Wels, W. S. (2016). ErbB2/HER2-Specific NK Cells for Targeted Therapy of Glioblastoma. *Journal of the National Cancer Institute*, *108*(5). <http://doi.org/10.1093/jnci/djv375>
- Zhang, G., Liu, R., Zhu, X., Wang, L., Ma, J., Han, H., ... Gao, B. (2013). Retargeting NK-92 for anti-melanoma activity by a TCR-like single-domain antibody. *Immunology and Cell Biology*, *91*(10), 615–24. <http://doi.org/10.1038/icb.2013.45>
- Zufferey, R., Donello, J. E., Trono, D., & Hope, T. J. (1999). Woodchuck hepatitis virus posttranscriptional regulatory element enhances expression of transgenes delivered by retroviral vectors. *Journal of Virology*, *73*(4), 2886–2892. <http://doi.org/10.1128/JVI.73.4.2886-2892.1999>
- Zufferey, R., Dull, T., Mandel, R. J., Bukovsky, A., Quiroz, D., Naldini, L., & Trono, D. (1998). Self-inactivating lentivirus vector for safe and efficient in vivo gene delivery. *Journal of Virology*, *72*(12), 9873–80. <http://doi.org/10.1128/JVI.72.12.9873-9880.1998>

APPENDIX

APPENDIX A: Chemicals Used in This Study

<u>Chemicals and Media Components</u>	<u>Company</u>
Agarose	Sigma, Germany
Ampicillin Sodium Salt	CellGro, USA
Boric Acid	Molekula, UK
Bradford Reagent	Sigma, Germany
Distilled Water	Merck Millipore, USA
DMEM	Thermo Scientific, USA
DMSO	Sigma, Germany
DNA Gel Loading Dye, 6X	NEB, USA
DPBS	Sigma, Germany
EDTA	Applichem, Germany
Ethanol	Sigma, Germany
Ethidium Bromide	Sigma, Germany
Fetal Bovine Serum	Thermo Scientific, USA
HEPES Solution, 1 M	Sigma, Germany
Hydrochloric Acid	Merck Millipore, USA
Isopropanol	Sigma, Germany
Kanamycin Sulfate	Thermo Scientific, USA
LB Agar	BD, USA
LB Broth	BD, USA
L-glutamine, 200 mM	Sigma, Germany
MEM Vitamin Solution, 100X	Sigma, Germany
MEM Non-essential Amino Acid Solution	Sigma, Germany
2-Mercaptoethanol	Sigma, Germany
Methanol	Sigma, Germany
PIPES	Sigma, Germany
Sodium Pyruvate Solution, 100 mM	Sigma, Germany

APPENDIX B: Equipment Used in This Study

<u>Equipment</u>	<u>Company</u>
Autoclave	Hirayama, HiClave HV-110, Japan
Balance	Sartorius, BP221S, Germany
Centrifuge	Schimidzu, Libror EB-3200 HU, Japan Eppendorf, 5415D, Germany Eppendorf, 5702, Germany
CO ₂ incubator	Binder, Germany Thermo Fisher Scientific, USA
Countess II FL automated cell counter	Thermo Fisher Scientific, USA
Deepfreeze	-80°C, Forma, Thermo Electron Corp., USA -20°C, Bosch, Turkey
Electrophoresis Apparatus	Biorad Inc., USA
Filters (0.22 µm and 0.45µm)	Merck Millipore, USA
Flow cytometer	BD FACScanto, USA
Gel Documentation	Biorad, UV-Transilluminator 2000, USA
Heater	Thermomixer Comfort, Eppendorf, Germany
Hemocytometer	Hausser Scientific, Blue Bell Pa., USA
Ice Machine	Scotsman Inc., AF20, USA
Incubator	Memmert, Modell 300, Germany Memmert, Modell 600, Germany
Laminar Flow	Heraeus, HeraSafe HS12, Germany Heraeus, HeraSafe KS, Germany
LightCycler® 480	Roche, Switzerland
Liquid Nitrogen Tank	Taylor-Wharton, 3000RS, USA
Magnetic Stirrer	VELP Scientifica, ARE Heating Magnetic Stirrer, Italy
Microliter Pipettes	Gilson, Pipetman, France Isolab, Germany Thermo Fisher Scientific, USA
Microscope	Zeiss, Primo Vert, Germany Olympus IX70 inverted, USA
Microwave Oven	Bosch, Turkey
pH meter	WTW, pH540 GLP MultiCal, Germany
Refrigerator	Bosch, Turkey
Shaker Incubator	New Brunswick Sci., Innova 4330, USA
Spectrophotometer	Schimidzu, UV-1208, Japan Schimidzu, UV-3150, Japan
Thermocycler	Eppendorf, Mastercycler Gradient, Germany
Vortex	Velp Scientifica, Italy

APPENDIX C: Commercial Kits Used in This Study

<u>Commercial Kit</u>	<u>Company</u>
Calcium Phosphate Transfection Kit	Sigma-Aldrich, USA
FITC Annexin V Apoptosis Detection Kit	BD Biosciences, USA
High-Capacity cDNA Reverse Transcription Kit	Thermo, USA
InsTAclone PCR Cloning Kit	Thermo, USA
NuceloSpin® Gel and PCR Clean up	Macherey-Nagel, USA
NuceloSpin® Plasmid Miniprep Kit	Macherey-Nagel, USA
NuceloSpin® Plasmid Midiprep Kit	Macherey-Nagel, USA
PathScan® Immune Cell Signaling Antibody Array Kit (Fluorescent Readout)	Cell Signaling Technology, USA
PureLink® HiPure Plasmid Midiprep Kit	Invitrogen, USA
PureLink® Genomic DNA Mini Kit	Invitrogen, USA
Quick-RNA™ Miniprep Kit	Zymo Research, USA
TaqMan® Gene Expression Assays	Thermo, USA
Vivapure® LentiSELECT 40	Sartorius, Germany

APPENDIX D: Antibodies Used in This Study

<u>Antibody</u>	<u>Company</u>
Mouse APC anti-CD56 (NCAM 16.2)	BD Biosciences, USA
Mouse AF647 anti-STAT3 (pS727) (Clone 49)	BD Biosciences, USA
Mouse PE anti-IRF-7 (pS477/pS479) (Clone K47-671)	BD Biosciences, USA
Mouse AF647 anti-RIG-I (Clone IMG2M6F10)	Imgenex, Novus, USA
Mouse AF647 IgG1κ (Clone MOPC-31C)	Imgenex, Novus, USA

APPENDIX E: DNA Ladder

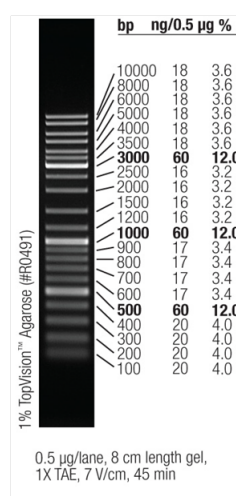


Figure E1. 10kb Gene Ruler DNA Ladder Mix (Fermentas)

APPENDIX F: Plasmid Maps

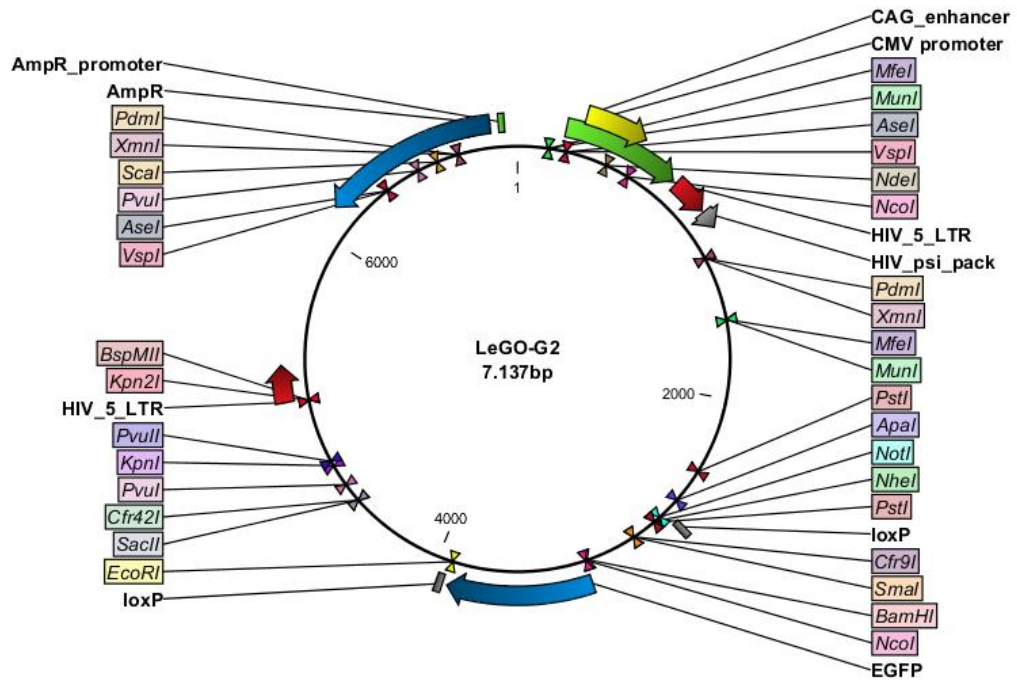


Figure F1. The vector map of LeGO-G2.

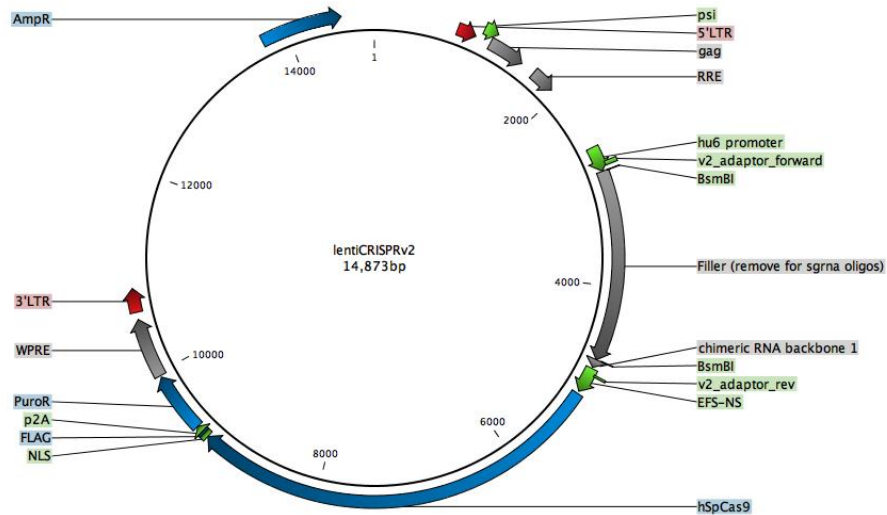
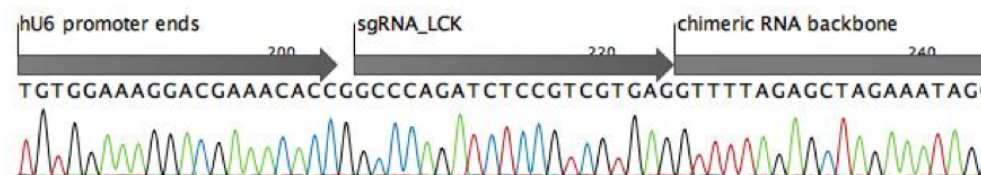
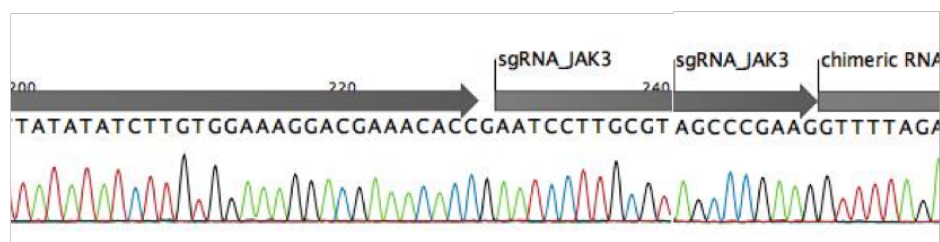
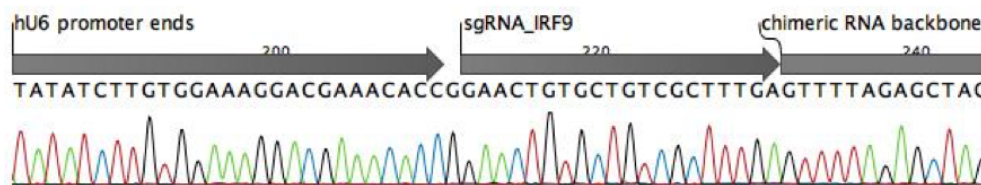
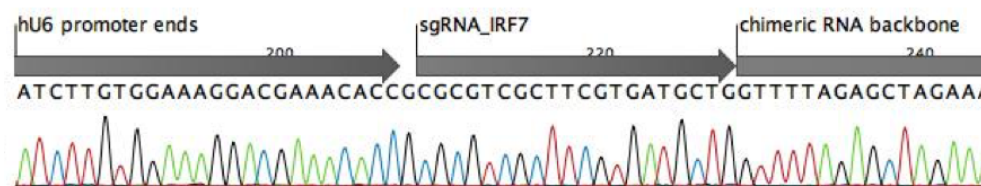
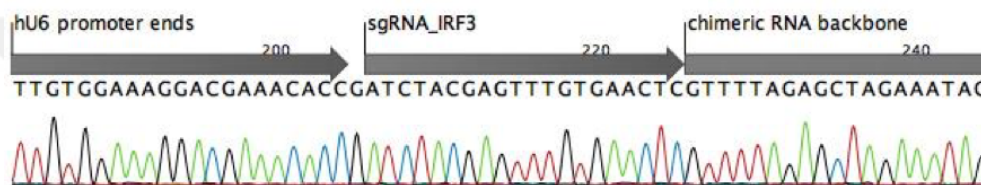
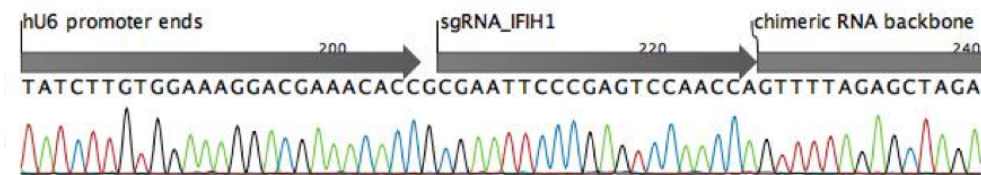
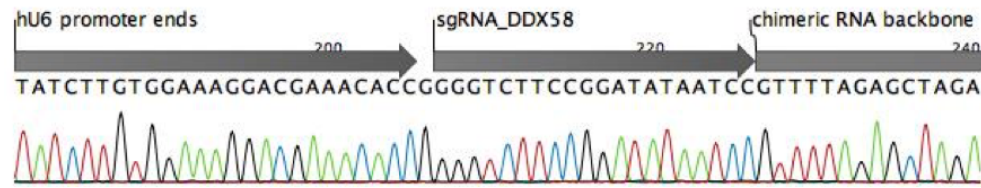
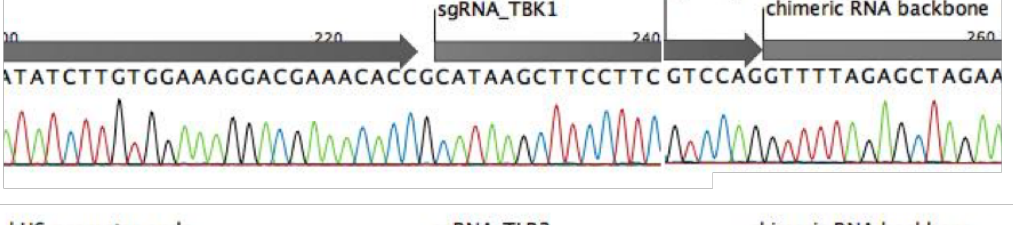
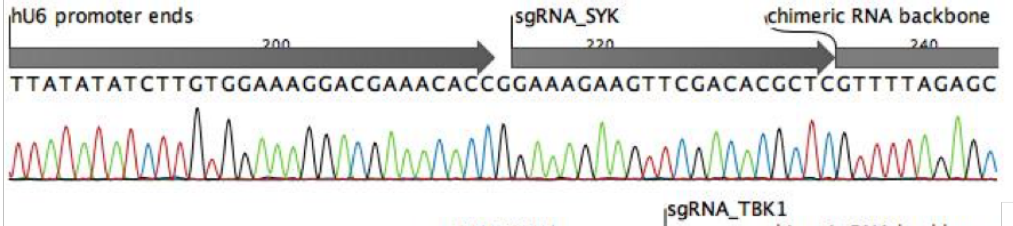
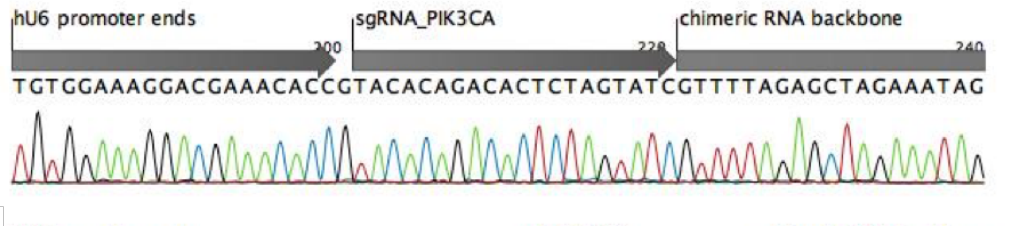
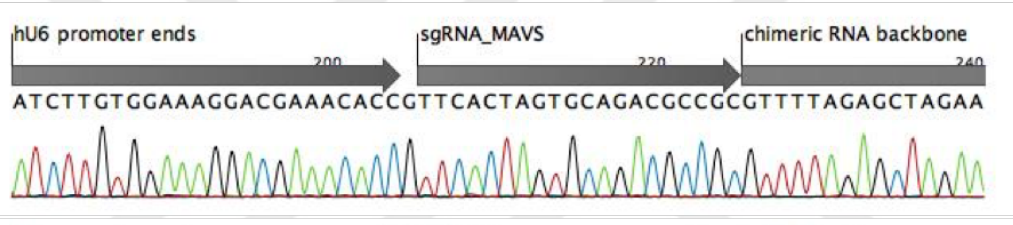
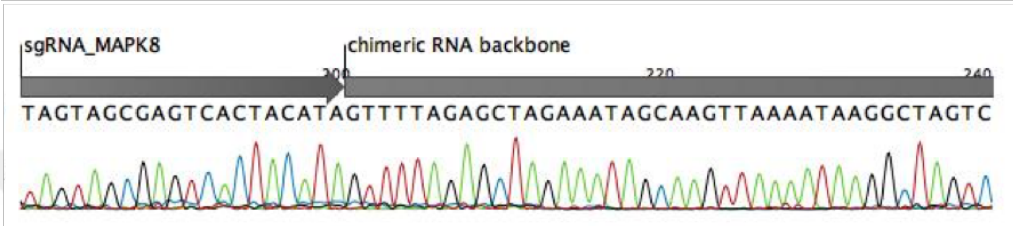
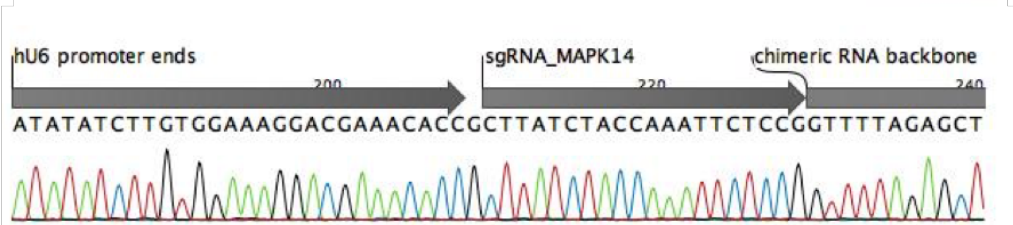
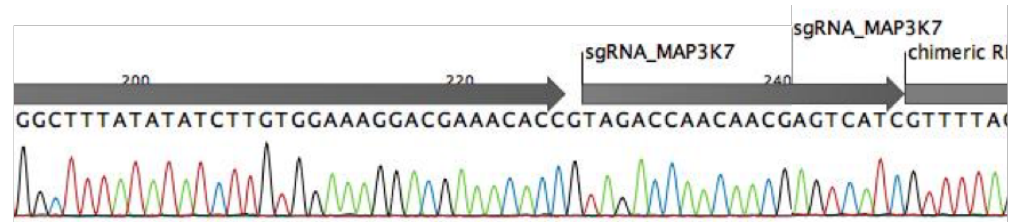


Figure F2. The vector map of lentiCRISPRv2.

APPENDIX G: Sequencing Results





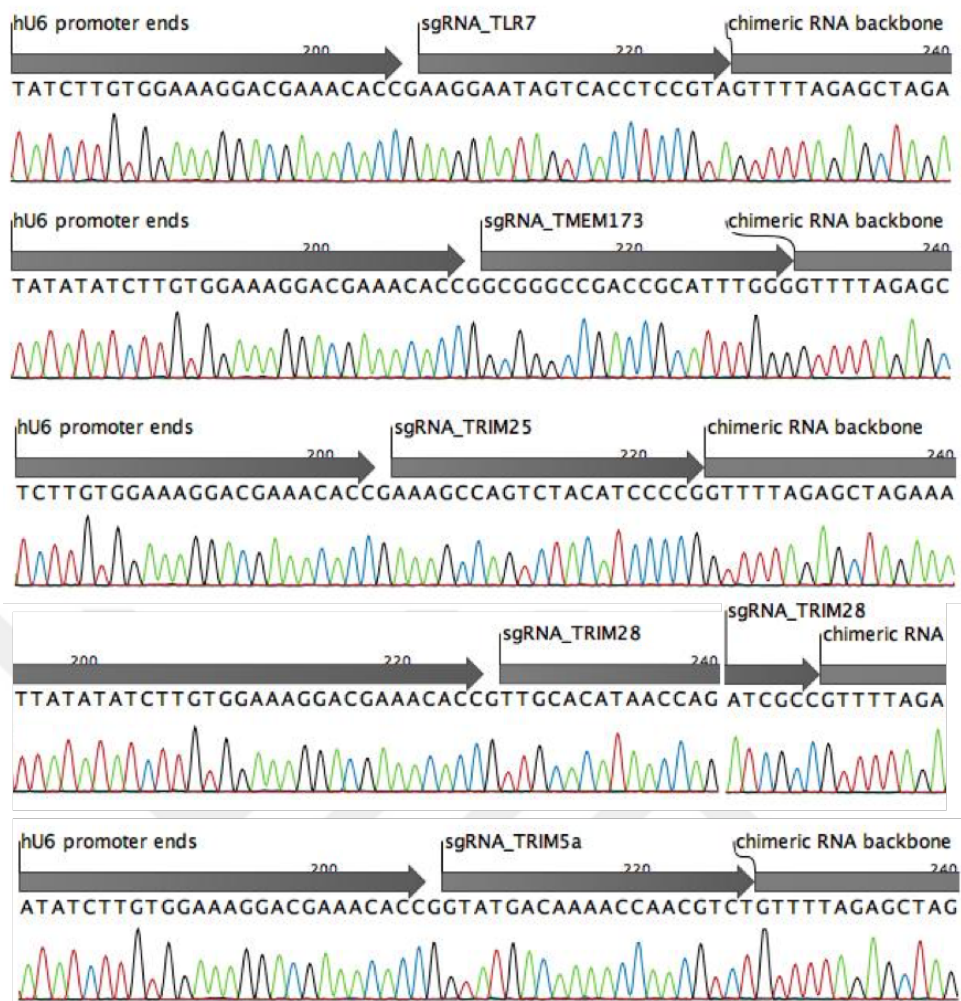


Figure G1. Sequencing results of lentiCRISPR constructs.

APPENDIX H: CRISPR Target Sites

CLOSE-UP

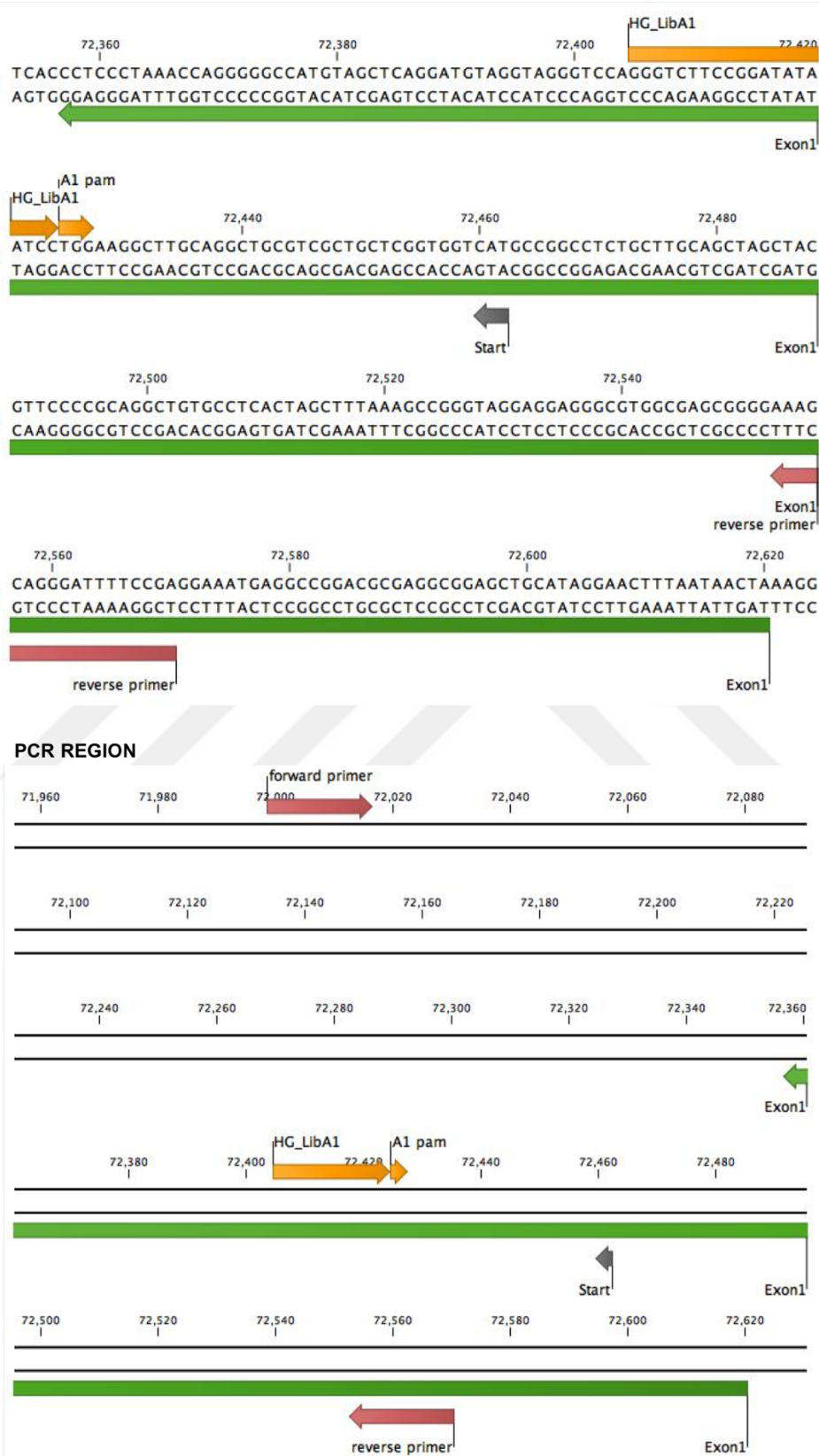


Figure H1. DDX58 (lentiCRISPR design) genomic DNA region.

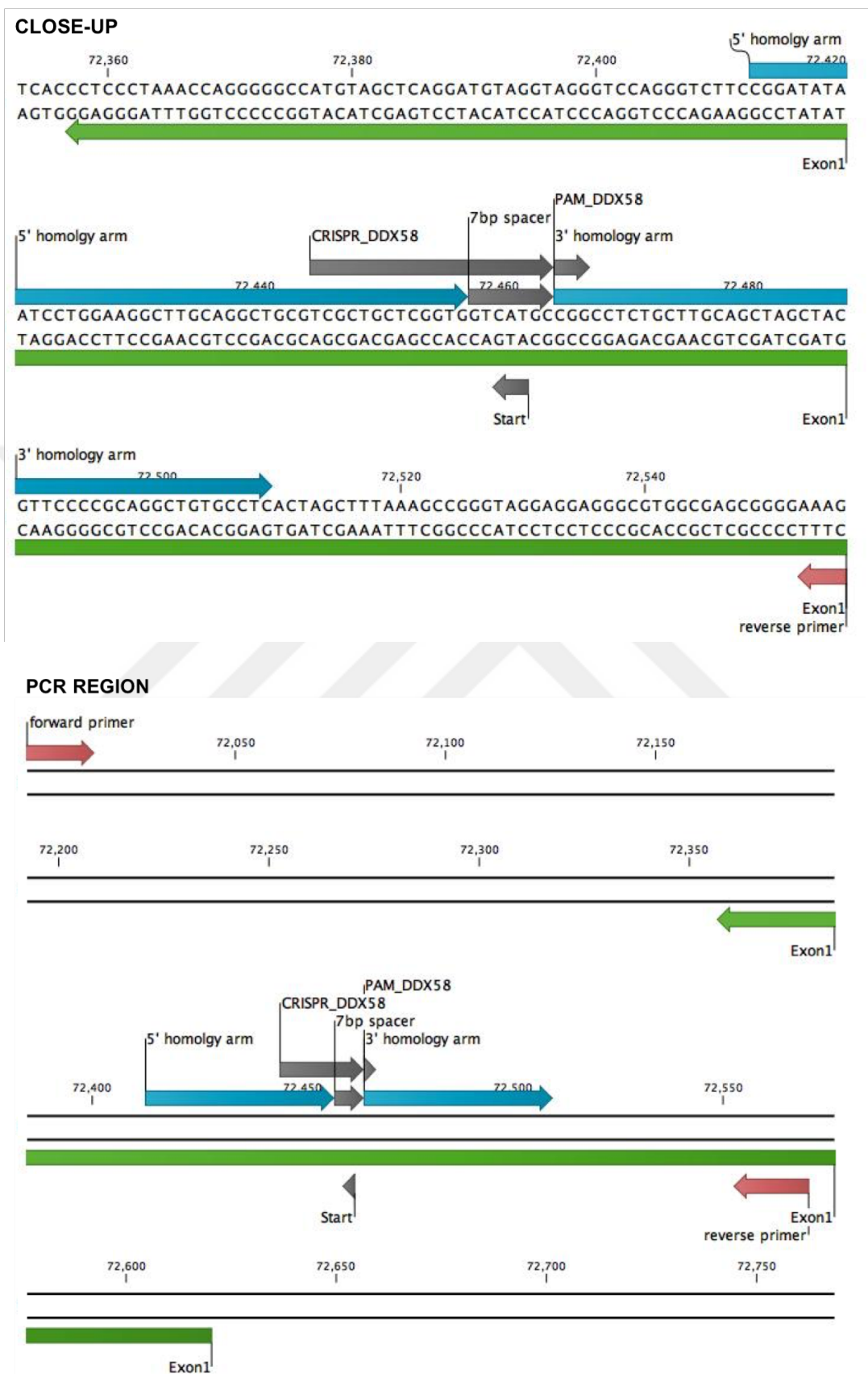
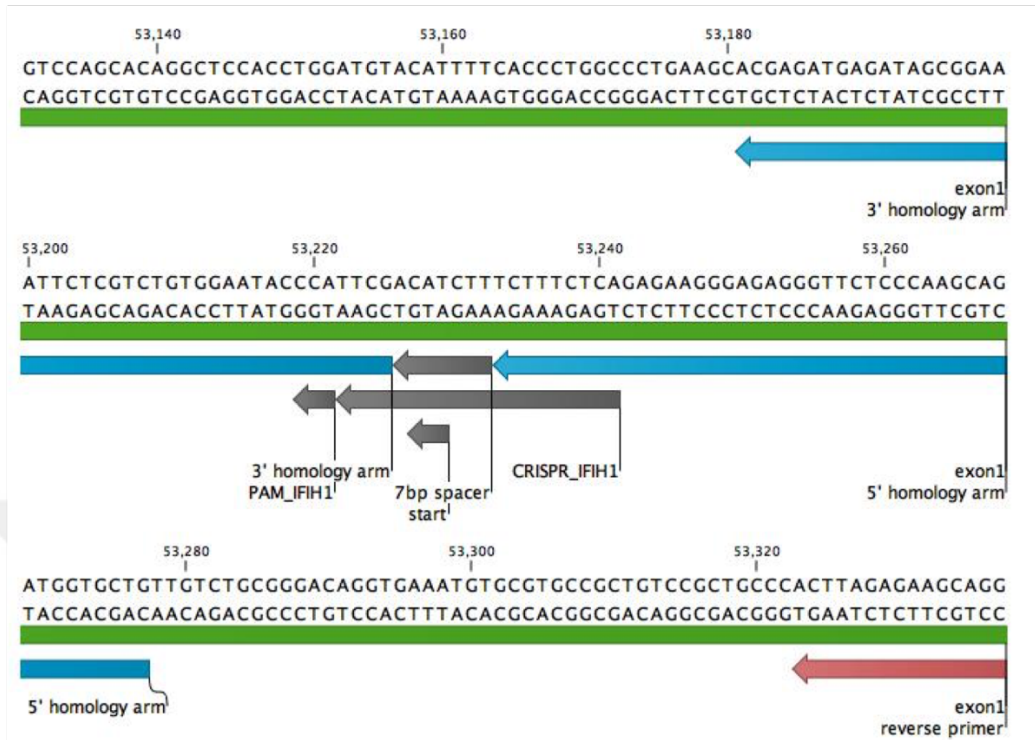


Figure H2. DDX58 (pspCas9(BB) design) genomic DNA region.

CLOSE-UP



PCR REGION

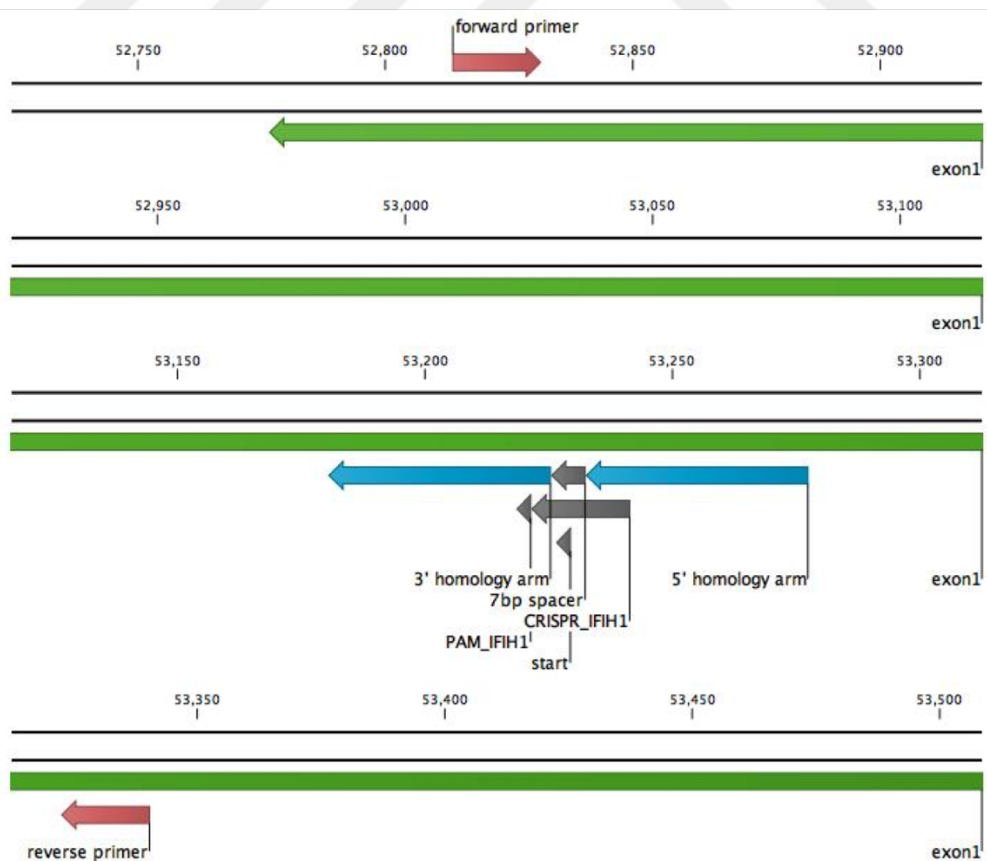
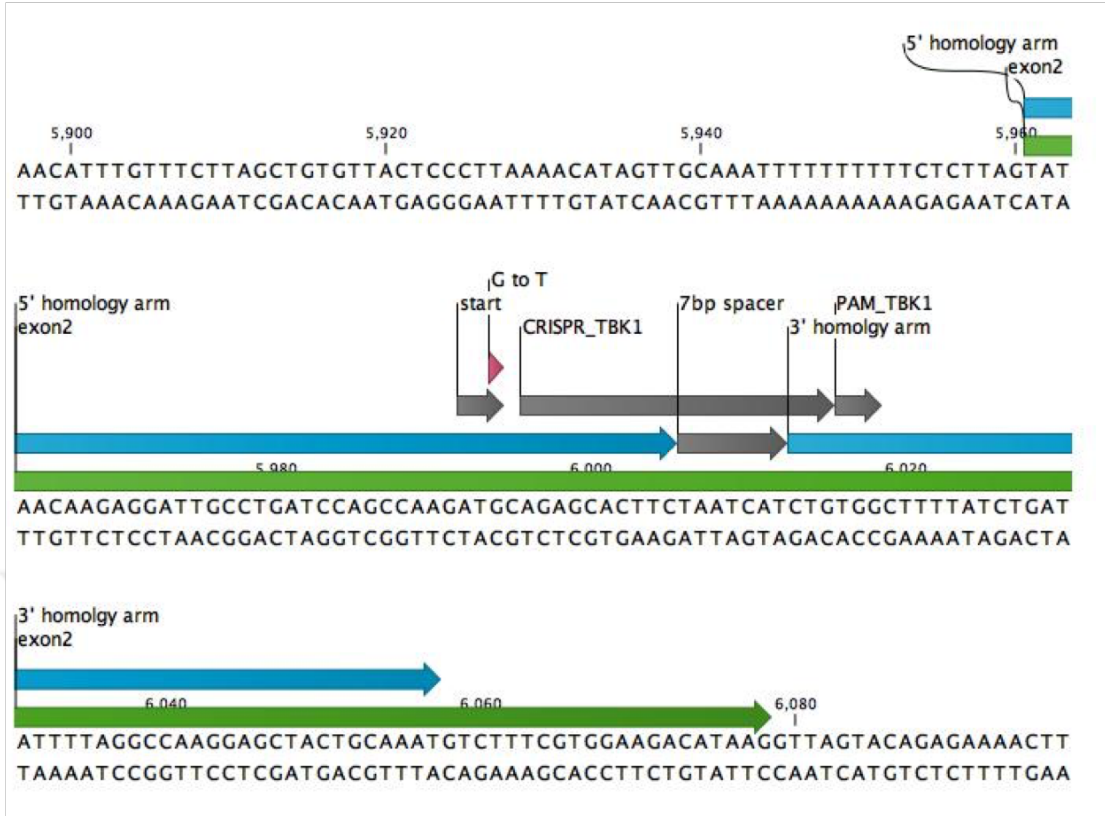


Figure H3. IFIH1 (pspCas9(BB) design) genomic DNA region.

CLOSE-UP



PCR REGION

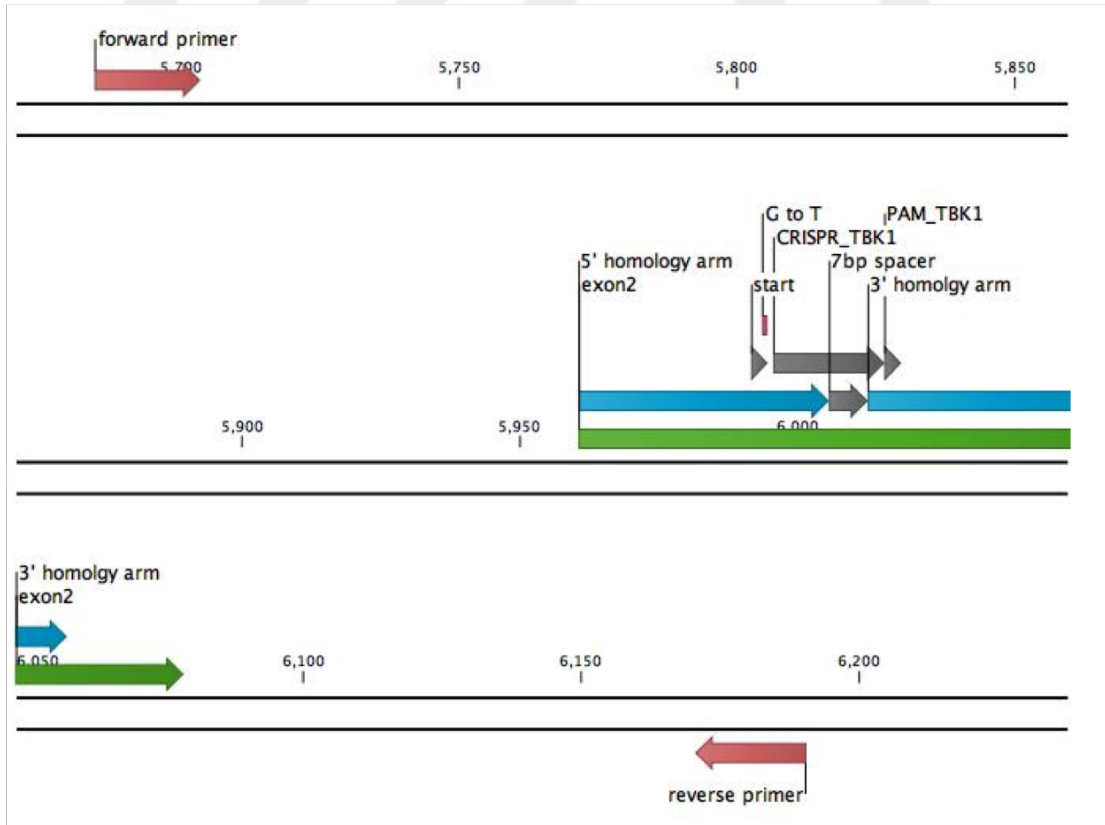
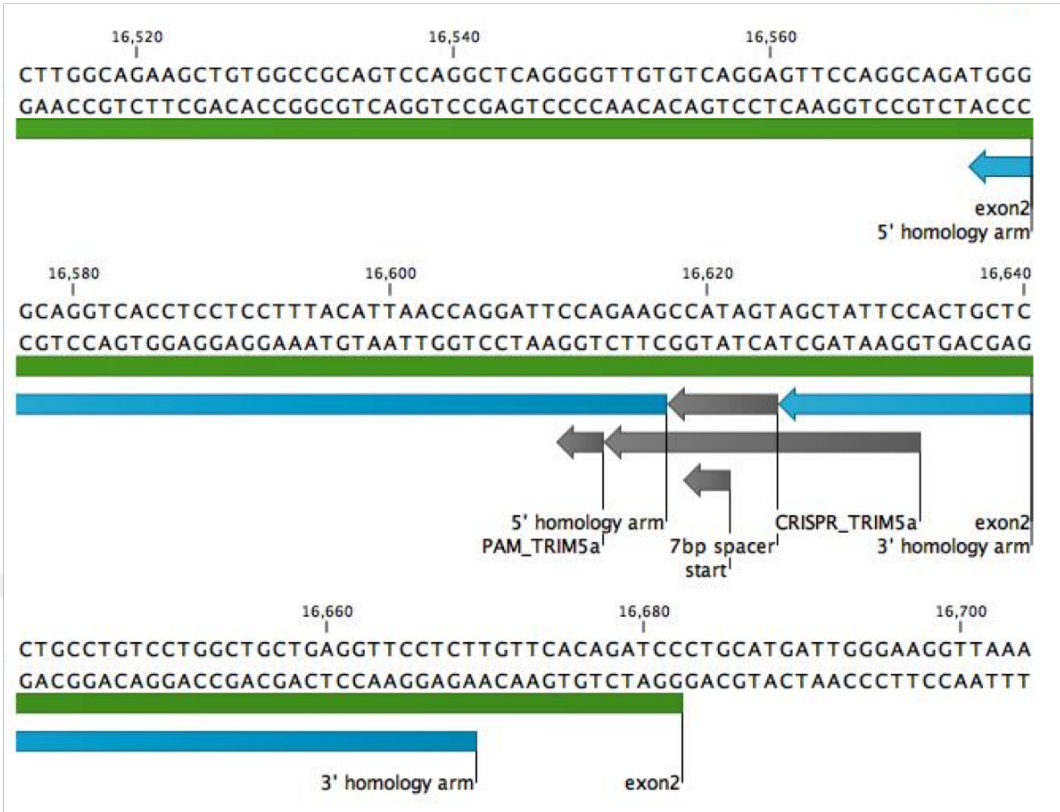


Figure H4. TBK1 (pspCas9(BB) design) genomic DNA region.

CLOSE-UP



PCR REGION

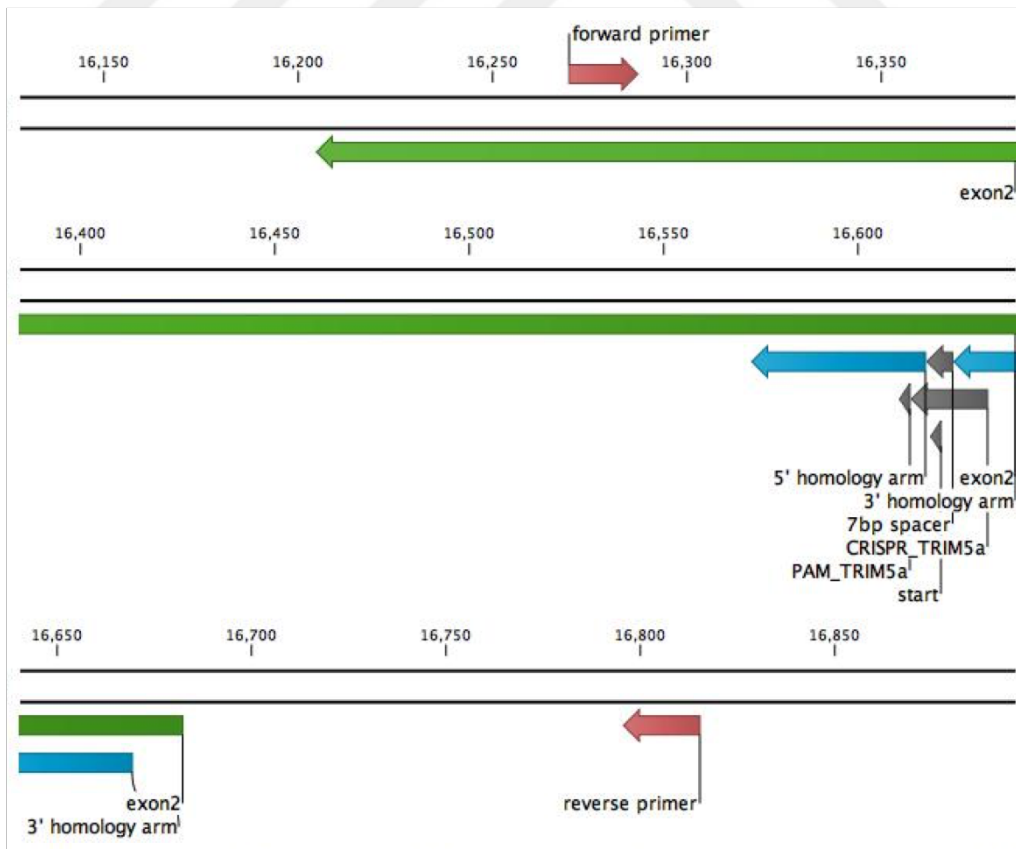


Figure H5. TRIM5α (pspCas9(BB) design) genomic DNA region.

APPENDIX I: Immune Cell Signaling Array Results

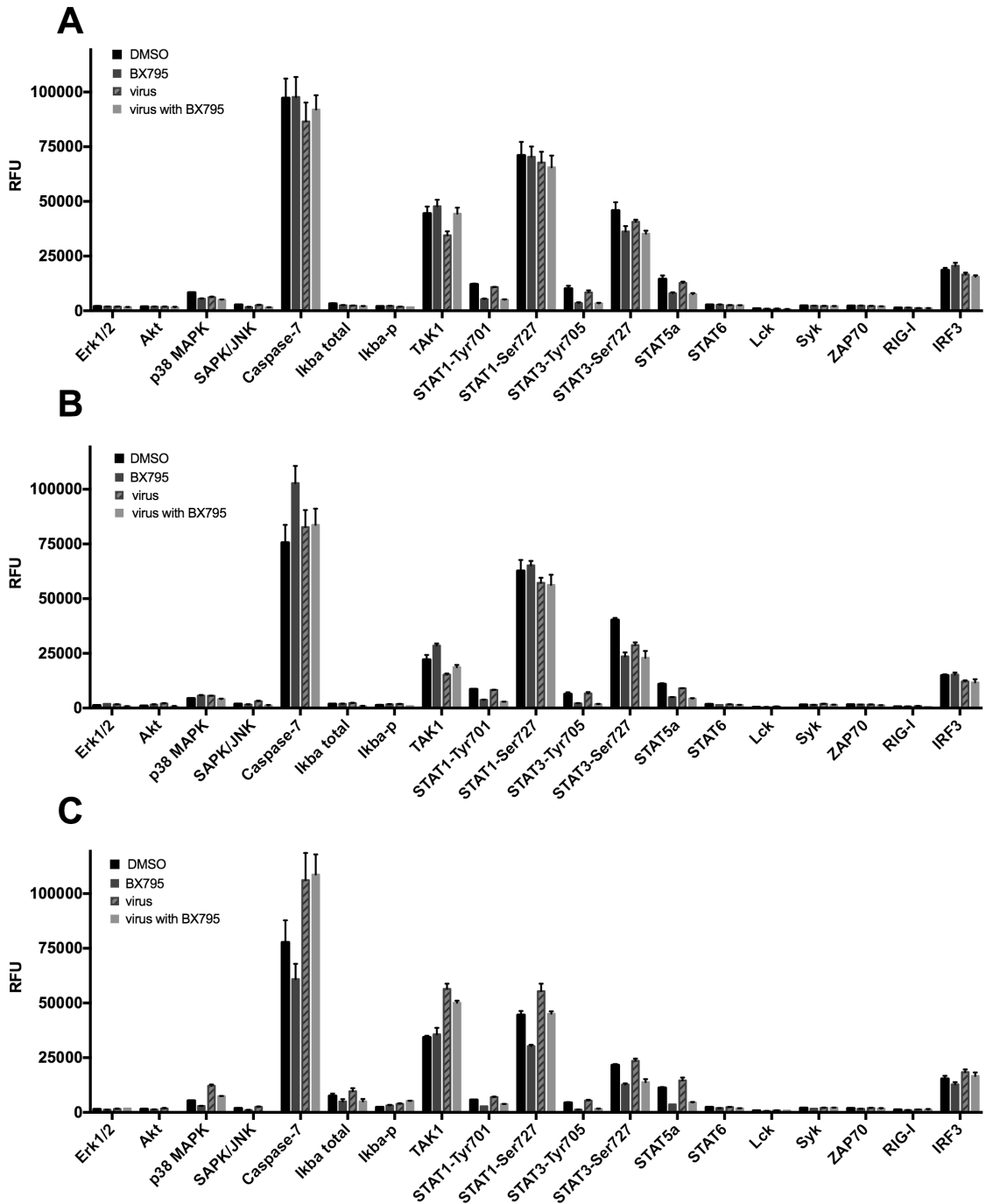


Figure 11. Immune cell signaling array with 15-30-90 minute-transductions. Serum-free NK-92 cells were treated with DMSO alone (black), 6 μ M BX795 alone (dark grey), viral vector at MOI=20 (striped) or viral vector with 6 μ M BX795 (light grey) for (A) 15, (B) 30 or (C) 90 minutes. The average of two blots for each protein were plotted. RFU: relative fluorescence unit. Error bars indicate SD.

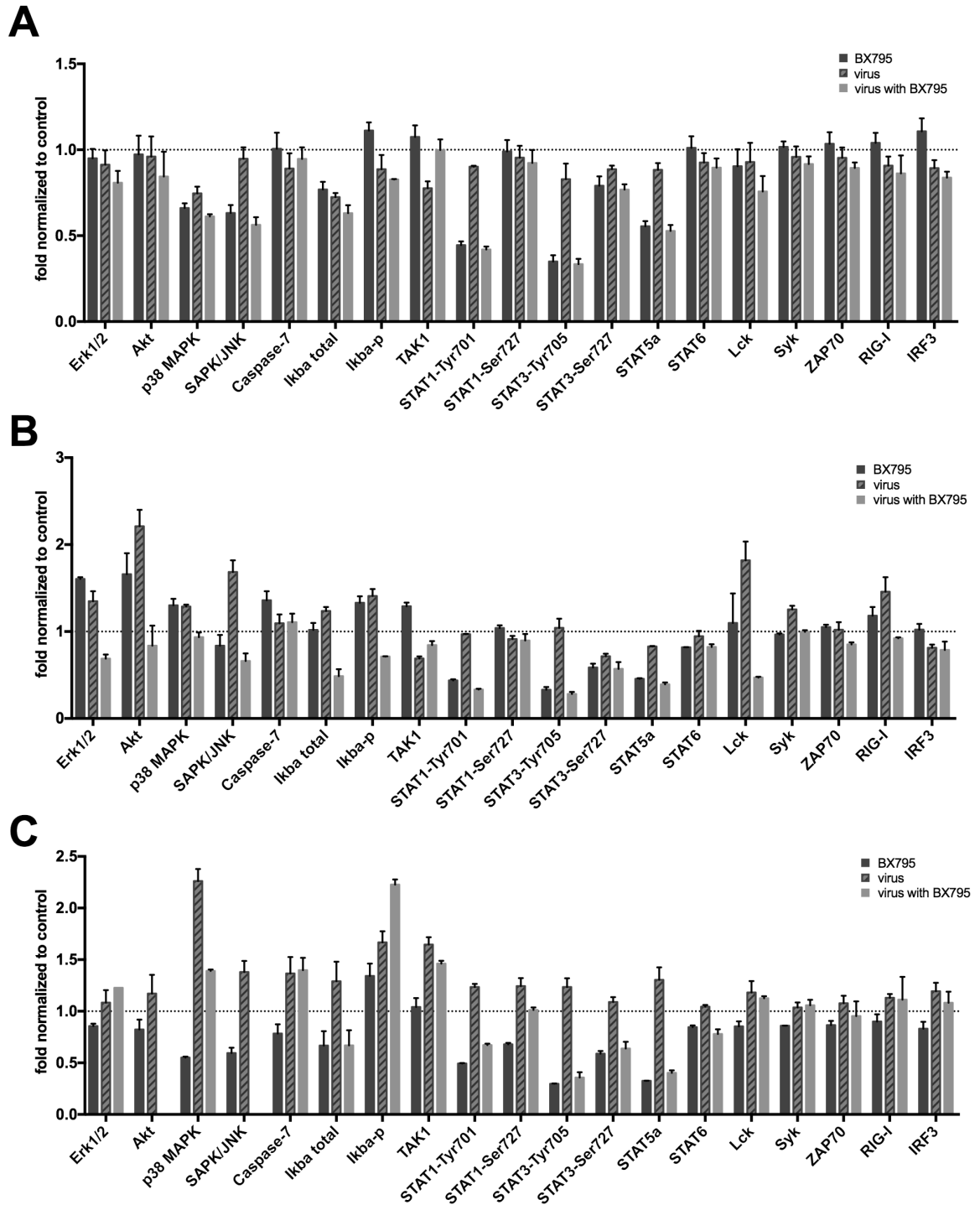


Figure 12. Immune cell signaling array with 15-, 30-, 90-minute transductions normalized to control. Serum-free NK-92 cells were treated with DMSO alone, 6 μ M BX795 alone (dark grey), viral vector at MOI=20 (striped) or viral vector with 6 μ M BX795 (light grey) for (A) 15, (B) 30 or (C) 90 minutes and each signal value was normalized to that of DMSO control for each time point. The average of two blots for each protein were plotted. Dashed line indicates the level of DMSO control sample. Error bars indicate SD.

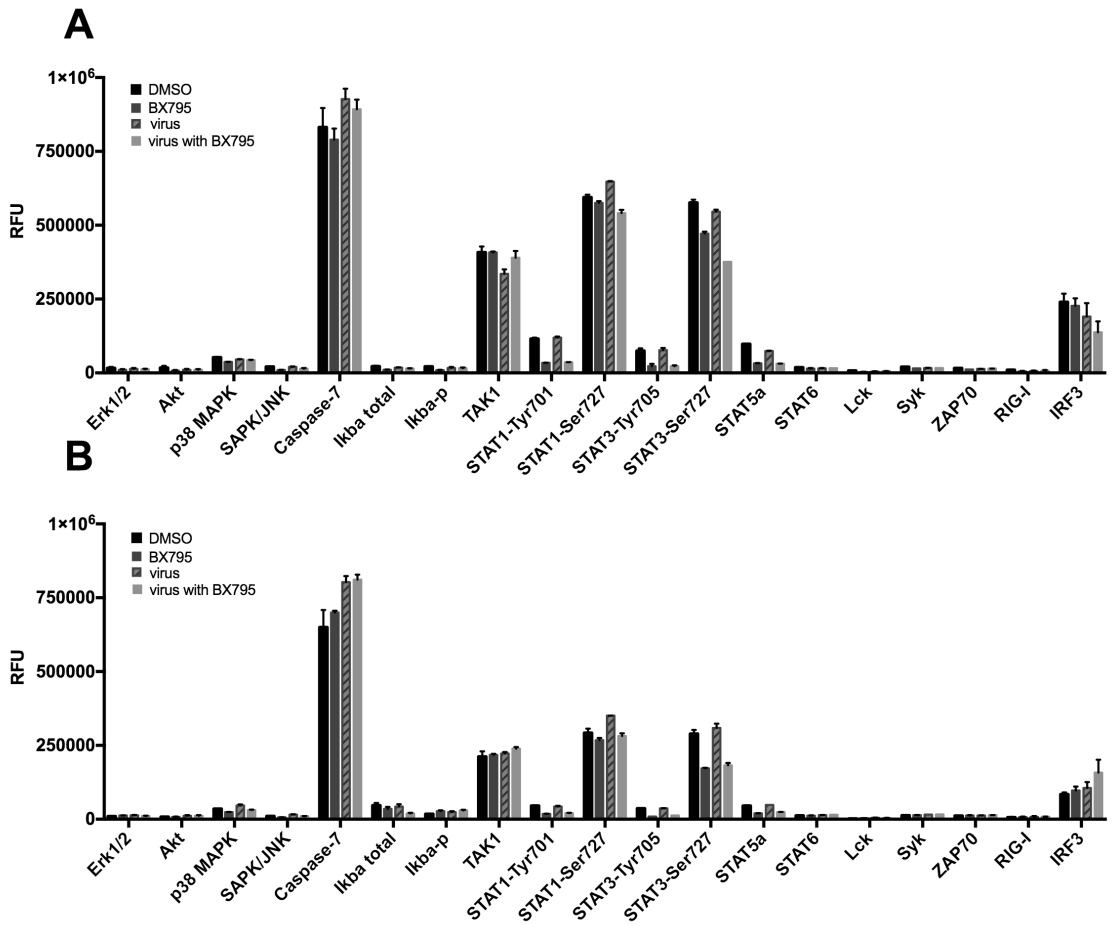


Figure 13. Immune cell signaling array with 30- and 90-minute transductions. Serum-free NK-92 cells were treated with DMSO alone (black), 6 μ M BX795 alone (dark grey), viral vector at MOI=20 (striped) or viral vector with 6 μ M BX795 (light grey) for (A) 30 and (B) 90 minutes in the presence of IL-2. The average of two blots for each protein were plotted. RFU: relative fluorescence unit. Error bars indicate SD.

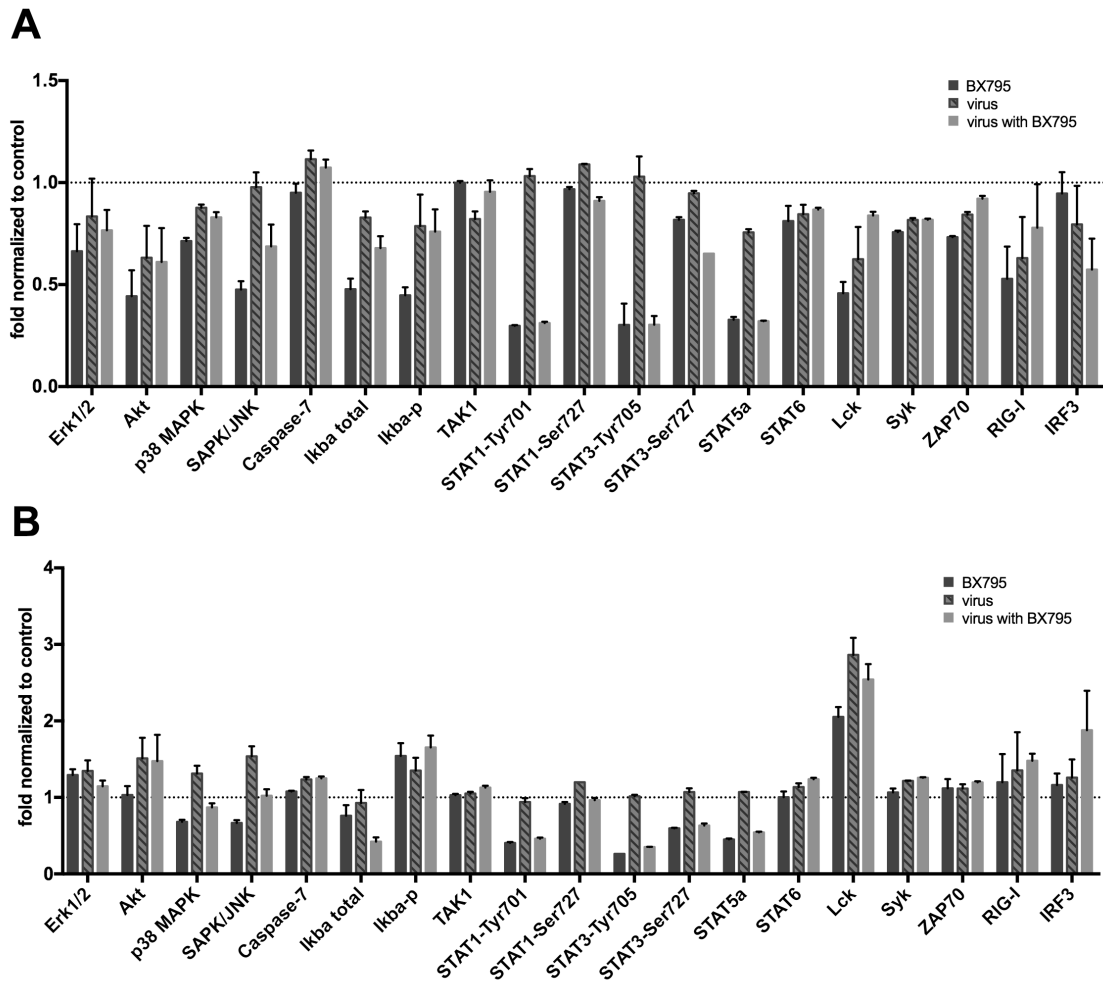


Figure 14. Immune cell signaling array with 30- and 90-minute transductions normalized to control. Serum-free NK-92 cells were treated with DMSO alone, 6 μ M BX795 alone (dark grey), viral vector at MOI=20 (striped) or viral vector with 6 μ M BX795 (light grey) for (A) 30 and (B) 90 minutes in the presence of IL-2. Each signal value was normalized to that of DMSO control for each time point. The average of two blots for each protein were plotted. Dashed line indicates the level of DMSO control sample. Error bars indicate SD.